Bridging Chasms with Polyphosphides[1]

HANS-GEORG VON SCHNERING* and WOLFGANG HÖNLE

Max-Planck-Institut für Festkörperforschung, Stuttgart, FRG

Received July 23, 1987 (Revised Manuscript Received November 10, 1987)

Contents

I.	Introduction	243
II.	The Compounds	243
III.	Preparation	244
IV.	Structure and Bonding	248
V.	Bond Distances, Bond Angles, and Electron Density	255
VI.	Polyphosphides from Solution	258
VII.	Gas-Phase Species	259
VIII.	The P^-/S Analogy	259
IX.	Thermochemistry	259
X.	Phase Transitions and Plastically Crystalline Phases	261
XI.	Phosphorus/Arsenic Mixed Crystals	262
XII.	Vibrational, Electronic, and Magnetic Properties	264
XIII.	Chemical Reactions	266
XIV.	Donor Properties	267
XV.	Solid-State Volumes	268
XVI.	Defect Structures	268
XVII.	The Eulerian Polyhedra Theorem	269
XVIII.	Epilogue	269
XIX.	References	269

I. Introduction

Marianne Baudler revealed the beauty of phosphane chemistry in a recent review,[2] making the following article apparently needless. One may gain the impression that this brilliant progress[3,4] was yielded by purposeful syntheses followed by excellent NMR work and sometimes by crystal structure analyses. But this is only part of the truth, because the main structural principles realized in catenated phosphorus systems were already offered by the simple binary solid phosphides, representing the derivatives of molecular and polymeric phosphanes to some extent. Furthermore, the crystalline phases can already be seen as complexes, because definite assignments exist between the coordination of the metal atoms and the donor functions of the polyanions. Bridging the unnatural gap between molecular chemists and solid-state chemists is still topical today, and it should be remembered that the creation of numerous chemical divisions has nothing to do with science but with politics. Today, when Inorganic Chemistry is believed to be Complex Chemistry and Solid-State Chemistry seems to be degenerated to Material Science, it may be useful to demonstrate the whole spread of the chemistry of solids and their relations in general. There is really a lot of individualism in collectives, but the latter can be more than the sum of the former. It is of course rather irrelevant which materials are used to demonstrate the intimate relations between molecules and complexes on one side, and real solids on the other. We think that the metal polyphosphides are quite suitable for this purpose, because it becomes clear now that even phosphorus follows carbon with regard to the multivarious phosphanes and their derivatives.

In the past two decades remarkable progress has occurred.[5-13] We owe this decisive progress to modern methods of synthesis and to the unambiguous characterization of the compounds. But we should not forget the pioneering work of Krebs[14-18] and Klemm.[19-21] Numerous unusual compounds were discovered by systematic investigations, and some of the previously described compounds were revised. Especially in the field of the main-group-element phosphides one can hardly expect new fundamental types, and, therefore, it seems reasonable to order the facts in line.

It has been known for a long time that phosphorus can be combined with nearly all elements. Especially compounds with high phosphorus content occur quite frequently, and these polyphosphides deserve general interest for several reasons: (1) they exhibit an unexpected wealth of composition and structures that represent the stepwise dismantling of group 5 element structures by the electron transfer of the electropositive metals; (2) they correlate herewith the field of typical collective solids (cf. NaCl, where clear separation into smaller units is impossible) with the field of molecules; (3) they disclose new routines to novel molecules acting as precursors; and (4) they cover a whole range of physical properties related to their stoichiometry and structure.

Special characteristics of phosphorus should be emphasized; viz., P atoms are per se structural elements of surfaces because of their maximal threefold homoatomic connectivity. Phosphorus is thereby distinguished from the diagonally related carbon. Indeed, even the crystalline phosphorus modifications demonstrate the strong correlations between structure and reactivity, because the structures represent the main ways of forming surfaces with different curvature and strain. Specifically the elemental forms are white phosphorus with droplike P_4 molecules, Hittorf's violet phosphorus with tubes like rolled-up surfaces, and black phosphorus with strain-free corrugated layers. These principles are continued in the numerous derivatives of these principal structures that are represented by the polyphosphides.

II. The Compounds

The present knowledge of phosphides is schematized in Figure 1 and compiled in Tables I–V, and we tried to complete this survey. The crystal structures are characterized by the short Pearson symbol,[22] and the phosphorus partial structures are symbolized by a bond

0009-2665/88/0788-0243$06.50/0

Hans-Georg von Schnering was born 1939 in Ranis (East Germany), studied in Münster and Göttingen (West Germany), and received his Diploma and Ph.D. degree (1960) at the University of Münster under the direction of Professor W. Klemm and Professor R. Hoppe, respectively. He was Full Professor of Inorganic Chemistry in Münster (1966–1975) and presently is a Scientific Member of the Max-Planck-Gesellschaft and Director at the Max-Planck-Institut für Festkörperforschung (Stuttgart). Professor von Schnering received the Alfred Stock Award of the Gesellschaft Deutscher Chemiker (1981). He is Dr.h.c. of the University of Geneva, Switzerland, and is a member of the Heidelberg Academy of Science and of the Academia Leopoldina, Halle. His research interests concern solid-state chemistry, especially synthetic, structural, and bonding studies of metal-cluster compounds and homonuclear-bonded polyanions and structural chemistry in general, including lattice energy and periodic potential surfaces in solids. He is editor-in-chief of *Zeitschrift für Kristallographie* and is a member of the Kuratorium of *Angewandte Chemie*.

Wolfgang Hönle received his Diploma and Ph.D. degree (1975) in inorganic chemistry at the University of Münster/FRG under the direction of Professor H. G. von Schnering. Presently he is a permanent scientific co-worker at the Max-Planck-Institut für Festkörperforschung in Stuttgart/FRG. His main research interests are polyanionic and polycationic compounds and their preparative and structural aspects as well as their properties. In addition he also serves as an assistant editor of *Zeitschrift für Kristallographie*.

key and by their linkage principles. The connectivity symbols (0b), (1b), (2b), and (3b) are valid for the P–P linkage and stand for P atoms with zero, one, two, or three homoatomic bonds. The formal charges correspond with the Zintl–Klemm rules[19,23] if the metal atoms are present as M^{n+} cations. The formal oxidation state per P atom (Figure 1) is calculated according to

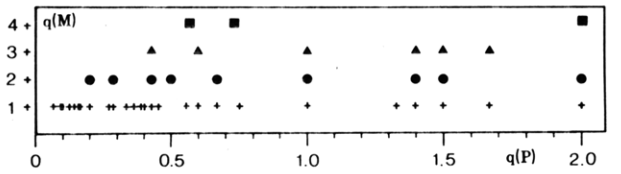

Figure 1. Occurence of metal polyphosphides MP_x with respect to the formal charges $q(P)$ and $q(M)$ in the range $q(P) \leq 2$. For the calculation of $q(P) = q(M)/x$ cf. text.

$-(3a + 2b + 1c)/(a + b + c + d)$, where a, b, c, and d are the bond key numbers (Table I). Isolated atoms or groups are symbolized as ( ), whereas for infinite polymeric partial structures the symbol $^{m}_{\infty}$( ) is used (m is the dimensionality of the P–P network). References for the individual compounds, compiled in Tables I–V, are only given there; further references are given in the text at the appropriate locations.

Let us take the existence of higher polyphosphides as a rough measure of their stability relative to that of lower phosphides. This treatment is fairly good because the compounds are prepared under more or less similar conditions with respect to the phosphorus pressure. It follows from the tables and figure 1 that the thermal stability with respect to decomposition into lower phosphides and P_4(g) is related to the cation size r(M) and to the formal cation charge q(M). Therefore, for the free energy of a generalized decomposition reaction

$$MP_n(s) = MP(s) + [(n - 1)/4]P_4(g)$$

$\Delta G_R(M_1) > \Delta G_R(M_2)$ holds if $r(M_1) < r(M_2)$ and/or $q(M_1) > q(M_2)$. In other words, the relative stability of a phosphide with a given stoichiometry increases with increasing size and with decreasing charge of the cation. For example, the maximal P/M ratio is reached for the compositions CaP_3, Sr_3P_{14}, and BaP_{10} (cation size) and LaP_7, BaP_{10}, and KP_{15} (cation charge), respectively. These relations correspond quite well with the relative stabilities of salt hydrates, salt ammoniates, and, at least, complex compounds. In a simple way, the formation of a polyphosphide from a monophosphide and P_4(g) may be compared with the formation of a metal carbonate from the metal oxide and CO_2. In both cases the free energy gain increases with increasing r(M) and with decreasing q(M), respectively, by lattice energy arguments. Compounds with P^{3-} have been included only for completeness in the case of main-group elements and rare-earth metals. The nonexistence of Rb_3P and Cs_3P is noticeable, as well as the unknown crystal structure of Ca_3P_2, one of the widely used phosphides.

III. Preparation

In principle, all metal phosphides and polyphosphides can be synthesized from the elements in stoichiometric ratios. However, there are several problems to master: (i) *Caution*: The syntheses must be guided very carefully. The exothermic reactions often give rise to explosive violence caused by local overheating. Especially the oxide layers on metals imply using unsuitably high temperatures for starting the phosphorination, which easily can produce a temperature of about 1200–1300 K in the reaction zone; e.g., CaP_3 melts (mp 1260 K) when the elements react at the "oven temperature" of 650 K. It should be remembered that the critical point of red phosphorus is at T_c = 908 K (p = 130 bar) and, therefore, phosphorus should be mostly bonded below

T_c. (ii) At higher temperatures P(white) transforms into the red modification, of which the vaporization for adjusting the equilibrium pressure is very slow (kinetic hindrance). (iii) High reaction temperatures are often necessary because of the passivating coating of the metals by oxides or lower phosphides. On the other hand, disadvantages of high reaction temperatures include the decomposition of polyphosphides into lower phosphides and P_4(g) as well as reactions of the components with the container material. (iv) To perform complete syntheses, several grindings and annealing procedures are necessary, as the metals are frequently covered in the first reaction step by a metal-rich phosphide. In general, these metal-rich phosphides have the highest melting points in the binary systems M/P. Therefore, the reaction rate of the inner parts of the metals with P is controlled by the diffusion of P (or M) through the metal-rich layers.

1. Synthesis from the Elements

The important progress of recent years is based on optimization of well-known procedures, the development of new methods, the application of new container materials, and the improved knowledge of single reaction steps. In particular, the ampule technique with different temperature zones and the application of molten salts as solvents need to be mentioned.

Ampule Technique[8,11,27,37,43]

This technique is generally used for the preparation of all kinds of phosphides. The corrosion of the outer ampule is prevented by the use of one or two inner containers from selected materials stable against corrosion. Tubes of Mo, Nb, and Ta replace the steel or iron container and allow, for example, the preparation of numerous alkali-metal phosphides as pure materials at temperatures up to 1100–1200 K. A typical size is length = 10 cm; outer diameter = 1.5 cm.

Two Temperature Zones

Two-zone furnaces allow the adjustment of different temperatures when the metal and phosphorus are loaded at different positions of the ampule. Thus, the decomposition pressure of the chosen metal phosphide (higher T) can be adjusted by the (lower T) equilibrium pressure of red phosphorus, which allows greater control over the reaction rate.

Phosphorus Pressure

The vaporization of red phosphorus is strongly hindered. So, one measures under usual reaction conditions at 600 K a pressure of about 3×10^{-4} bar instead of the equilibrium value of about 5×10^{-2} bar. Therefore, older experiments need large P excesses and much higher temperatures, and after reaction they lead to the precipitation of the P excess in all parts of the ampules. This is no longer a problem, because it was found that small amounts of iodine and even sulfur erase this hindrance completely and lead to fast adjustment of the equilibrium pressure.[275]

Molten Reaction Media[8,144,154,199,339-341]

Low-melting metals (Ga, In, Sn, Bi, Pb, Hg) and salts (halides of the alkali metals and rare-earth metals) are suitable reaction media as long as the desired phosphide is thermodynamically more stable than other phases formed under reaction conditions (intermetallic phosphides of the low-melting metals, binary and ternary halides, phosphide halides). The effectiveness is governed by the solubility of the metal and phosphorus and even of some metal phosphide species at higher temperatures, as well as the ability to remove the oxide covers. However, the method is strongly limited by the necessary separation procedures following the reaction. Molten Ga and In are suitable because only GaP and InP exist with high decomposition pressures. In the case of Sn/P, at higher temperatures, a miscibility gap of a tin-rich and a phosphorus-rich melt exists. Since Bi, Hg, and Pb form no binary phosphides at all, they have been used, e.g., for the preparation of crystalline black and red phosphorus. Other examples include the synthesis of CrP_4, MnP_4, and p-SiP_2 without high-pressure techniques from molten Sn and the synthesis of LaP_2, LaP_5, and LaP_7 from molten KCl.

Arc Melting[5]

Especially high-melting metal-rich phosphides can be prepared by arc melting, followed by annealing with additional P in silica tubes up to 1470 K.

High-Pressure Techniques[200]

The main advantage is the possibility to counterbalance the decomposition pressures $p(MP_x)$ on one side with the formation of very-high-pressure modifications on the other. With this technique one obtains several unexpected high-pressure phases, e.g., SnP, GeP, GeP_3, GeP_5, InP_3, and WP_4. However, some of the so-called high-pressure phases, e.g., CrP_4, MnP_4, and p-SiP_2, are preparable by other methods. In addition, P(black) is formed in Pb or Bi fluxes as small single crystals.

2. Alternative Procedures

Thermal Decomposition[56]

The thermal decomposition of higher phosphides under controlled conditions is a very suitable method to prepare pure compounds with medium P/M ratio. In some cases, crystals can be grown, but usually only microcrystalline samples are found. Some compounds were prepared this way (e.g., Sr_3P_5 and SrP_2), which were never obtained in suitable quality by any other procedure.

Chemical Transport Reactions

Numerous metals form gaseous halides that allow for chemical transport reactions to prepare and purify metal phosphides. But only in some cases, e.g., Fe/P or in the case of III/V semiconductors, are there detailed investigations.[276-280]

Preparation in Liquids[1,342,343]

Due to the solubility of alkali metals M in NH_3(l), the phosphides M_3P and the yellow M_3P_7 (in the literature formerly erroneously called M_2P_5) have been prepared in NH_3(l). In the past two decades several very effective procedures have been worked out. These methods mainly yield *solvated phosphides*, which are sometimes amorphous and of high reactivity, especially in solution

TABLE I. Binary Polyphosphides of s, p, and f Elements[a]

compd	color	structure type	structure symbol	P–P bond key 0b	1b	2b	3b	anionic partial structure	ref
Li_3P	black	Na_3As[b]	h P 8	1	0	0	0	(P^{3-})	24, 25
LiP	black	LiAs	m P 16	0	0	1	0	$^1_\infty(P^-)$ helical chain	26
Li_3P_7 (α)	yellow	α-Li_3P_7	o P 80	0	0	3	4	(P_7^{3-}) cage	27
Li_3P_7 (β)	yellow	β-Li_3P_7	o P 80	0	0	3	4	(P_7^{3-}) cage	27
$Li_3P_{8.33}$	red	$Li_3P_{8.33}$	h P *	0	0	9	16	(P_7^{3-}) and (P_{11}^{3-}) cages (2:1)	28
LiP_5	black	LiP_5	o P 24	0	0	1	4	$^3_\infty(P_5^-)$ cond *cyclo*-P_6 and *cyclo*-P_{18}	29
LiP_7	ruby red	LiP_7	t I 128	0	0	1	6	$^1_\infty(P_7^-)$ helical tubes	29
LiP_{15}	dark red	KP_{15}	a P 32	0	0	1	14	$^1_\infty(P_{15}^-)$ tube	30
Na_3P	blue, refl	Na_3As[b]	h P 8	1	0	0	0	(P^{3-})	24, 25
NaP	black	NaP	o P 16	0	0	1	0	$^1_\infty(P^-)$ helical chain	31
Na_3P_7 (α)	yellow	α-Na_3P_7	o p 80	0	0	3	4	(P_7^{3-}) cage	32, 33
Na_3P_7 (β)	yellow	β-Rb_3P_7	c F 40	0	0	3	4	(P_7^{3-}) cage	32, 33
Na_3P_{11} (α)	orange	α-Na_3P_{11}	o P 56	0	0	3	8	(P_{11}^{3-}) cage	34
Na_3P_{11} (β)	red	β-Na_3P_{11}	t * 112	0	0	3	8	(P_{11}^{3-}) cage	32
NaP_7	ruby red	LiP_7	t I 128	0	0	1	6	$^1_\infty(P_7^-)$ helical tubes	29, 30
NaP_{15}	dark red	KP_{15}	a P 32	0	0	1	14	$^1_\infty(P_{15}^-)$ tube	30
K_3P	green, refl	Na_3As[b]	h P 8	1	0	0	0	(P^{3-})	35, 25
KP	black	NaP	o P 16	0	0	1	0	$^1_\infty(P^-)$ helical chain	31
K_4P_6 (α)	black	Rb_4P_6	o F 40	0	0	(4+	2)	(P_6^{4-}) planar *cyclo*-P_6	36, 37
K_4P_6 (β)	black	β-K_4P_6	o F 80	0	0	(4+	2)	(P_6^{4-}) planar *cyclo*-P_6	37
K_3P_7 (α)	yellow	?	?	0	0	3	4	(P_7^{3-}) cage	38
K_3P_7 (β)	orange	β-Rb_3P_7	c F 40	0	0	3	4	(P_7^{3-}) cage	33, 38
K_3P_{11} (α)	red	α-Na_3P_{11}	o P 56	0	0	3	8	(P_{11}^{3-}) cage	33
K_3P_{11} (β)	red	β-Rb_3P_7	c P 28	0	0	3	8	(P_{11}^{3-}) cage	33, 38
$KP_{10.3}$	dark brown	$KP_{10.3}$	t P 1488					complex tubular superstructure	40
KP_{15}	red	KP_{15}	a P 32	0	0	1	14	$^1_\infty(P_{15}^-)$ tube	41
Rb_4P_6	black	Rb_4P_6	o F 40	0	0	(4+	2)	(P_6^{4-}) planar *cyclo*-P_6	36, 42
Rb_3P_7 (α)	yellow	α-Cs_3P_7	t P 40	0	0	3	4	(P_7^{3-}) cage	33, 38
Rb_3P_7 (β)	red	β-Rb_3P_7	c F 40	0	0	3	4	(P_7^{3-}) cage	33, 38
Rb_3P_{11} (α)	orange-brown	α-Na_3P_{11}	o P 80	0	0	3	8	(P_{11}^{3-}) cage	33, 38
Rb_3P_{11} (β)	red	β-Cs_3P_{11}	c F 56	0	0	3	8	(P_{11}^{3-}) cage	33, 38
RbP_7	dark red	CsP_7	o P 32	0	0	1	6	$^1_\infty(P_7^-)$ linear chain of cages	40
$RbP_{10.3}$	dark brown	$KP_{10.3}$	t P 1488					complex tubular superstructure	40
RbP_{11}	red	RbP_{11}	m P 48	0	0	2	20	$^1_\infty(P_7^-)$ and $^1_\infty(P_{15}^-)$ tubes (1:1)	40
RbP_{15}	red	KP_{15}	a P 32	0	0	1	14	$^1_\infty(P_{15}^-)$ tube	40
Cs_4P_6	black, refl	Rb_4P_6	o F 40	0	0	(4+	2)	(P_6^{4-}) planar *cyclo*-P_6	42
Cs_3P_7 (α)	yellow	α-Cs_3P_7	t P 40	0	0	3	4	(P_7^{3-}) cage	38, 43
Cs_3P_7 (β)	orange	β-Rb_3P_7	c F 40	0	0	3	4	(P_7^{3-}) cage	38, 43
$Cs_3P_{8.3}$ (β)	orange	β-Rb_3P_7	c F 40/56					(P_7^{3-}) and $^1_\infty(P_{15}^-)$ tubes (1:1)	38, 43
Cs_3P_{11} (α)	red	?	?	0	0	3	8	(P_{11}^{3-}) cage	33, 38
Cs_3P_{11} (β)	red	β-Rb_3P_7	c F 56	0	0	3	8	(P_{11}^{3-}) cage	33, 38, 44
CsP_7	red-brown	CsP_7	o P 32	0	0	1	6	$^1_\infty(P_7^-)$ linear chain of cages	45
CsP_{11}	red	RbP_{11}	m P 48	0	0	2	20	$^1_\infty(P_7^-)$ and $^1_\infty(P_{15}^-)$ tubes (1:1)	45
CsP_{15}	red	KP_{15}	a P 32	0	0	1	14	$^1_\infty(P_{15}^-)$ tube	106
Be_3P_2	brown	Mn_2O_3	c I 80	1	0	0	0	(P^{3-})	46
Be_3P_2	ocher-brown	Be_3P_2	t I 160	1	0	0	0	(P^{3-})	47
BeP_2	red	BeP_2	t I 12	0	0	2	0	$^1_\infty(P^-)$ chain with shortrange order	48, 49
Mg_3P_2	yellow	Mn_2O_3	c I 80	1	0	0	0	(P^{3-})	46, 50
MgP_4	black, refl	CdP_4	m P 10	0	0	2	2	$^2_\infty(P_4^{2-})$ cond *cyclo*-P_{10}	51–53
Ca_3P_2	red-brown	?	?	2	0	0	0	(P^{3-})	54
CaP	black, refl	Na_2O_2	h P 12	0	2	0	0	(P_2^{4-}) dumbbell	55
Ca_3P_5	red	?	?						56, 58
CaP_3	black	CaP_3	a P 8	0	0	2	1	$^2_\infty(P_3^{2-})$ cond *cyclo*-P_{14} corr	59
Sr_3P_2	black	Th_3P_4, def.	c I 28	2	0	0	0	(P^{3-})	60
SrP	black-purple	Na_2O_2	h P 12	0	2	0	0	(P_2^{4-}) dumbbell	55
Sr_3P_4	black	Sr_3As_4	o F 56	0	2	2	0	(P_4^{6-}) chain	56, 57
SrP_2	met lustre	$BaAs_2$	m P 18	0	2	0	0	$^1_\infty(P_2^{2-})$ cis–trans helical chain	58
SrP_3	black	SrP_3	m C 32	0	0	2	1	$^2_\infty(P_3^{2-})$ cond *cyclo*-P_6 and *cyclo*-P_{22}	61
Sr_3P_{14}	red, transp	Ba_3P_{14}	m P 34	0	0	3	4	(P_7^{3-}) cage	62
Ba_3P_2	gray, refl	Th_3P_4, def.	c I 28	2	0	0	0	(P^{3-})	63
Ba_3P_4	black	Sr_3As_4	o F 56	0	2	2	0	(P_4^{6-}) chain	57
BaP_2	black, refl	$BaAs_2$	m P 18	0	2	0	0	$^1_\infty(P_2^{2-})$ cis–trans helical chain	58
BaP_3	black, refl	BaP_3	m C 16	0	0	2	1	$^1_\infty(P_3^{2-})$ linear chain of *cyclo*-$P_6(1,4)$	64
Ba_3P_{14}	red, transp	Ba_3P_{14}	m P 34	0	0	3	4	(P_7^{3-}) cage	61
BaP_{10}	black, refl	BaP_{10}	o C 44	0	0	1	6	$^2_\infty(P_{10}^{2-})$ linked tubes	65
Sc_3P		Fe_3C	o P 16	1	0	0	0	(P^{3-})	66
Sc_7P_3		Ru_7B_3	h P 20	3	0	0	0	(P^{3-})	66
Sc_3P_2		Cr_3C_2	o P 20	2	0	0	0	(P^{3-})	67
Sc_3P_2		Hf_3P_2	o P 20	2	0	0	0	(P^{3-})	67
ScP	black, refl	NaCl	c F 8	1	0	0	0	(P^{3-})	68
YP	black, refl	NaCl	c F 8	1	0	0	0	(P^{3-})	68
YP_5	black, refl	NdP_5	m P 12	0	0	3	2	$^2_\infty(P_5^{3-})$ cond *cyclo*-P_{12} corr	69
LaP	black	NaCl	c F 8	1	0	0	0	(P^{3-})	70
LaP_2	black, refl	LaP_2	m I 48	0	4	4	0	(P_3^{5-}) and (P_5^{7-}) chains (1:1)	71, 72
LaP_5	black, refl	LaP_5	m P 24	0	0	3	2	$^2_\infty(P_5^{3-})$ cond *cyclo*-P_{12} corr	70, 73

TABLE I (Continued)

compd	color	structure type	structure symbol	P–P bond key 0b	1b	2b	3b	anionic partial structure	ref
LaP_7	black	LaP_7	m P 32	0	0	3	4	$^3_\infty(P_7^{3-})$ cond *cyclo*-P_7 and *cyclo*-P_{20}	74
CeP	black	NaCl	c F 8	1	0	0	0	(P^{3-})	70
CeP_2 (HT)	black	LaP_2	m I 48	0	4	4	0	(P_3^{5-}) and (P_5^{7-}) chains (1:1)	70, 72, 76
CeP_2 (LT)	black	$NdAs_2$	m P 12	0	2	2	0	(P_4^{6-}) chain	75, 76
CeP_5	black	LaP_5	m P 24	0	0	3	2	$^2_\infty(P_5^{3-})$ cond *cyclo*-P_{12} corr	70, 73
CeP_7	black	LaP_7	m P 32	0	0	3	4	$^3_\infty(P_7^{3-})$ cond *cyclo*-P_7 and *cyclo*-P_{20}	77
PrP	black	NaCl	c F 8	1	0	0	0	(P^{3-})	70, 78
PrP_2	black	$NdAs_2$	m P 12	0	2	2	0	(P_4^{6-}) chain	70, 75
PrP_5	black	NdP_5	m P 12	0	0	3	2	$^2_\infty(P_5^{3-})$ cond *cyclo*-P_{12} corr	70, 79
PrP_7	black	LaP_7	m P 32	0	0	3	4	$^3_\infty(P_7^{3-})$ cond *cyclo*-P_7 and *cyclo*-P_{20}	77
NdP	black	NaCl	c F 8	1	0	0	0	(P^{3-})	70, 80
NdP_2	black	$NdAs_2$	m P 12	0	2	2	0	(P_4^{6-}) chain	81
NdP_5	black	NdP_5	m P 12	0	0	3	2	$^2_\infty(P_5^{2-})$ cond *cyclo*-P_{12} corr	73
SmP	black	NaCl	c F 8	1	0	0	0	(P^{3-})	70, 82
SmP_5	black	NdP_5	m P 12	0	0	3	2	$^2_\infty(P_5^{3-})$ cond *cyclo*-P_{12} corr	73, 83, 84
Eu_3P_2	black	Ba_3P_2	c I 28	1	0	0	0	(P^{3-})	85
Eu_4P_3	black	Th_3P_4, dist	c I 28	1	0	0	0	(P^{3-})	86
Eu_5P_4	black	Eu_5As_4	o C 36	2	2	0	0	(P^{3-}) and (P_2^{4-}) dumbbell	86
EuP	black	NaCl	c F 8	1	0	0	0	(P^{3-})	87
Eu_3P_4	black	Sr_3As_4	o F 56	0	2	2	0	(P_4^{6-}) chain	57
EuP_2	gray-black	EuP_2	m P 18	0	0	2	0	$^1_\infty(P^-)$ cis–trans helical chain	88
EuP_3 (α)	gray-black	$EuAs_3$	m C 16	0	0	2	1	$^2_\infty(P_3^{2-})$ cond *cyclo*-P_{14} corr	88, 89
EuP_3 (β)	gray-black	SrP_3	m C 32	0	0	2	1	$^2_\infty(P_3^{2-})$ cond *cyclo*-P_6 and *cyclo*-P_{22} corr	88–90
EuP_7	black	EuP_7	m P 32	0	0	2	5	$^2_\infty(P_7^{2-})$ cond *cyclo*-P_6 and *cyclo*-P_8 corr	91
GdP	black	NaCl	c F 8	1	0	0	0	(P^{3-})	92
GdP_5	black	NdP_5	m P 12	0	0	3	2	$^2_\infty(P_5^{3-})$ cond *cyclo*-P_{12} corr	93
TbP	black	NaCl	c F 8	1	0	0	0	(P^{3-})	92
TbP_5	black	NdP_5	m P 12	0	0	3	2	$^2_\infty(P_5^{3-})$ cond *cyclo*-P_{12} corr	83, 84
DyP	black	NaCl	c F 8	1	0	0	0	(P^{3-})	92
DyP_5	black	NdP_5	m P 12	0	0	3	2	$^2_\infty(P_5^{3-})$ cond *cyclo*-P_{12} corr	83, 84
HoP	black	NaCl	c F 8	1	0	0	0	(P^{3-})	94
HoP_5	black	NaP_5	m P 12	0	0	3	2	$^2_\infty(P_5^{3-})$ cond *cyclo*-P_{12} corr	83, 84
ErP	black	NaCl	c F 8	1	0	0	0	(P^{3-})	94
ErP_5	black	NdP_5	m P 12	0	0	3	2	$^2_\infty(P_5^{3-})$ cond *cyclo*-P_{12} corr	83, 84
TmP	black	NaCl	c F 8	1	0	0	0	(P^{3-})	94
TmP_5	black	NdP_5	m P 12	0	0	3	2	$^2_\infty(P_5^{3-})$ cond *cyclo*-P_{12} corr	83, 84
YbP	black	NaCl	c F 8	1	0	0	0	(P^{3-})	94
YbP_5 (α)	black	NdP_5	m P 12	0	0	3	2	$^2_\infty(P_5^{3-})$ cond *cyclo*-P_{12} corr	83, 84
YbP_5 (β)	black	β-YbP_5	m P 24	0	0	3	2	$^2_\infty(P_5^{3-})$ cond *cyclo*-P_{12} corr	83, 84
LuP	black	NaCl	c F 8	1	0	0	0	(P^{3-})	70
LuP_5	black	NdP_5	m P 12	0	0	3	2	$^2_\infty(P_5^{3-})$ cond *cyclo*-P_{12} corr	83, 84
ThP	black	NaCl	c F 8	1	0	0	0	(P^{3-})	95
Th_3P_4	black	Th_3P_4	c I 28	4	0	0	0	(P^{3-})	96, 102
ThP_2	black	Ca_2Si	o P 12	1	0	1	0	(P^{3-}) and $^1_\infty(P^-)$ chain?	97
Th_2P_{11}	black	Th_2P_{11}	m P 156	0	2	21	10	$^1_\infty(P_{16}^{10-})$ band (cond *cyclo*-P_6, P_8) and *cyclo*-P_8 (chair)	98
ThP_7	black	ThP_7	o P 32	0	0	4	3	$^3_\infty(P_7^{4-})$ cond *cyclo*-P_6 and *cyclo*-P_{12}	99
Pa_3P_4	black	Th_3P_4	c I 28	4	0	0	0	(P^{3-})	100
PaP_2	black	Fe_2As	t P 6	1	0	0	0	(P^{3-})	100
UP	black	NaCl	c F 8	1	0	0	0	(P^{3-})	101
U_3P_4	black	Th_3P_4	c I 28	4	0	0	0	(P^{3-})	102
UP_2	black	UP_2	t I 24	1	0	0	0	(P^{3-})	103
UP_2 (HT)	black	Cu_2Sb	t P 6	1	0	0	0	(P^{3-})	103
PuP		NaCl	c F 8	1	0	0	0	(P^{3-})	163
CmP		NaCl	c F 8	1	0	0	0	(P^{3-})	104
BkP		NaCl	c F 8	1	0	0	0	(P^{3-})	105
Cu_3P (LT)	gray	Cu_3As	h P 24	1	0	0	0	(P^{3-})	107, 25
Cu_3P (HT)	gray	Cu_3P	h P 8	1	0	0	0	(P^{3-})	108
CuP_2	black	CuP_2	m P 12	0	0	2	2	$^2_\infty(P_4^{2-})$ cond *cyclo*-P_{10}	109, 110
Cu_2P_7	black	Cu_2P_7	m C 72	0	0	2	5	$^2_\infty(P_7^{2-})$ tubular frag (P_{12}^{4-}) and (P_{16}^{4-})	110
AgP_2	black	CuP_2	m P 12	0	0	2	2	$^2_\infty(P_4^{2-})$ cond *cyclo*-P_{10}	109, 110
Ag_3P_{11}	black	Ag_3P_{11}	m C 28	0	0	3	8	$^2_\infty(P_{11}^{3-})$ tubular frag (P_{11}^{3-})	111
Au_2P_3	black	Au_2P_3	m C 20	0	0	2	1	$^1_\infty(P_3^{2-})$ chain of *cyclo*-P_6 (1,6)	112
Zn_3P_2	black	Zn_3P_2	t P 40	2	0	0	0	(P^{3-})	113, 118
Zn_7P_{10}	black	Cd_7P_{10}	o F 126	2	0	8	0	(P^{3-}) and $^1_\infty(P^-)$ helical chain	114
ZnP_2	red-orange	ZnP_2	t P 24	0	0	2	0	$^1_\infty(P^-)$ helical chain	115
ZnP_2	black	$ZnAs_2$	m P 24	0	0	2	0	$^1_\infty(P^-)$ semispiral chain	116
ZnP_4	?	ZnP_4	t P 20	0	0	2	2	CdP_4 analogous?	117
Cd_3P_2	black	Zn_3P_2	t P 40	2	0	0	0	(P^{3-})	113
Cd_6P_7	steel gray	?	c * *						118
Cd_7P_{10}	steel gray	Cd_7P_{10}	o F 126	2	0	8	0	(P^{3-}) and $^1_\infty(P^-)$ helical chain	119
CdP_2 (LT)	dark red	CdP_2	o P 12	0	0	2	0	$^1_\infty(P^-)$ helical chain	120
CdP_2 (HT)	red	ZnP_2	t P 24	0	0	2	0	$^1_\infty(P^-)$ helical chain	121
CdP_4	black	CdP_4	m P 10	0	0	2	2	$^2_\infty(P_4^{2-})$ cond *cyclo*-P_{10}	122
B_6P	transp	B_6P	h R 14	1	0	0	0	(P^{3-})	123

TABLE I (Continued)

compd	color	structure type	structure symbol	P–P bond key 0b	1b	2b	3b	anionic partial structure	ref
BP	gray-black	ZnS	c F 8	1	0	0	0	(P^{3-})	124
$B_{12}(P,B)_2$	gray-black	$B_{12}(P,B)_2$	h R 42	1	0	0	0	(P^{3-})	125
AlP	pea green	ZnS	c F 8	1	0	0	0	(P^{3-})	126
GaP	orange-red	ZnS	c F 8	1	0	0	0	(P^{3-})	126
InP (α)	gray	ZnS	c F 8	1	0	0	0	(P^{3-})	126
InP (β)		NaCl	c F 8	1	0	0	0	(P^{3-})	127
InP_3	black, met	SnP_3	h R 24	0	0	1	0	(P_6^{6-}) *cyclo*-P_6 (chair)	128
TlP_5		TlP_5	o P 24	0	0	1	4	$^2_\infty(P_5^-)$ linked tubes	129
SiP	yellow	SiP	o C 48	1	0	0	0	(P^{3-}) and Si_2 dumbbell	130
SiP(hp)		ZnS	c F 8	1	0	0	0	(P^{3-})	131
SiP (I–IV)	high-pressure forms								131
SiP_2 (β)	red	$GeAs_2$	o P 24	2	0	2	0	(P^{3-}) and $^1_\infty(P^-)$ chain	131, 132
SiP_2	gray	p-FeS_2	c P 12	0	2	0	0	(P_2^{4-}) dumbbell	133–135
GeP	black	GaTe	m C 24	1	0	0	0	(P^{3-}) and Ge_2 dumbbell	132
GeP (I–VIII)	high-pressure forms								136
GeP(hp)			t I 4	1	0	0	0	(P^{3-})	137
GeP(hp)		ZnS	c F 8	1	0	0	0	(P^{3-})	136
GeP_2		FeS_2?	c P 12	0	2	0	0	(P_2^{4-}) dumbbell	136
GeP_3(hp)	black	SnP_3	h R 24	0	0	1	0	(P_6^{6-}) *cyclo*-P_6 (chair)	137, 138
GeP_5(hp)	black		h R *						137
Sn_4P_3	met lustre	Bi_4Se_3	h R 7	2	0	0	0	(P^{3-})	139, 140
SnP(hp)		NaCl	c F 8	1	0	0	0	(P^{3-})	141
SnP(hp)		GeAs	t I 4	1	0	0	0	(P^{3-})	141
SnP	dull, met	SnP	h P 16						142
SnP_3	silicon-like	SnP_3	h R 8	0	0	1	0	(P_6^{6-}) *cyclo*-P_6 (chair)	138
Sn_3P_4	gray	?	h * *						139
$AlSiP_3$	black	$AlSiP_3$	o P 20	2	1	0	0	(P^{3-}) and (P_2^{4-}) dumbbell	153
$CeSiP_3$	black	$CeSiP_3$	o P 40	2	0	1	0	(P^{3-}) and $^1_\infty(P^-)$ chain	155
Cu_4SnP_{10}	gray	Cu_4SnP_{10}	c F 60	0	0	6	4	(P_{10}^{6-}) adamantane	154
$Li_4Eu_3P_4$	black	$Li_4Sr_3Sb_4$	o I 22	2	2	0	0	(P^{3-}) and (P_2^{4-}) dumbbell	76
$MPbP_{14}$ (M = Hg, Cd, Zn)	black	$HgPbP_{14}$	o P 64	0	0	4	10	$^1_\infty(P_{14}^{4-})$ tube with M in the frame	15, 18
$MSnP_{14}$ (M = Hg, Cd, Zn)	black	$HgPbP_{14}$	o P 64	0	0	4	10	$^1_\infty(P_{14}^{4-})$ tube with M in the frame	164, 356

[a] Phosphides with isolated P^{3-} anions (monophosphides) have been included for completeness. For the symbols cf. text. [b] See ref 25 for different choice of unit cell.

(section VI). Moderate thermal decomposition of these solvates leads to amorphous or microcrystalline *solvent-free* phosphides.

Reduction of Phosphates[7]

Due to the evolution of gaseous products, the reduction of phosphates can only be performed in open systems. The purity of the phosphides produced by these older methods has not always been examined. Well-known examples are the reduction of $Ca_3(PO_4)_2$ and $Fe_2P_2O_7$ by carbon and hydrogen to form Ca_3P_2 and FeP, respectively. Disadvantages are the necessity of an open system and the fact that only classical phosphides can be prepared. The same holds for the reactions of oxides and chlorides with PH_3.

Replacement[7]

Reactions of metals or metal chlorides with other phosphides by a replacement reaction can be performed in the case of transition-metal phosphides, which show high thermal stability or are stable for dissolving the byproducts ($Ca_3P_2 + 2Ta \rightarrow 2TaP + 3Ca$ and $Ca_3P_2 + 2CrCl_3 \rightarrow 2CrP + 3CaCl_2$). Also in these cases the purity of the phosphides is questionable.

Molecular Beam Methods

MBE is suitable for common semiconductors such as GaP. The deposition of various kinds of P is possible and the preparation of higher polyphosphides like KP_{15} as thin films has been studied recently.[281] Sometimes new compounds were found,[40] which have not been prepared before by the ampule technique (section VII).

Electrolysis

Phosphides like FeP[282] and W_4P[283] were prepared by electrolysis of phosphates. Up to now there is no evidence for the formation of polyphosphides by this procedure.

IV. Structure and Bonding

1. General Relations

According to their structures and physical properties the polyphosphides are valence compounds in a classical sense. All valence electrons are in localized states and, therefore, these compounds are (or should be) insulators or semiconductors. Nevertheless some compounds are semimetals or even metals if conduction bands are formed by sufficient overlap, but their structures are often still in accordance with the picture of localized states. The same is true, e.g., for gray arsenic, which is semimetallic but has (3b)As atoms in accordance with the number of valence electrons. Close relationships between stoichiometry, number of valence electrons, structural principles, and physical properties can be derived by the Mooser–Pearson $8 - n$ rule[284] as an ex-

TABLE II. Representative Polyphosphides of the Transition Metals[a]

compd	type	M	symbol	bond key 0b	1b	2b	3b	polyanionic structure	ref
M_5P_4	Ni_5P_4	Ni	h P 30	4	3	0	1	(P^{3-}) and (P_4^{6-}) pyramidal	175
MP	NiP	Ni	o P 16	0	2	0	0	(P_2^{4-}) dumbbell	176
	MnP	Cr, W, Mn, Ru, Fe, Co	o P 8	0	2	0	0	$^1_\infty(P^{n-})$ chain with half-bonds	177, 178
M_3P_4	Cr_3S_4	Re	m C 14	0	2	0	0	(P_2^{4-}) dumbbell and chains, resp	179
M_2P_3	Tc_2As_3	Tc						(P^{3-}) and (P_2^{4-}) dumbbell	180
M_4P_7	V_4P_7	V, Nb	h P 29	1	*	*	0	(P^{3-}) and ?	181
MP_2	Co_2Si	Ti, Zr, Hf (*Pnma*)	o P 12	1	0	1	0	(P^{3-}) and $^1_\infty(P^-)$ chain	182, 183
	$OsGe_2$	V, Nb, Cr, W ($C2/m$)	m C 12	2	2	0	0	(P^{3-}) and (P_2^{4-}) dumbbell	184–187
	MoP_2	Mo, W ($Cmc2_1$)	o C 12	2	2	0	0	(P^{3-}) and (P_2^{4-}) dumbbell	187
	$NbSb_2$	Ta ($C2$)	m C 12	2	2	0	0	perhaps $OsGe_2$ type?	182, 185
	FeS_2 (m)	Fe, Ru, Os, Ni (*Pnnm*)	o P 6	0	2	0	0	(P_2^{4-}) dumbbell	188, 205, 214
	FeAsS	Co, Rh, Ir ($P2_1/c$)	m P 12	0	2	0	0	(P_2^{4-}) dumbbell	189–191
	NiP_2	Ni, Pd ($C2/c$)	m C 12	0	0	1	0	$^1_\infty(P^-)$ chain	176, 190, 192
	FeS_2 (p)	Ni, Pt ($Pa\bar{3}$)	c P 12	0	2	0	0	(P_2^{4-}) dumbbell	193, 205
M_6P_{13}	Re_6P_{13}	Re	h R 38	3	4	6	0	(P^{3-}) and (P_2^{4-}) dumbbell and (P_4^{6-}) chain and *cyclo*-P_6 (chair)	194
M_2P_5	Nb_2P_5	Nb	o P 28	2	0	2	1	(P^{3-}) and $^2_\infty(P_3^{2-})$ cond *cyclo*-P_8	195
	Re_2P_5	Re	a P 28	1	4	3	2	$2(P^{3-})$ and (P_2^{4-}) dumbbell and (P_4^{6-}) chain and $^1_\infty(P_{12}^{12-})$ branched chain	196
MP_3	ReP_3	Tc, Re	o P 16	0	1	1	1	$^1_\infty(P_3^{3-})$ branched chain	197
	$CoAs_3$	Co, Rh, Ir, Pd, Ni	c I 32	0	0	4	0	(P_4^{4-}) plane *cyclo*-P_4	198, 190
	RuP_3	Ru	a P 16	0	1	1	1	$^1_\infty(P_6^{6-})$ branched chain	199
MP_4	CrP_4	Cr, Mo, V	m C 20	0	0	2	2	$^2_\infty(P_4^{2-})$ cond *cyclo*-P_{10}	200, 189
	ReP_4	Tc, Re	o P 40	0	0	2	2	$^2_\infty(P_4^{2-})$ cond *cyclo*-P_{10}	201, 202
	OsP_4 (β)	Ru, Os	a P 15	0	0	2	2	$^2_\infty(P_4^{2-})$ cond *cyclo*-P_{10}	203
	OsP_4 (α)	Ru, Os, (Cd) (Mg)	m P 10	0	0	2	2	$^2_\infty(P_4^{2-})$ cond *cyclo*-P_{10}	204
	MnP_4 (2)	Mn	a P 10	0	0	2	2	$^2_\infty(P_4^{2-})$ cond *cyclo*-P_{10}	206, 207
	MnP_4 (6)	Mn	a P 30	0	0	2	2	$^2_\infty(P_4^{2-})$ cond *cyclo*-P_{10}	208
	MnP_4 (8)	Mn	m C 80	0	0	2	2	$^2_\infty(P_4^{2-})$ cond *cyclo*-P_{10}	209
	FeP_4 (α)	Fe	m P 30	0	0	2	2	$^2_\infty(P_4^{2-})$ cond *cyclo*-P_{10}	210
	FeP_4 (β)	Fe	o C 20	0	0	2	2	$^2_\infty(P_4^{2-})$ cond *cyclo*-P_{10}	211
	FeP_4 (γ)	Fe	m C 40	0	0	2	2	$^2_\infty(P_4^{2-})$ cond *cyclo*-P_{10}	212
	WP_4	W	t I 20	*	*	*	*	?	213

Ternary Polyphosphides

compd	symbol	bond key 0b	1b	2b	3b	anionic partial structure	ref
$Ln_6Ni_6P_{17}$ (Ln = La, Ce, Pr)	c I 58	1	12	0	4	(P^{3-}) and (P_4^{6-}) pyramidal	150
$Ln_6Pd_6P_{17}$ (Ln = La, Ce)	c I 58	1	12	0	4	(P^{3-}) and (P_4^{6-}) pyramidal	151
$LaCo_8P_5$	o P 28	6	4	0	0	(P^{3-}) and (P_2^{n-}) (n = 2.5; half bond) dumbbell	152
$Co_2Re_5P_{12}$	o P 38	1	5	0	0	(P^{3-}) and (P_2^{4-}) dumbbells	156
MFe_2P_{12} (M = Mo, W)	o P 60	0	0	4	2	$^1_\infty(P_6^{4-})$ chain of *cyclo*-P_6 (1,2) boat	157
MMn_2P_{12} (M = Ti, Nb, Mo, W)	m C 60	0	0	4	2	$^3_\infty(P_{12}^{8-})$ cond *cyclo*-P_{18}	158
$MnCoP_4$	o P 6	0	1	0	0	(P_2^{4-}) dumbbell	159
$LnFe_4P_{12}$[b]	c I 34	0	0	4	0	(P_4^{4-}) planar *cyclo*-P_4	160, 161
$LnRu_4P_{12}$[b]							162
$LnOs_4P_{12}$[b]							
$LnCo_4P_{12}$[b]							
MT_2P_2							
M = La, Ce, Pr; T = Co[c]	t I 10; $ThCr_2Si_2$						168
M = La, Ce; T = Fe[c]							168
M = U, La, Ce; T = Ni[c]							169
M = Eu; T = Ni[c]							170
M = Ln; T = Pd[c]							171
M = Ca, Sr, La; T = Pd, Ni, Co, Ru, Fe[c]							172–174, 357
M = Th, U; T = Co	o P 10; $CaBe_2Ge_2$						168
M = Ba; T = Pd	o P 5; $CeMg_2Si_2$						172

[a] For the symbols, see text. [b] Filled skutterudite ($CoAs_3$) = $\square Co_4As_{12}$. [c] These compounds have a (P_2^{n-}) dumbbell, where n and hence the P–P bond length varies with composition.

tended Grimm–Sommerfeld rule[285] or by the Zintl–Klemm formalism.[19,23] Generally, for a compound A_mB_n with electronegativities $\chi_A < \chi_B$ one can proceed (e_A and e_B are the number of valence electrons of A and B)[8]

$$\sum_m e_A + \sum_n e_B + k = 8n$$
$$\text{with } k = -\sum e_{AA} + \sum e_{BB} - \sum e^* \qquad (1)$$

where the term k accounts for the number of electrons involved in A-to-A bonds and B-to-B bonds as well as the number of electrons e^* that are not involved in any localized bond. Alternatively, one can proceed

$$A \rightarrow A^{p+}; \quad B \rightarrow B^{q-}$$
$$\text{with } |mp| = |nq| \text{ for } A_mB_n \qquad (2)$$

In this electron-transfer process "pseudoelements" $A^* = A^{p+}$ and $B^* = B^{q-}$ are formed that show the structural principles of the corresponding isoelectronic elements with the whole spread of bond types.

Both concepts lead to identical structural predictions that are in accordance with the experiments. However,

TABLE III. Polyphosphide Halides and Chalcogenides[a]

compd	color	structure type	structure symbol	P–P bond key 0b	1b	2b	3b	anionic partial structure	ref
$K_4P_{21}I$	red	$K_4P_{21}I$	o C 104	0	0	3	18	$^2_\infty(P_7^-)$ cond P_7^- norbornane	143
$Rb_4P_{21}I$	dark red	$K_4P_{21}I$	o C 104	0	0	3	18	$^2_\infty(P_7^-)$ cond P_7^- norbornane	40
Ba_2P_7Cl	ruby red	Ba_2P_7Cl	m P 20	0	0	3	4	(P_7^{3-}) cage	144
$Au_7P_{10}I$	black	$Au_7P_{10}I$	n P 18	0	0	6	4	$^2_\infty(P_{10}^{6-})$ cond *cyclo*-P_{12}	112
$Cu_2P_3I_2$	black	$Cu_2P_3I_2$	m P 112	0	0	0	3	$^1_\infty(P_{12}^0)$ chain of cond (P_8^0) and (P_4^0)	145
$Ag_2P_3I_2$	black	$Cu_2P_3I_2$	m P 112	0	0	0	3		145
Cd_2P_3X	red-black	Cd_2P_3X	m C 24	0	0	3	0	$^1_\infty(P^-)$ chain (X = Cl, Br, I)	146, 147
$Cd_4P_2I_3$	orange	$Cd_4P_2I_3$	o P 72	1	1	0	0	(P^{3-}) and (P_2^{4-}) dumbbell	148
$Cd_7P_4Cl_6$	gray	$Cd_7P_4Cl_6$	c P 68	0	2	0	0	(P_2^{4-}) dumbbell	149
GdPS		GdPS	o P 24	0	0	1	0	$^1_\infty(P^-)$ chain and (S^{2-})	165
$Nb_2P_2S_2$; $Nb_2P_2Se_2$		$Nb_2P_2S_2$	o I 12	0	2	0	0	(P_2^{4-}) dumbbell, further weak interactions	167
$Pd_2P_2S_2$; $Pd_2P_2Se_2$		$Pd_2P_2S_2$	o P 24	0	2	0	0	$(S–P–P–S)^{4-}$ anion	166

[a] For the symbols, cf. text.

TABLE IV. Polyphosphide Solvates and Salts

compd	method	anionic partial structure	ref
$MP_5(solv)_x$ (M = Li, Na, K)	^{31}P NMR	(P_5^-) planar *cyclo*-P_5	229, 37
$M_4P_6(solv)_x$ (M = K, Rb, Cs)	^{31}P NMR	(P_6^{4-}) planar *cyclo*-P_6	42
$[(Li)(tmeda)]_3P_7$	X-ray	(P_7^{3-}) nortricyclene	230
$Li_3(en)_5P_7$	X-ray	(P_7^{3-}) nortricyclene	231
$Li_3P_7(solv)_3$, amorphous	^{31}P NMR	(P_7^{3-}) nortricyclene	232, 233
$[Rb(en)]_3P_7$	X-ray	(P_7^{3-}) nortricyclene	234
$Cs_3P_{11}(en)_3$	X-ray	(P_{11}^{3-}) "ufosane"	235
$Na_4P_{14}(en)_6$	X-ray	(P_{14}^{4-}) cond P_7^{2-}	236
$Li_2P_{16}(thf)_8$	^{31}P NMR	(P_{16}^{2-}) from (P_9^-) and (P_7^-)	237–239
$Na_2P_{16}(crown)_3(thf)_2$	^{31}P NMR	(P_{16}^{2-})	240
$[P(ph)_4]_2P_{16}$	X-ray	(P_{16}^{2-})	241
$M_3P_{19}(solv)_x$ (M = Li, Na, K)	^{31}P NMR	(P_{19}^{3-}) from (P_9^-) and $(P_5^-)_2$	242
$M_3P_{21}(solv)_x$ (M = Li, Na)	^{31}P NMR	(P_{21}^{3-}) trimer of (P_7^-)	243
$[Li(crown)_2]_2P_{21}(thf)_2$	X-ray	(P_{21}^{3-}) trimer of (P_7^-)	244
$M_4P_{26}(solv)_x$ (M = Li, Na)	^{31}P NMR, X-ray	(P_{26}^{4-}) from $(P_9^-)_2$ and (P_8^{2-})	245

TABLE V. Binary Phosphorus Sulfides and Selenides[a]

compd	bond key (P) 0b 3+	1b 2+	2b 1+	3b ±0	bond key (S) 1b	2b	corresponding polyanionic structure	ref
$P_{14}S$	0	0	2	12	0	1	$^1_\infty(P_{15}^-)$ tube	215
P_4S_3 (α)	1	0	3	0	0	3	(P_7^{3-}) nortricyclene cage	216, 217
P_4S_3 (β)	1	0	3	0	0	3	(P_7^{3-}) as α, plastically crystalline	218
P_4S_4 (α)	4	0	0	0	0	4	(P_8^{4-}) realgar cage	219
P_4S_4 (β)	2	2	0	0	0	4	(P_8^{4-}) norbornane (S) bridged	220
P_4S_5 (α)	1	2	1	0	1	4	(P_8^{4-}) norbornane (S) bridged and S=	221
P_4S_5 (β)	2	2	0	0	0	5	(P_9^{5-}) noradamantane	222
$P_4S_{6.5}$	2	2	0	0	3	10	(P_9^{5-}) noradamantane and exo S=	223
P_4S_7	2	2	0	0	2	5	(P_9^{5-}) noradamantane and 2 S=	221
P_4S_9	4	0	0	0	3	6	(P_{10}^{6-}) adamantane and 3 S=	224
P_4S_{10}	4	0	0	0	4	6	(P_{10}^{6-}) adamantane and 4 S=	221
$P_{14}Se$	0	0	2	12	0	1	$^1_\infty(P_{15}^-)$ tube	215
P_4Se_3 (α)	1	0	3	0	0	3	(P_7^{3-}) nortricyclene cage	225
P_4Se_3 (β)	1	0	3	0	0	3	(P_7^{3-}) as α, plastically crystalline	226
P_4Se_4 (α, β)[b]								227
P_4Se_5	1	2	1	0	1	4	(P_8^{4-}) norbornane (Se) bridged and Se=	228

[a] Note the changed formal charges in the P–P bond key with respect to the phosphides. [b] Claimed to be isotypic to the sulfides.

one cannot predict all structural details because k is composed of three unknown terms $\sum_i$ in Scheme 1. This corresponds to the fact that the formal ions A^{p+} and B^{q-} do not need to use all remaining electrons to form covalent homonuclear bonds. In spite of such limitations, both schemes are extraordinarily helpful because they allow the combination of (*a*) stoichiometry (= number of valence electrons), (b) structure (= distribution of valence electrons), and (c) physical properties. By knowing the relationship a ↔ b for a given solid, one can rationalize magnetic and electrical properties, i.e. c, and vice versa.

The application of the $8 - n$ rule leads to the same result as one gets by looking at the polyphosphides as derivatives of phosphanes: [P< = CH<], [PH< = CH_2< = S<], [PH_2– = CH_3– = Cl–]. In the following we will refer to the congruent concept of formal ions according to the simple scheme

$$P< \triangleq P^{\pm 0} = (3b) \quad \text{for threefold-linked atoms}$$

$$P< \triangleq P^{1-} = (2b) \quad \text{for twofold-linked atoms}$$

$$P– \triangleq P^{2-} = (1b) \quad \text{for onefold-linked atoms}$$

$$P \triangleq P^{3-} = (0b) \quad \text{for nonlinked atoms}$$

where the linkages exclusively describe the homonuclear P–P bonds.

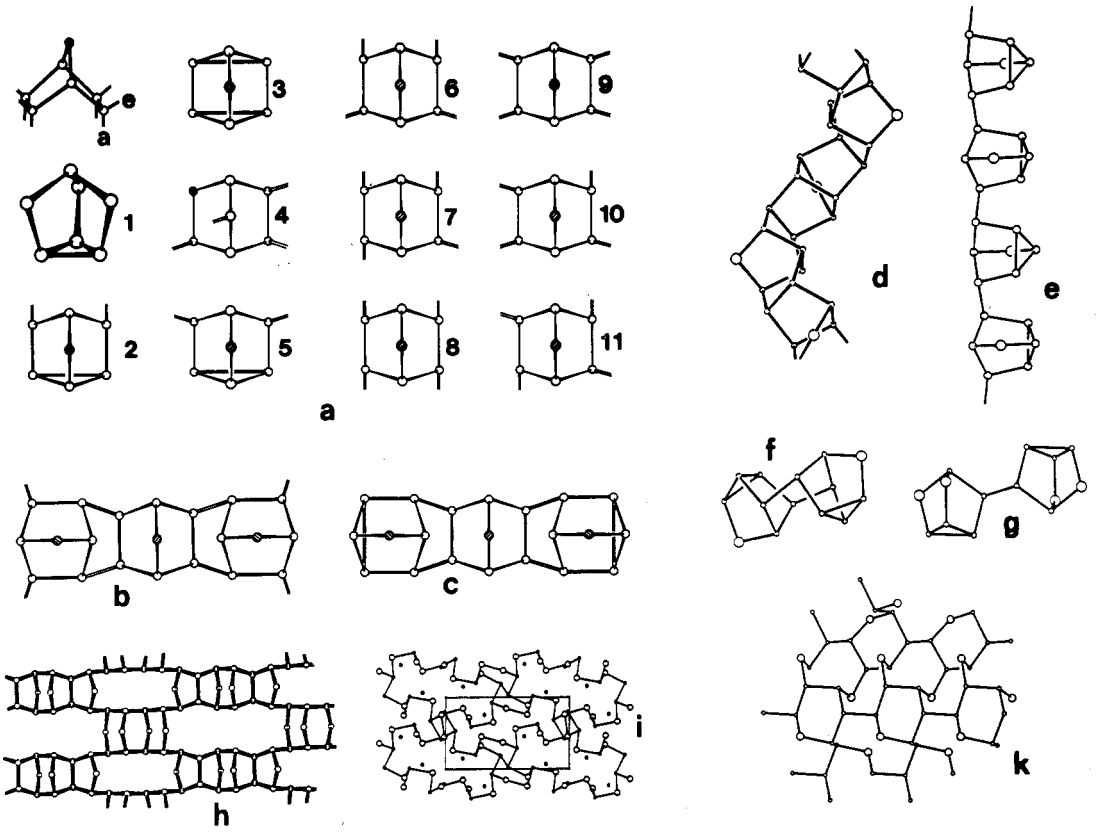

Figure 2. (a) Representatives of the heptaphosphanorbornane (top left) with axial (a) and equatorial (e) connectivities. i denotes intramolecular saturation of bonds. (1) P_7^{3-}; (2) $(a_2i_2)P_7^-$ (end-on type of oligomeric P_{21}^{3-}); (3) $(i_4)P_7^-$ (possible oligomeric structure of P_7H); (4) LiP_7 type; (5) $(e_2i_2)P_7^-$ (CsP_7 type); (6) $(a_2e_2)P_7^-$ (end-on type of polymeric P_{21}^{3-}); (7) $(a_3e)P_7^-$ (unknown); (8) $(a_4)P_7^-$ (unknown); (9) $(e_4)P_7^-$ (central part of oligomeric and polymeric P_{21}^{3-} as well as of P(Hittorf); (10) $(a)_3)P_7^-$ (unknown); (11) $(a_2e_2)P_7^-$ (unknown). (b) $^2_\infty(P_{21}^{3-})$, as built from type $(6)_2$ and type 9. (c) (P_{21}^{3-}), as built from type $(2)_2$ and type 9. (d) Helical unit $^1_\infty(P_7^-)$ as in LiP_7 and NaP_7 built from type 4. (e) CsP_7; $^1_\infty(P_7^-)$ chain of cages of type 5. (f) (P_{14}^{2-}), hypothetical dimer of type 2. (g) P_{14}^{4-}; as found in $Na_4P_{14}(en)_6$. (h) $^2_\infty(P_7^{2-})$ network of tubular fragments in Cu_2P_7. (i) $^3_\infty(P_7^{3-})$ in LaP_7. (k) $^2_\infty(P_7^{2-})$ in EuP_7.

Thus, the remarkable variation of stoichiometry (Tables I–V) can be rationalized by only a few simple structural subunits, which are parts of the structures of both known or hypothetical modifications of phosphorus. Quite obviously, the problem of finding new patterns with the simple graphs ≪<– can be solved by phosphorus with charming variations. Independent of the ratio of the different subunits, there exist many of realizations for the polyanionic structures, which yield the formation of isolated polycycles and of one- (1D), two- (2D), and three-dimensional (3D) polymers. Moreover, one has to take into account the numerous variations with respect to their conformation. There is no doubt that the electron transfer as ruled out in scheme 2 takes place in the compounds that belong to the Zintl phases in a broader sense. In the past years this has been shown quantitatively by complete ab initio calculations in some critical cases. The extent of this transfer is not equivalent to integer charges but as expected with a scale factor.

2. Heptaphosphides with P_7^{n-} Anions

The heptaphosphides of the cations M^{n+} (n = 1–4) give beautiful examples for a general discussion of the structural possibilities (Figure 2) (see Chart I). An isolated P_7^{1-} is not known, but type 3 may be a possible structure for the phosphane P_7H. For P_7^{1-} oligomers and polymers, one derives two structural families that have a 1,4-bridged six-membered ring in common (boat conformation, norbornane system). In the *first* family the $(2b)P^{1-}$ is at the bridging position. In the *second* family the $(2b)P^{1-}$ is a member of the P_6 ring (type 4). The four remaining bonds allow for different structures with regard to equatorial (e) and axial (a) connections, e.g., type 8 and type 9. Types 7, 8, 10, and 11 are further possibilities but structures are not known. Types 2 and 5 are generated by intramolecular saturation of the two axial bonds in type 6 and type 9.

CHART I

unit	linkage	realized in	Figure
P_7^{1-}	oligomeric	$(Li\text{-}crown_2)_3P_{21}(thf)_2$	2c
$[(3b)_6(2b)_1P_7]$	polymeric	CsP_7, type 5	2e
		NaP_7, type 4	2d
		$K_4P_{21}I$, types 6 and 9	2b
P_7^{2-}	oligomeric	$Na_4P_{14}(en)_6$	2g
$[(3b)_5(2b)_2P_7]$	polymeric	EuP_7, Cu_2P_7	2k, 2h
P_7^{3-}	oligomeric	Li_3P_7 to Cs_3P_7	2l
$[(3b)_4(2b)_3P_7]$		Ba_3P_{14}, Ba_2P_7Cl	
	polymeric	LaP_7	2i
P_7^{4-}	oligomeric	?	
$[(3b)_3(2b)_4P_7]$	polymeric	ThP_7	17

The first family generates 1D and 2D polyanionic structures. $K_4P_{21}I$ (=$KI{\cdot}3KP_7$) shows a structure with the fourfold equatorial-bonded type 9 as well as with the partially axial-bonded type 6. The formation of oligomeric P_{14}^{2-} and P_{21}^{3-}, however, can be realized in a simple way by combining type 2 with type 9. The formation of the type 5 cage leads to the CsP_7 structure type and one realizes that only a small further step forms an isolated P_7^{3-} group with the structure of the well-known P_4S_3 molecule. On the other hand, type 4

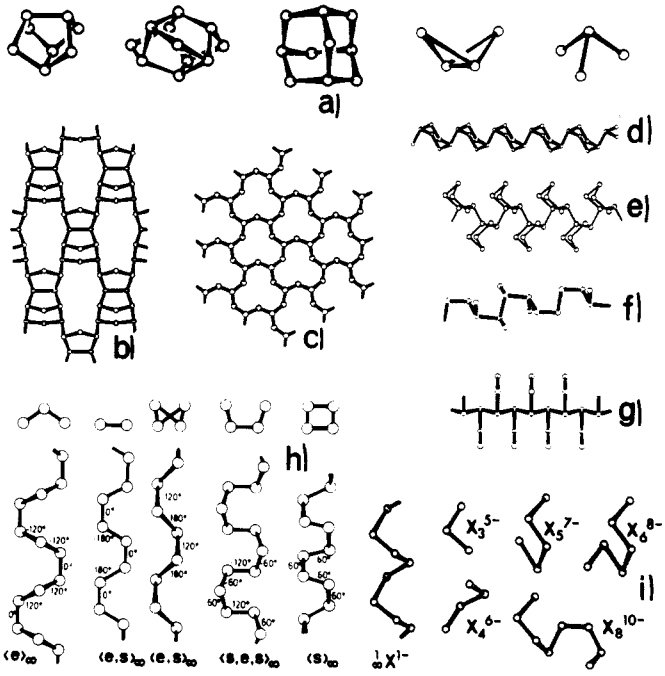

Figure 3. (a) Molecular units (left to right) P_8^{4-}, P_{11}^{3-}, P_{10}^{6-}, P_4^{2-}, and P_6^{6-}. (b) $^2_\infty(P_{11}^{3-})$ of Ag_3P_{11}. (c) $^1_\infty(P_{10}^{6-})$ of $Au_7P_{10}I$. (d) Chain of six-membered rings (chair conformation) as found in BaP_3 and Au_2P_3. (e) Chain of six-membered rings (boat conformation, 1,2 connection) from $MoFe_2P_{12}$. (f) Branched $^1_\infty(P^-)$ from RuP_3. (g) Branched $^1_\infty(P^-)$ from ReP_3. (h) Different conformations of $^1_\infty(X^-)$ torsion angles and their projections along the helix axes. (i) Infinite and finite chains $X_n^{(n+2)-}$ with n = 3, 4, 5, 6, and 8.

units as members of the second family wind in a quite natural way, a helical structure, which is realized in the LiP_7 structure type. LiP_7 and NaP_7 crystallize with this structure of helical tubes, whereas RbP_7 and CsP_7 have a more linear structure with connected P_7 cage units. The cavities for the cations are too small for K^+ in the helical structure but are too large in the other, and indeed the reaction of potassium and phosphorus (P:K ratio = 7:1; without iodine) leads only to mixtures of lower and higher phosphides. But in the presence of iodine, $K_4P_{21}I$ ("Ersatz-KP_7") is formed. From the unit cell volumes, space filling in this compound is evidently better than in both MP_7 structures (section XV). Only rubidium forms both compounds with nearly the same space filling.

A monomeric P_7^{2-} is not possible (section XVII), but the dimeric P_{14}^{4-} is known from the solvated $Na_4P_{14}(en)_6$. EuP_7 is a Eu(II) compound with a polymeric P_7^{2-} structure of two-dimensional puckered layers resulting from a network of six-membered rings (chair conformation; axial and equatorial linkage). For a description of P_7^{2-} in Cu_2P_7, see section IV.6.

The isolated quasi-molecular P_7^{3-} cage is the essential building unit of the bright yellow alkali-metal phosphides M_3P_7 (formerly called erroneously M_2P_5) and of the red alkaline-earth phosphides Sr_3P_{14} and Ba_3P_{14} as well as of the chloride phosphide Ba_2P_7Cl. These compounds are extremely reactive (section XIII), and the compounds M_3P_7 are unique in their behavior; e.g., they transform to plastically crystalline modifications and they are volatile in vacuo.

The heptaphosphides of the rare-earth metals La, Ce, and Pr behave quite differently: the structure contains a polymeric polyanionic network $^3_\infty(P_7^{3-})$ with seven-membered and large twenty-membered rings, which, nevertheless, can be related in a simple way to the P_7^{3-} cage.

ThP_7 is the only yet known compound with a P_7^{4-} substructure. The 3D network is formed by a condensed system of six-membered and twelve-membered rings yielding characteristic crown-shaped cavities occupied by Th atoms (Figure 17).

3. Ufosane P_{11}^{3-}, Adamantane P_{10}^{6-}, *cyclo*-P_6^{4-}, *cyclo*-P_6^{6-}, and *cyclo*-P_4^{4-}

No simple compound is known with the adamantane-like P_{10}^{6-} cage. This is remarkable, because in that region of stoichiometry some compounds exist. Obviously, the units P_7^{3-} and P_6^{4-} are more stable, and therefore, the P_{10}^{6-} cage is observed only in the ternary phase Cu_4SnP_{10} with Cu(I) and Sn(II). A polymeric tubular 2D isomer was found in $Au_7P_{10}I$ (Figure 3).

Just as the cages P_7^{3-} and P_{10}^{6-} are derivatives of the tetrahedral P_4 molecule, the P_{11}^{3-} cage—characteristic for the M_3P_{11} alkali-metal phosphides—is a derivative of the not yet known phosphacubane. This magnificently shaped chiral group is a system of six five-membered rings with D_3 symmetry. Both enantiomers are present in the crystal. The M_3P_{11} phases also transform into plastically crystalline modifications. On the other hand, the Ag_3P_{11} structure is built of $^2_\infty(P_{11}^{3-})$ tubular polymers (Figure 3).

The compounds M_4P_6 of the alkali metals K, Rb, and Cs were found to have a unique structure with planar and isometric P_6 rings. The structure is a defect variant of the AlB_2 type (section XVI), and it is clearly shown that the unusually short P–P bond distance of about 215 pm is not affected by the metal substructure. Indeed, these compounds were the first examples for an unsaturated P–P bond system, although it was not possible to decide between a disordered double bond or a quasi-aromatic 2π system (Pauling bond order (PBO) = 1.167 from the P–P distance). It should be pointed out that the corresponding arsenides also exist. Polymers of P_6^{4-} were found in BaP_3, Au_2P_3, and the $MoFe_2P_{12}$ phases as well.

cyclo-P_6^{6-} has the usual chair conformation and is observed as part of the Th_2P_{11} structure. The six-membered rings are inserted in a complicated 2D phosphorus substructure and act as doubly tridentate ligands for Th. *cyclo*-P_6^{6-} is also part of the arsenic-like structures of SnP_3, GeP_3, and InP_3. The skutterudite structure type ($CoAs_3$ and derivatives) is formed by some transition-metal triphosphides (M^{3+}) and is characterized by planar *cyclo*-P_4^{4-}.

4. Polyanionic Chains

In principle, all catenations of the type $(2b)X_n(1b)Y_2$ ($0 \leq n \leq \infty$; X,Y, any chain link) belong to the large family of chain structures (Figure 3d–i). In this section only compounds with single atoms or with branches at X will be discussed, whereas the others are described at the appropriate places, e.g., finite or infinite chains of cages (CsP_7, $Na_4P_{14}(en)_6$) or rings (BaP_3, Au_2P_3, $MoFe_2P_{12}$).

The 1D polyanion $^1_\infty(P^-)$ is characteristic for the monophosphides of the alkali metals and the diphosphides of divalent metals but is also present in SiP_2 ($GeAs_2$ type), $CeSiP_3$, and GdPS as part of the phos-

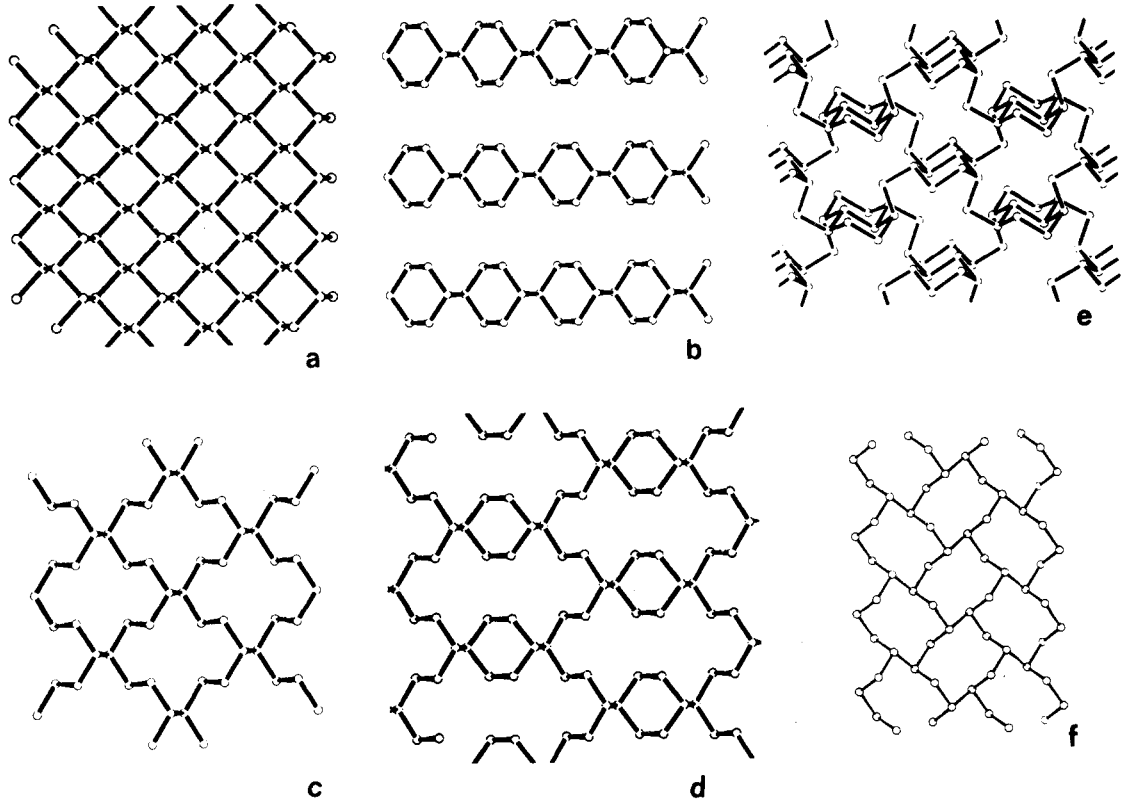

Figure 4. Black phosphorus (a) and its derivatives BaP_3 (b), CaP_3 and α-EuP_3 (c), and SrP_3 and β-EuP_3 (d). The $^3_\infty(P_5^-)$ network of LiP_5 (e) and the condensed P_{10} rings of MgP_4 (f).

phide substructure (Tables I–V). There is a series of structures that provides impressive examples of configurational and conformational variability, which obviously is forced by the external conditions, such as size and coordination of the cations. Figure 3h demonstrates how the sequence of torsional angles labels the chains, including fourfold helices as well as chains with changing rotational direction. The cation coordination may even change the configuration of a $(P^-)_\infty$ polyanion. This is observed, e.g., in the RuP_3 structure, where a branched isomer $^1_\infty(P_3^{3-}) = {}^1_\infty[(3b)P^0(2b)P^-(1b)P^{2-}]$ is present, that is with three different states of charge according to an internal bond disproportionation. ReP_3 and Re_2P_5 behave similarly.

With increasing charge transfer a stepwise dismantling of the 1D infinite chains takes place, yielding finite $P_n^{(n+2)-}$ chains ($2 \le n \le 8$; including As and Sb for comparison). Tables I–IV show that these polyanions are present in compounds of M^{2+} and M^{3+}. Two particularities should be mentioned here: (i) the coexistence of P_4^{6-} and P_8^{10-} in some structures and P_3^{5-} and P_5^{7-} in others; and (ii) the existence of the pyramidal isomer P_4^{6-} in Ni_5P_4 and in $La_6Ni_6P_{17}$.

5. 2D and 3D Nets

Structures with corrugated 2D and 3D polyanionic nets occur if the mean charge of P^{q-} is in the range $0.20 \le q \le 0.73$. The nets are formed by condensed and connected P_n rings of different sizes and conformations (n = 5, 6, 7, 8, 10, 12, 14, 18, 20, 22; Figure 4). Derivatives of black phosphorus are the triphosphides MP_3 of divalent Ca, Sr, Ba, and Eu. The structures are impressive examples of the disintegration of 2D networks by removing atoms in different ways. In all (P_3^{2-}) networks $^1/_4$ of the atoms are removed and necessarily $^2/_3$ of the remaining atoms are $(2b)P^-$. By removing only neighboring atoms the 1D BaP_3 structure is formed as a special case, containing infinite connected six-membered rings with chair conformation and axial linkage. This polyanionic structure is comparable with that of Au_2P_3 and can be regarded as the polymeric analogue of the planar hexagonal *cyclo*-P_6^{4-} discussed in section IV.3. In SrP_3 half of the P_6 rings remain complete but in CaP_3 all of them are opened and yield P_{14} rings. It is remarkable that α-EuP_3 follows CaP_3 and not SrP_3. The $^3_\infty(P_5^-)$ net of LiP_5 is, on the other hand, related to the pattern of black phosphorus as well as that of gray arsenic. One-dimensional bands of condensed six-membered rings are connected by two-fold-linked $(2b)P^-$, with these atoms occupying axial as well as equatorial positions (Figure 4e).

The pentaphosphides of the trivalent rare-earth metals form three very similar structures, with a mainly identical $^2_\infty(P_5^{3-})$ network, which can be derived from a structure similar to that of gray arsenic but with the six-membered rings in boat conformation (Figure 12). The charge transfer disintegrates this hypothetical structure by removing $^1/_6$ of the atoms and, therefore, yields a 2D net of condensed 12-membered rings. In that case $^3/_5$ of the remaining atoms are $(2b)P^-$. Especially interesting is the step-by-step adaptation of the 2D polyanionic net to the decreasing size of the Ln^{3+} cations, which takes place mainly by changing the dihedral P–P angles (section X).

The unique 2D substructure P_{11}^{8-} formed by Th_2P_{11} is more precisely described as $(P_{16}^{10-} + P_6^{6-})$. Puckered P layers consist of $^1_\infty(P_{16})$ bands with isolated P_6 rings inserted. The P_{16} bands are formed by condensed skew-boat P_6 rings and endo P_8 rings. The inserted P_6 chairs are partially opened and give rise therefore to a periodic structural modulation (section X). For the

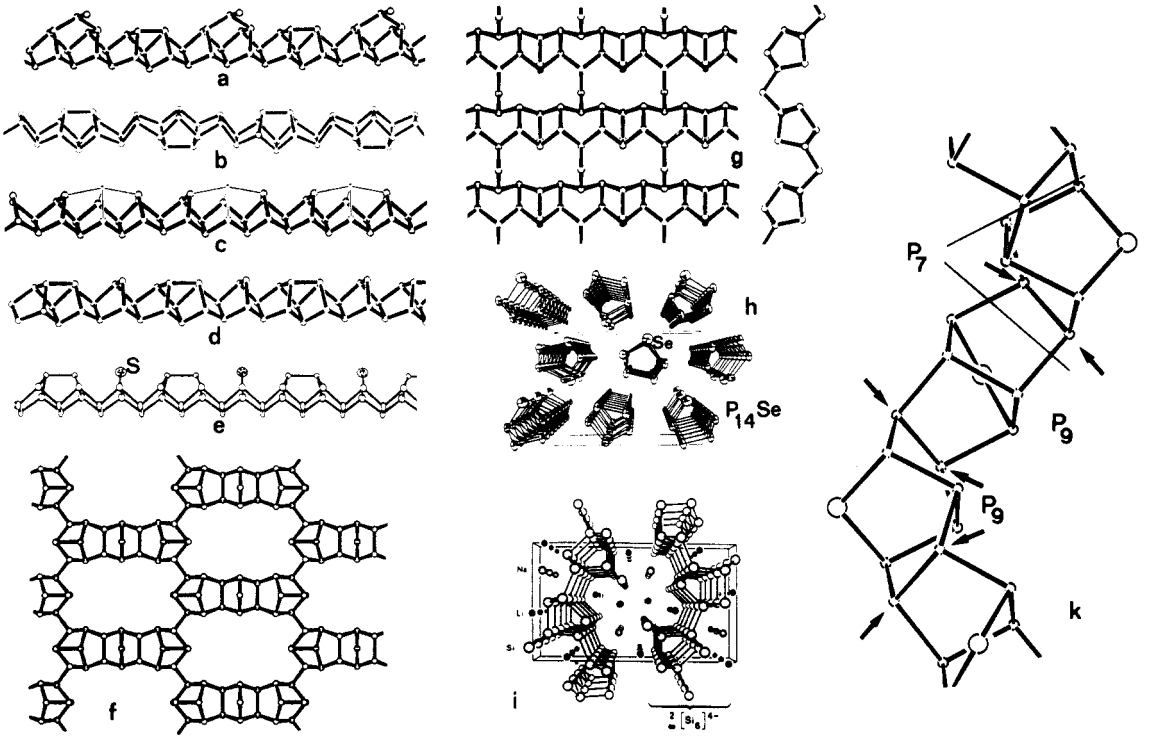

Figure 5. (a) Tubular unit in P(Hittorf); (b) $^1_\infty(P_{12}^{\pm 0})$ as built up from $P_8^{\pm 0}$ and $P_4^{\pm 0}$ in the structure of $Cu_2P_3I_2$; (c) framework $^1_\infty(P_{14}M^{II})$ as in the structure of the $HgPbP_{14}$ type (M^{II} indicated by small spheres); (d) $^1_\infty(P_{15}^-)$ from MP_{15}; (e) $^1_\infty(P_{14}S)$ (isoelectronic with P_{15}^-); (f) $^2_\infty(P_{21}^{3-})$ framework from $K_4P_{21}I$; (g) arrangement of linked pentagonal tubes as found in BaP_{10} and TlP_5 (seen perpendicular and parallel to the puckered layer); (h) perspective view of $P_{14}Se$ tube arrangement; (i) $^2_\infty(Si_6^{4-})$ as a linked tube arrangement of pentagonal tubes; (k) alternative descriptions of poly$(P_7^-)_n$ (thin lines indicate P_7); the common atoms of condensed P_9 units (symmetry 2-C_2) are indicated by arrows).

networks $^2_\infty(P_7^{2-})$, $^3_\infty(P_7^{3-})$, and $^3_\infty(P_7^{4-})$, see section IV.2. As noted in section IV.3, the $^2_\infty(P_{10}^{6-})$ net of $Au_7P_{10}I$ is a polymeric isomer of the adamantane cage. This net contains P_{12} rings, whereas P_{18} rings are present in the $^2_\infty(P_{12}^{8-})$ net of $TiMn_2P_{12}$. The tetraphosphides of divalent M^{2+} (Mg, Cd, transition metals) and the diphosphides of monovalent Cu^+ and Ag^+ form $^2_\infty(P_4^{2-})$ nets. They have condensed P_{10} rings in common, but with a rich variation in their linkages (Figure 4).[11,12]

6. Tubular Structures

As pointed out, rolling up tubes is the special contribution of phosphorus to curved 2D surface structures (Figure 5). The tubular character of the Hittorf phosphorus structure is preserved in the polyanionic linkage of the compounds with the smallest $(P^-):(P^0)$ ratio. The $Cu_2P_3I_2$ structure is unique, because this ratio is zero; i.e., this structure is formed by insertion of elemental phosphorus in CuI! The tubular $^1_\infty(P_{12}^0)$ substructure consists of connected P_8 cages of realgar type and planar P_4 rings. Needle-shaped crystals are typical for the alkali-metal compounds MP_{15}, MP_{11}, and $MP_{10.3}$ (Table I). The fivefold $^1_\infty(P_{15}^-)$ tubes represent the polymerization of alternating P_7^{1-} and $P_8^{\pm 0}$ units, the former a norbornane derivative and the latter comparable with the As_4S_4 molecule (Figure 3a). In principle, the sequence of P_7^- and P_8 may be variable, but now the 1:1 structure seems to be the optimized modulation in crystalline compounds. In $KP_{10.3}$ and $RbP_{10.3}$ units like P_{35}^- were identified in a preliminary study, although the 20-year analysis of that extremely complicated nonintegral twofold superstructure has not proved this unambiguously. On the other hand, the structures of the very closely neighbored RbP_{11} and CsP_{11} are characterized by $^1_\infty(P_{15}^-)$ tubes and $^1_\infty(P_7^-)$ chains of type 5 (Figure 2). When looking for general structural relations that may be responsible for the stability of crystalline phases, one has to keep in mind that the repetition lengths of P_{15}^- and P_7^- chains correspond as $\tau(P_{15}^-) = 2\tau(P_7^-)$. Therefore, a whole series of compounds with twin-slab structures may exist in a very narrow compositional range, differing slightly in energy but, of course, having very different kinetics. Linear fivefold tubes are also characteristic of the ternary $HgPbP_{14}$ phases and of the chalcogenides $P_{14}S$ and $P_{14}Se$, respectively. Lead and sulfur act as heteroatoms in the frame (section VIII). The above-mentioned alternation of P_7^- and $P_8^{\pm 0}$ subunits is a necessary condition to form strain-reduced tubular structures. Thus, no $^1_\infty(P_5^-)$ structures exist in crystalline compounds. LiP_5 has solved the problem by forming a strain-free 3D structure with P_6 chairs (Figure 4e) (section IV.5). Another possibility is demonstrated with TlP_5 and BaP_{10}, where the curvature of $^1_\infty(P_5^-)$ tubes is compensated by the formation of an upside-down polymerization of those tubes and results in a corrugated complex 2D structure of alternating parallel and antiparallel fivefold tubes that are partially opened at the roofs.

Winding up those tubes to spirals results in the structures of LiP_7 and NaP_7, as shown in section IV.2. This unit is especially interesting with respect to its dimensionality. It represents, on one hand, a more complicated 1D chain, where the chain links are connected via two bonds in both directions, typical for the tubelike chains under discussion here. On the other hand, by looking at the tubes as rolled-up surfaces, the phosphorus substructure of LiP_7 is a wringed 2D

structure that results in different curvature and strain in the central and peripheral regions (cf. section XI). The structures of $K_4P_{21}I$, Ag_3P_{11}, and Cu_2P_7 (with polymers of P_7^-, P_{11}^{3-}, and P_7^{2-}) are characterized by 2D arrangements of connected short tubelike parts, whose connections result in larger P_n rings, appropriate as cavities for the other atoms.

There is one very impressive detail in all tubular chains and in structures with shorter or longer parts of these, namely, the wavelike development along the chain direction. This also occurs in suitable molecules. The reason is the difference in strain of units like P_8 (like As_4S_4), P_7 (norbornane), and P_9, caused by positive and negative curvature with respect to the roofs of the tubes. It should be pointed out that the value of curvature can be pictured with the help of a simple model kit, which works very precisely as a *s*tructure *m*odel *a*nalog computer (SMAC), and allows for bending bonds while keeping local bond angles unchanged.[348]

7. Alternative Descriptions

The description of polymeric structures in terms of selected subunits is arbitrary to some extent. We have chosen subunits that are known as isolated clusters. In some cases it is of value to look for alternative ways of fractionation. A good example is the helical $^1_\infty(P_7^-)$ chain of LiP_7, which indeed can be fractionated into overlapping sequences of *polymerized* P_7^- units (Figure 2d). On the other hand, one may discuss this structure in terms of *condensed* $P_9^- = [P_{2/2}P_5^-P_{2/2}]$ units in order to demonstrate the twofold symmetry elements perpendicular to the helical axis (Figure 5k). Another example is the P_{16}^{2-} unit, either a *polymer* of $2P_7 + P_2$ and alternatively of $P_9 + P_7$ or a *condensate* of two P_9 units (Figure 9). It is very important to be free in this respect because only in this way can one relate the different structures with their synthesis and reactions. Similar arguments are true in the discussion of polycyclic units. For systematics we have chosen a six-membered P_6 ring as the primary unit and the five-membered rings result from further connections. For a deeper understanding of the obvious preference for five-membered rings in phosphorus structures, one perhaps should change this argument. But, it is true that tubular and some polycyclic subunits of these are the only ones containing P_5 (and P_4 and P_3) rings.

8. Solid-State Isomerism

Structural phase transitions in solids change the coordination of atoms in a broad sense (cf. graphite and diamond, P modifications). Usually such modifications are not named isomers, but may belong to them, taking the definition of isomers not too strictly (e.g., pentane and neopentane). This also holds for structures of different compounds, if one looks at selected partial structures. In solid-state structures of cluster anions—and the polyphosphides in a way belong to that group—one observes all limiting cases of formal charge distribution within different isomeric polyanionic networks. Some examples were given in the above section, e.g.

$$CoP_3 \mid [(2b)P^-]_3 \triangleq {}^1_\infty(P^-)$$
$$= {}^1_\infty\{[(3b)P^0][(2b)P^-][(1b)P^{2-}]\} \mid RuP_3$$

$$Sr_3P_4 \mid (P_4^{6-}) = \{[(3b)P^0][(1b)P^{2-}]_3\} \mid Ni_5P_4$$

Whereas in these examples both "isomers" are homogeneous with respect to their partial structures, the following are characterized by heterogeneous partial structures. Such heterogeneous mixtures, locked in a "flask" or "crystal", would hardly be named isomers. Examples are

$$CeSiP_3 \mid 2(0b)P^{3-} + {}^1_\infty(P^-) = (0b)P^{3-} + (P_2^{4-}) \mid AlSiP_3$$

$$\alpha\text{-}CeP_2 \mid 2P_4^{6-} = P_3^{5-} + P_5^{7-} \mid \beta\text{-}CeP_2$$

This isomerism is especially important in the case of crystalline modifications of the same compound, because in the course of phase transitions, rearrangements may occur similar to polycomponent reactions.

9. Further Relationships

Fivefold tubes occur very often among partial structures of polyphosphides. Other elements also make use of these structural principles. The red ZnP_2 belongs to this group. The $^1_\infty(P^-)$ polyanionic helices are interconnected by the Zn cations to a 3D structure that can be characterized by heterosubstituted fivefold tubes. Another example is the $GeAs_2$ structure, which is also adopted by the red form of SiP_2. Interesting variants are the 2D partial structures Si_6^{4-} in Li_3NaSi_6,[286] the very similar partial structure $Si_3As_3^-$ in KSi_3As_3,[287] and also the structure of *allo*-Ge[288] and its precursor $Li_{12}Ge_7$.[289]

V. Bond Distances, Bond Angles, and Electron Density

1. P–P Single Bond

The P–P single-bond distance now may be best derived from the three crystalline and well-characterized phosphorus modifications, namely, the triclinic β-P(white),[290] the monoclinic P(violet, Hittorf),[291] and the orthorhombic P(black).[292] Including the second-order distances in the case of P(black), the *P*auling *b*ond *o*rder[293] algorithm with $\sum PBO = 3$ results in d_1(white) = 220.9 pm, d_1(violet) = 221.5 pm, and d_1(black) = 222.8 pm, respectively. This sequence reflects the decreasing strain in the three structures [P_4 with four *cyclo*-P_3; tubular condensed *cyclo*-P_5 and *cyclo*-P_6 (boat); corrugated layer of *cyclo*-P_6 (chair)]. The shortening in the strained units corresponds quite well with the results in small carbon rings, etc. We think, therefore, that the value of the nearly strain-free P(black) structure is the best approximation for the single-bond distance $d_1(P^{\pm 0})$ = 222.8 pm and the respective covalent radius $r(P^{\pm 0})$ = 111.4 pm.

2. Polyphosphide P–P Bonds

Figure 6 illustrates the range of P–P bond lengths according to the most important structural functions. With the *dumbbells* P_2^{4-} an overall mean value of $\bar{d}$(P–P) ~ 223 (6) pm is observed, showing significant variations with structure type. With strong electropositive cations $\bar{d}$ = 229 (3) pm is considerably larger than $\bar{d}$ = 221 (2) pm with neutral molecules. Transition-metal diphosphides of M(IV) show a value $\bar{d}$ ~ 223 (6) pm,

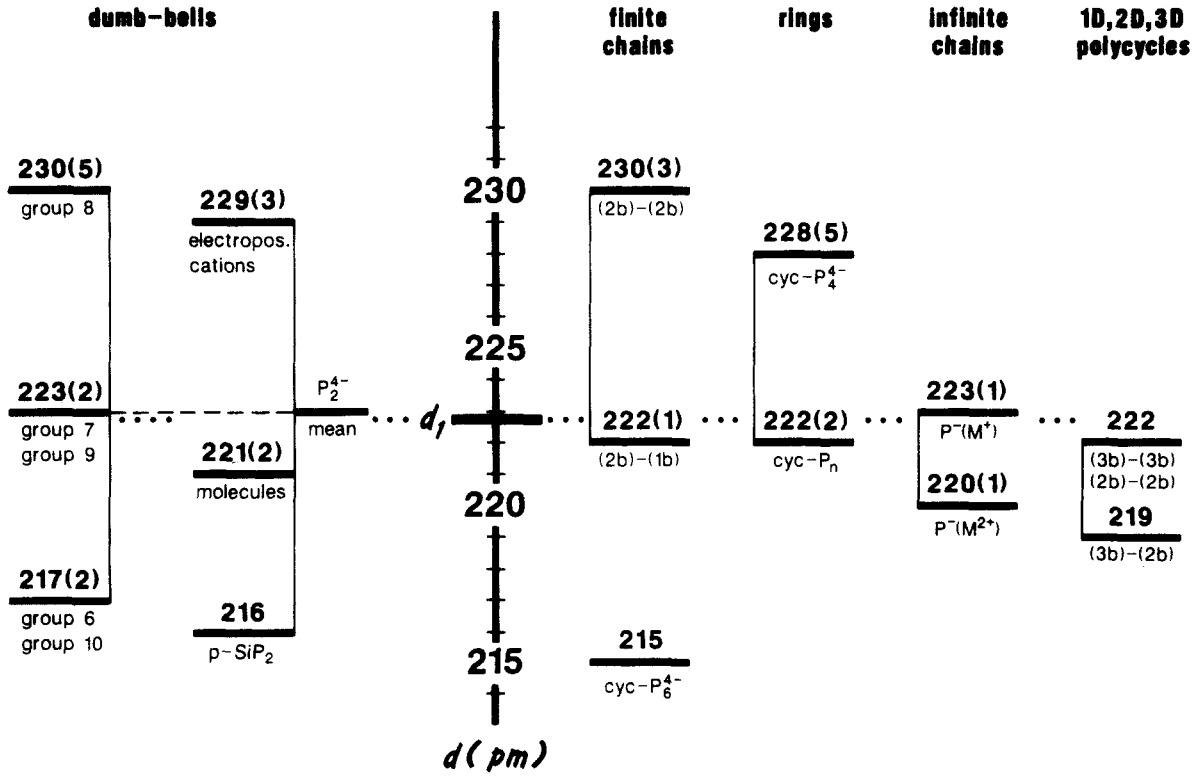

Figure 6. Bond lengths d(P–P) in polyphosphides (cf. text) (d_1(P–P), level dotted).

but the bond lengths are obviously tunable by the valence electron concentration (VEC); i.e., $\bar{d}$(group 6) = 217 (2) pm, $\bar{d}$(group 7) = 223 (2) pm, $\bar{d}$(group 8) = 230 (5) pm, $\bar{d}$(group 9) = 223 (2) pm, and $\bar{d}$(group 10) = 217 (4) pm ≙ d(SiP_2) = 216 pm. These relations correspond quite well to the stronger tendency for metal oxidation by charge transfer in group 8 and to the stronger tendency for metal reduction in the other groups (accompanied by M_2 pairing in groups 6, 7, and 9). The phosphide halides of Cd are of some interest, because one group shows $\bar{d}$ = 231 (4) pm corresponding to the electropositive M^{2+}, but the other group (219 pm) indicates metal reduction [tendency for Cd(I)?]. The *cyclo*-P_n^{n-} and the corresponding neutral molecules are characterized by $\bar{d}$ = 222 (2) pm. The bond lengths in the transition-metal skutterudites (e.g., CoP_3) are much larger with $\bar{d}$ = 228 (5) pm in the P_4^{4-} rings, possibly also generated by redox charge transfer. In the *helical* $^1_\infty(P^-)$ units $\bar{d}$ = 221 (2) pm, but with significant alterations by the cation charge: $\bar{d}(M^+)$ = 223 (1) pm and $\bar{d}(M^{2+})$ = 220 (1) pm. The range is that of the *cyclo*-P_n^{n-}. The structures of *finite chains* $P_n^{(n+2)-}$ demonstrate unambiguously the differences between central and terminal bonds: (2b)–(2b) = 230 (3) pm, but (2b)–(1b) = 222 (1) pm. Obviously, the shortening by polarity differences in the latter exceeds the lengthening by larger mean charges. In the *polycyclic 1D, 2D, and 3D* structures the bond lengths are strongly influenced by the P/M ratio and different strain in the different arrangements; e.g., the (2b)–(2b) distances are most affected by the ring sizes. Furthermore, there are differences between main-group compounds and transition-metal compounds. Therefore, the individual values cover large ranges, 230 ≥ (3b)–(3b) ≥ 217 pm, 224 ≥ (3b)–(2b) ≥ 214 pm, and 226 ≥ (2b)–(2b) ≥ 219 pm, but, in general, d(3b–3b) = d(2b–2b) > d(3b–2b), with mean values of about 222, 222, and 219 pm, respectively. Again the shortening of (3b)–(2b) distances reflects the bond polarity. Unfortunately, the mean values of (3b)–(3b) and (2b)–(2b) hide some important details. In flexible structures like the $^2_\infty(P_5^{3-})$ network of the rare-earth pentaphosphides, (3b)–(3b) = 219 pm is shorter than (2b)–(2b) = 221 pm, as expected. But in other structures, e.g., in the ladder-like spines of the tubular type, the internal strain in the (3b)–(3b) bond regions results in remarkable stretching of those bonds.

Temperature- and pressure-dependent structure determinations reveal very small changes of the P-to-P bonds, which is demonstrated with p-SiP_2.[294] Between 60 and 293 K, e.g., d(P–P) increases from 215.6 to 216.2 pm. The change in d(Si–P), on the other hand, is larger (238.6 to 239.8 pm), reflecting the different bond order of these two bonds.

3. Bond Angles P–P–P

Bond angles within the polyphosphide skeletons are not easy to systematize, as they cover a broad range of values from 60° up to 120°. The mean values found in P(black) and P(violet) are 100.2° and 101.2°, respectively, and correspond with those found for sufficiently determined crystal structures of polyphosphides. It should be pointed out that in unstrained parts of polyphosphide networks, the bond angles cover the narrow range 98°–104°. Large deviations from the mean values obviously exist with *cyclo*-P_3 and *cyclo*-P_4 as well as in transition-metal phosphides, which are forced by the metal coordination. The bond angles approach the upper limit with $^1_\infty(P^-)$ structures, which indicates opposite bond bending than in strained rings. In polycyclic cages in which small and large rings are condensed, special problems occur, because, e.g., the endocyclic 60° values of P_3 are compensated by unreasonably large exocyclic angles.

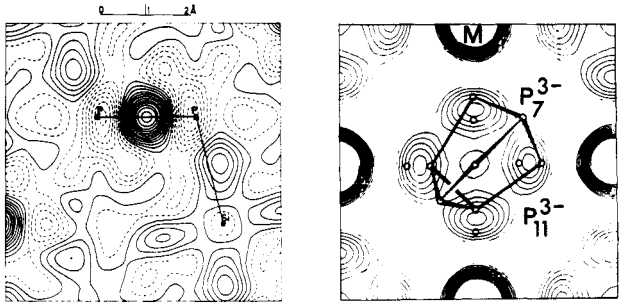

Figure 7. (Left) Deformation densities ρ_{X-N} of SiP_2 in the (110) plane containing the P–P dumbbell and the bend bond Si–P. The contour interval is 0.5 e/Å^3; continuous and dashed curves indicate positive and negative electron densities, respectively. (Right) Typical electron densities in the plastically crystalline phases of M_3P_7 and M_3P_{11}. One of the possible orientations of a P_7^{3-} anion is superimposed.

4. M–P Bonds

In general, all P atoms are involved in M–P interactions according to the number of their lone pairs. Therefore, the M–P_n arrangements can be regarded as complexes (section XIV). The metal coordination follows the usual expectations. The transition metals try to reach octahedral coordination (only few exceptions), but the cations of the electropositive main-group elements exhibit a rich variety. In other words, the coordination polyhedra are determined by radius ratios more than by topological preferences. The anionic (1b)P^{2-} and (2b)P^- as well as the neutral (3b)P^0 species complete their coordination to a quasi-tetrahedral one, even if main-group cations are involved. Only few exceptions are known, e.g., Li_3P_7. With covalent M–P bonds, the number $(m + n)$ of available lone pairs of a polyanion P_m^{n-} is strongly related to the metal coordination number; namely, CN(M) $\leq (m + n)$. If CN(M) $> (m + n)$ ion–ion and ion–dipole interactions dominate. The relation d[M$^-$(2b)P] > d[M$^-$(3b)P] is true in most cases. By analyzing the distances using the above-cited PBO algorithm, one discovers a remarkable discrepancy: for the P atoms one obtains $\sum$PBO(P) = 3 and 4 including all P–P and P–M bonds, but the correct valency of the electropositive metals is reached only by neglecting the contacts P–M to the (3b)P^0, i.e., if only the M–P^{n-} contacts are taken into account.

5. Electron Density

Determinations of electron densities have been carried out only for a few P-containing compounds. Naturally, the most interesting results would be provided by the electron density of the strained P_4 molecule. Even in the triclinic low-temperature modification of white phosphorus (β-P(white)),[290] however, the thermal motions are still so large that no detailed conclusions can be made. It has been proved for the crystalline modification of α-P_4S_3 that in both independent molecules bent bonds are present in the P_3 ring. Special interest should be paid to the p-SiP_2 structure. The large electron density maximum, observed within the P–P bond, corresponds to the very short P–P distance (215 pm) and is a good hint for a considerable amount of back-bonding P→Si according to the formulation Si^{2+} and $(P{=}P)^{2-}$. In this structure (the crystal symmetry $Pa\bar{3}$ does not allow either point symmetry $\bar{4}3m$ at the P atom site nor $m\bar{3}m$ at the Si atom site) there are also strong indications for bent Si–P bonds[135] (Figure 7).

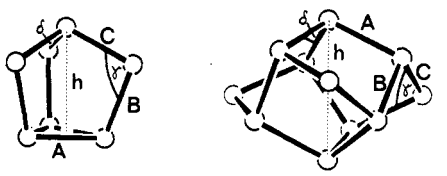

Figure 8. Y_7^{3-} and Y_{11}^{3-} with the labels of bond lengths, pertinent bond angles, and the heights of the polyanion (cf. text).

The pyrite structure is an instructive example for tunable bond lengths in the polyanionic dumbbell. There are short bond lengths d(P–P) in SiP_2, large d(S–S) in FeS_2 and CoS_2, and normal ones in MnS_2 and NiS_2.[135,344] Under pressure d(S–S) becomes *larger* in CoS_2,[296] due to a M→X back-donation. This result can also be regarded as an intrinsic redox process. Further examples include the phosphides MT_2P_2 (Table II) in the $ThCr_2Si_2$ type, containing a formal P_2^{n-} dumbbell, for which detailed theoretical investigations have already been performed.[337,338] Compounds of the MnP type as well as ThP_7 should be mentioned here. Both structures contain unusually large P–P bond lengths. In the first case $^1_\infty(P^{n-})$ polyanions are present with $2 \leq n \leq 3$, which results in corresponding variations of d(P–P). In ThP_7 the simple electron-counting rules are fulfilled only by assigning to the longer bonds, d(P–P) = 240 pm, the bond order $^1/_2$. The compound $LaCo_8P_5$, containing isolated P^{3-} and P_2^{n-} with $n \simeq 2.5$, should be treated in an analogous way.

6. P_7 and P_{11} Cage Topology

The neutral heptaheteronortricyclenes P_4S_3, P_4Se_3, and P_7R_3 as well as the isoelectronic species P_7^{3-} (As_7^{3-} and Sb_7^{3-}) exhibit distinct differences in their topology. Endocyclic bond lengths and bond angles as well as the elevation h of the apical P atom with respect to the P_3 base show differences due to their function in the polycyclic cage (Figure 8).[311,345] For neutral compounds $A > B > C$ and $\gamma > \delta$ is valid, whereas for ionic cages $A > C > B$ and $\delta > \gamma$. On defining the ratio $\bar{Q} = h/A$, one obtains mean values of $\bar{Q}(P_7^{\pm 0}) \simeq 1.42$ and $\bar{Q}(P_7^{3-}) \simeq 1.33$. The lowered height h, the enlarged angle δ at the apical P atoms, and the smaller angle γ at the bridging P atom in P_7^{3-} are clear indications for the localization of negative charge at the (2b)P atoms. The Coulombic repulsion is responsible for the topological changes between neutral (h_{cov}) and ionic (h_{ion}) heptaheteronortricyclenes. This result has been confirmed by Böhm and Gleiter,[336] who calculated a localized charge of $q = -0.85$. A further support is the heights of the cages P_7^- and P_7^{2-} with values of about $h = {}^1/_3(h_{cov} + 2h_{ion})$ and $h = {}^1/_3(2h_{cov} + h_{ion})$, respectively. The homologues M_3P_7 (M = Li to Cs) exhibit more details: h(Li) > h(Na) > h(Rb) > h(Cs), which means Li_3P_7 has the tallest P_7 cage (Table VI). The small but significant variations can be understood in terms of progressive electron transfer in going from Li to Cs.

A similar, but less pronounced analysis can also be made for the P_{11} cages. The smaller changes that appear in localizing negative charges at the (2b)P atom positions are understandable with respect to the per se larger distance between the (2b)P atoms and therefore less repulsive interactions between them.

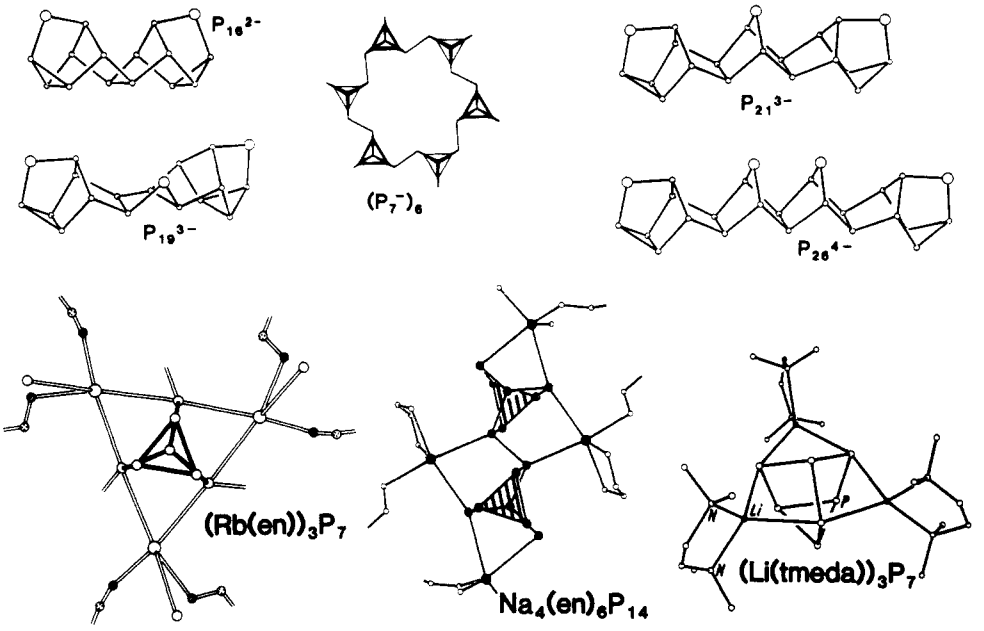

Figure 9. Structures of polyanions from solution. P_{19}^{3-} has been characterized by ^{31}P NMR spectroscopy, $(P_7^-)_6$ is hypothetical. Note the specific positions of the alkali metals with respect to the (2b)P^- atoms of the cages.

TABLE VI. Topological Details of Heptaheteronortricyclene and Ufosane Systems (Cf. Figure 8)

compd	A, pm	B, pm	C, pm	γ, deg	δ, deg	h, pm	$Q = h/A$	$\bar{Q}$
M_3P_7								
Li_3P_7	224.9	214.7	217.6	101.64	98.84	301.6	1.341	
$(Li(tmeda))_3P_7$[210]	225.5	215.0	220.4	98.1	101.8	302.2	1.340	
$Li_3(en)_5P_7$[231]	225.8	211.8	217.9	98.9	101.4	299.5	1.326	1.33
Na_3P_7[32,33]	226.2	210.5	219.5	99.6	100.6	300.0	1.326	
$(Rb(en))_3P_7$[234]	225.7	212.3	216.9	98.2	102.3	297.1	1.316	
Cs_3P_7[43]	228.7	212.0	216.2	98.4	102.6	296.9	1.298	
P_7R_3 (R = $M^{IV}(me)_3$,[311] $M^{IV}(ph)_3$[327])	222.0	218.9	218.3	102.3	98.4	315.4		1.42
M_3As_7								
Li_3As_7[231,298]	249.5	240.1	242.4	99.4	101.5	344.6	1.381	
Na_3As_7[231,298]	249.3	236.1	241.1	99.9	100.5	335.8	1.347	1.34
$(Rb(en))_3As_7$[231,298]	249.9	235.2	240.1	98.5	102.1	329.8	1.320	
$Cs_3As_7 \cdot NH_3$[298]	251.0	235.5	240.1	98.5	102.2	329.3	1.312	
As_7R_3 (R = $M^{IV}(me)_3$[324,297,231])	244.3	242.7	240.7	101.58	98.84	347.0		1.42
M_3P_{11}								
Na_3P_{11}[34]	224.7	217.4	220.4	95.8	102.0	378.6	1.685	1.69
K_3P_{11}[38]	224.4	217.4	220.5	95.9	102.2	379.1[a]	1.689	
$P_{11}R_3$ (R = $M^{IV}(me)_3$[326,32])	220.8	219.8	220.8	98.3	102.5	381.6		1.73
M_3As_{11}								
Rb_3As_{11}[38,297]	246.9	239.5	245.6	98.8	103.4	409.3[a]	1.658	
$(Rb(crypt))_3As_{11}$[297]	245.9	237.5	244.4	96.5	103.3	411.2	1.672	1.66
$(K(crypt))_3As_{11}$[354]	245.3	238.3	243.3	96.8	103.5	405.4	1.653	

[a] Powder determination.

We note in this context that similar relations are much more pronounced in the case of As_7R_3 and $As_{11}R_3$ as well as in their ionic compounds M_3As_7 and M_3As_{11}. Solvation, however, does not influence the observed results, as long as the solvation takes place in the outer sphere of the ion complexes (cf. Table VI).

VI. Polyphosphides from Solution

Reactions in solutions containing polyphosphides (section XIII)—may they be obtained by direct solvolysis of phosphides or in the course of suitable syntheses[1,343]—yield a whole bunch of new compounds. Some of them have been crystallized, while others have been characterized by ^{31}P NMR spectroscopy in solution. Table IV and Figure 9 give the present knowledge.

Solvent-free and solvated phases differ not only in some incidental details as coordination and bonding but primarily in the fact that corresponding compounds do not necessarily have to exist—and this is of general importance. Some examples include the following: (1) The thermodynamically stable modifications of LiP_7 and NaP_7 consist of polymeric norbornanes, whereas KP_7 does not exist (section IV). Therefore, one can expect corresponding transformation on desolvation of the P_{21}^{3-} salts. On the other hand, the MP_7 structures demonstrate how P_7^- anions can be adapted to the size of the cations via the different catenations of nortricyclenes as well as norbornanes. It cannot be excluded therefore that in mixed crystals or with other suitable cations also the trimers $(P_7^-)_3$ and other variants can be stabilized even in quasi-binary solvent-free compounds. The cyclic hexameric anion $(P_7^-)_6$ will be of special interest. (2) There are no stable phases in the binary system alkali metal/phosphorus between MP_7 and MP_{11} ($MP_{10.3}$), although their existence can be ex-

pected for structural reasons (section IV). Only solvated alkali-metal salts with P_{16}^{2-} ($\triangleq MP_8$) exist and therefore will disproportionate in the course of solvent abstraction. On the other hand, the solvent-free salt $(P(ph)_4)_2P_{16}$ is a nice example for the stabilization of new, quasi-binary phosphides using large cations. The same holds, if e.g., the alkali metals are completely separated from the anions by macrocyclic ligands. (3) The anions P_{19}^{3-} and P_{26}^{4-} (Figure 9) have no counterparts in the binary systems, although their topology corresponds to the schemes already observed. The ratio P/M = 6.33 and 6.50, respectively, is close to P/M = 7, the stoichiometry of the thermodynamically stable binary phases. (4) Somewhat different is the situation with P_{14}^{4-}, a dimeric nortricyclene system with P/M = 3.50. Although mixed crystals or ordered mixed phases with $2.33 \leq P/M \leq 3.66$ contain only isolated anions P_7^{3-} and P_{11}^{3-}, such dimers may exist, e.g., in the not yet identified part of the crystal structure of $Li_3P_{8.33}$ (section IV). (5) The remarkable monomeric P_5^-, an analogue of the cyclopentadienyl anion, is stabilized in solvent-free LiP_5 as a polymer. The corresponding NaP_5 and KP_5 do not exist.

The influence of the solvent can be seen by comparing the crystal structures of solvent-free Li_3P_7 and solvated Li_3P_7, e.g., $(Li(tmeda))_3P_7$. Whereas Li_3P_7 forms a 3D network using ion–ion and ion–dipole Li–P interactions, the solvated compound forms an isolated ion complex with the solvent completing the tetrahedral coordination of Li. In the solvated polyphosphides the metal atoms coordinate preferably the $(2b)P^-$ of the polyanion. This proves the donor quality of the $(2b)P^-$ atoms (section XIV). There is strong evidence that the pronounced formation of arrangements like solvated ion complexes reflects the structure of those polyphosphides even in solution. This point of view is supported by the alkali-metal-dependent position of the ^{31}P NMR signal, which indicates the valence tautomerism of M_3P_7(solv).

VII. Gas-Phase Species

In general, metal phosphides decompose by thermal stress vaporizing phosphorus. Only with highly volatile metals does one observe M(g) in addition.[300] Especially important is the behavior of the alkali-metal phosphides. K_3P and KP_{15} give off K and P, respectively, and yield K_3P_7 at least. The unique behavior of the bright yellow phosphides M_3P_7 (M = Na to Cs) was mentioned above, namely, that they can easily vaporize congruently.[301] Nevertheless, there is no evidence for gaseous MP_n species (mass spectra) under normal-pressure conditions. On the contrary, the congruent vaporization takes place with complete dissociation into the respective elements. It seems to be very probable that $M_3P_7^+$ (mass spectral conditions) immediately decomposes into P_4^+ and its fragments and, therefore, claims dissociative sublimation. On the other hand, this may be a question of temperature. Very important experiments were reported recently by Martin,[299] who studied the cluster formation from K(g) and P_4(g) at low pressure and low temperature (He gas). Under those conditions a complete series of $[K(K_3P_7)_m(K_2P_4)_n]^+$ moieties were identified (Figure 10), which show, with the help of K^+ as a carrier, the expected outstanding stability of K_3P_7. The second favored

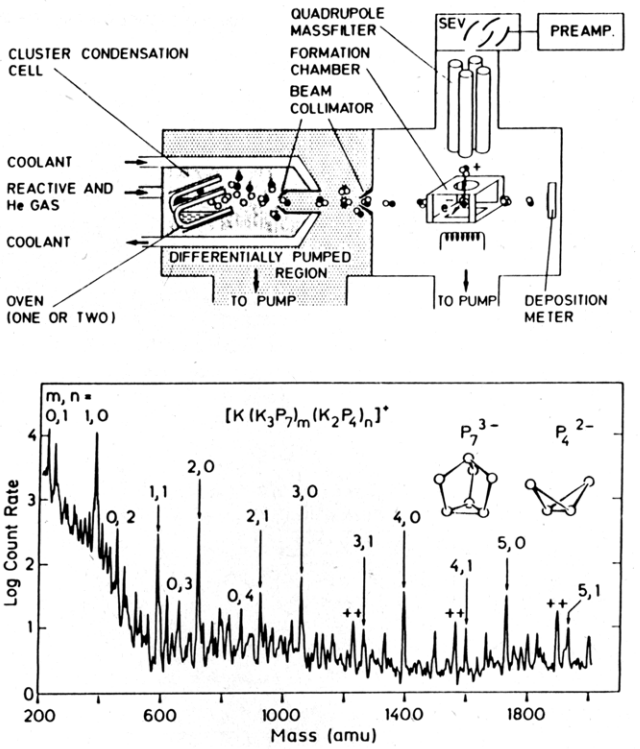

Figure 10. Experimental setup (top) for the cluster beam preparation, and typical mass spectra for the system K/P (bottom).[299]

molecule is K_2P_4, which is probably a derivative of the butterfly P_4^{2-} (Figure 3). Corresponding crystalline compounds of this composition are still unknown. The preparative utilization of this method has not yet begun.

VIII. The P^-/S Analogy

The analogy between the twofold covalently bonded isoelectronic $(2b)P^-$ and S follows from simple valence rules. Table V gives the known examples. Three compounds may be of interest: P_4S_3, which is the prototype of the heptaheteronortricyclene system P_7^{3-}; PdPS, containing $(P_2S_2)^{4-}$ anions, isostructural with P_4^{6-}; and the recently found $P_{14}S$ ($P_{14}Se$), which is isostructural with the tubelike polyanion P_{15}^- (Figure 5e). Because the electronegativity of sulfur (and selenium) is larger than that of phosphorus, these compounds are sulfides and, therefore, the phosphorus substructure must be discussed in terms of polyphosphonium cations. Both fragments, P_{15}^- in the ruby red KP_{15} and P_{14}^{2+} in the bright red $P_{14}S$, represent derivatives of the violet Hittorf's phosphorus in the lowest state of reduction and oxidation, respectively. They are comparable with the graphite compounds, but, whereas the graphite intercalation does not change the σ-bonded net of graphite, in the compounds of violet phosphorus the transfered electrons are always localized at a few special positions, forming defects in the structure of the element.

IX. Thermochemistry

Phosphorus-rich compounds like KP_{15}, BaP_{10}, LaP_7, and ThP_7 are delightful because of their crystalline behavior and their structures, which fit the almost accepted ideas of chemical bonding very well. One can hardly ask for the energy gain which may be related to

TABLE VII. Thermochemical Data According to $\Delta(\Delta H°_{298}) = \Delta H°_{298}(EuP_{x,F}) - \Delta H°_{298}(EuP_{y,F}) = -\Delta H^*_R + (x-y)\Delta H^V_T(P_{red})$ Enthalpies in kJ mol^{-1})

educt	product	T, K	ΔH^*_R	$\Delta(\Delta H°_{298})$
EuP_7	β-EuP_3	700	191.0	−71.8
α-EuP_3	EuP_2	800	53.0	−23.7
β-EuP_3	EuP_2	800	65.3	−36.0
EuP_2	$EuP_{1.33}$	900	34.8	−15.6
$EuP_{1.33}$	EuP	1100	20.0	−10.7

Enthalpies of Formation of the Europium Phosphides in kJ mol^{-1}

compd	$\Delta H°_{298}$/Eu		$\Delta H°_{298}$/atom			$\Delta H°_{298}$[a]
EuP	A		0.500	A		(−320)
Eu_3P_4	A	−10.7	0.429	A	−4.6	−992
EuP_2	A	−26.3	0.333	A	−8.8	−346
β-EuP_3	A	−62.3	0.250	A	−15.6	−382
α-EuP_3	A	−50.0	0.250	A	−12.5	−370
EuP_7	A	−134.1	0.125	A	−16.8	−454

Enthalpies and Entropies of Reaction (R) and Formation (F) in kJ mol^{-1} for MP_{15}

compd	$\Delta H°_{298,R}$	$\Delta S°_{298,R}$	$\Delta H°_{298,F}$	$S°_{298}$
LiP_{15}	556 (20)	798 (36)		
NaP_{15}	486 (15)	685 (30)	−153 (15)	364 (30)
KP_{15}	494 (8)	686 (14)	−126 (8)	398 (14)
RbP_{15}	489 (6)	696 (12)	−113 (6)	418 (12)
CsP_{15}	493 (6)	689 (12)	−108 (6)	433 (12)

[a] Referred to an estimated value of A for EuP.

a further phosphorination of a polyphosphide, e.g., $BaP_3 + {}^7/_4P_4 \rightarrow BaP_{10}$. Quite contrary, the existence is still accepted just as that of an object one can look at. It is therefore not surprising that information concerning the thermodynamic stability is very rare. We will demonstrate how important these data are.

1. The binary system Eu/P may be taken as an example of phases with a negligible metal partial pressure. The polyphosphides vaporize incongruently according to the reaction $aEuP_m(s) = aEuP_n(s) + P_4(g)$, where $a(m-n) = 4$. Vapor pressure measurements[89] yield the enthalpy and entropy of reaction and allow for the calculation of enthalpy and entropy of formation relative to that of EuP (Table VII). The stability regions of the europium polyphosphides are shown in Figure 11 (top). The large stability of β-EuP_3 and the small stability of EuP_2 are clearly demonstrated. β-EuP_3 has the largest vaporization enthalpy and transforms to α-EuP_3 at 960 K. EuP_2 is only stable above 750 K and below that temperature β-EuP_3 decomposes directly to Eu_3P_4. From the stability regions one can derive appropriate routines for the synthesis. Figure 11 (center) shows the standard enthalpies of formation per atom. It is remarkable that just the phosphorus-richest phases possess the largest atomic excess enthalpy. Another interesting detail is shown by the entropy of formation per mole of P_4(g) during the vaporization reaction. ΔS(600 K) increases slowly from Eu_3P_4 to EuP_2, α-EuP_3, and violet Hittorf's phosphorus (131, 144, 162, and 175 J K^{-1} mol^{-1}) but is much larger for β-EuP_3 and EuP_7 (212 and 215 J K^{-1} mol^{-1}). This effect seems to be related to the phosphorus partial structures. That is, there are, on the one hand, short P_4^{6-} chains, 1D chains $^1_\infty(P^-)$, twistable 2D nets $^2_\infty(P_3^{2-})$, and a strained network of connected tubes, but, on the other hand, 2D polyanions with strain-free P_6 and P_8 rings.

2. The phosphorus-richest alkali-metal polyphosphides MP_{15}(s) with M = Li, Na, K, Rb, and Cs were found to decompose under vacuum conditions in one step directly to the corresponding M_3P_7(s)[106] phases

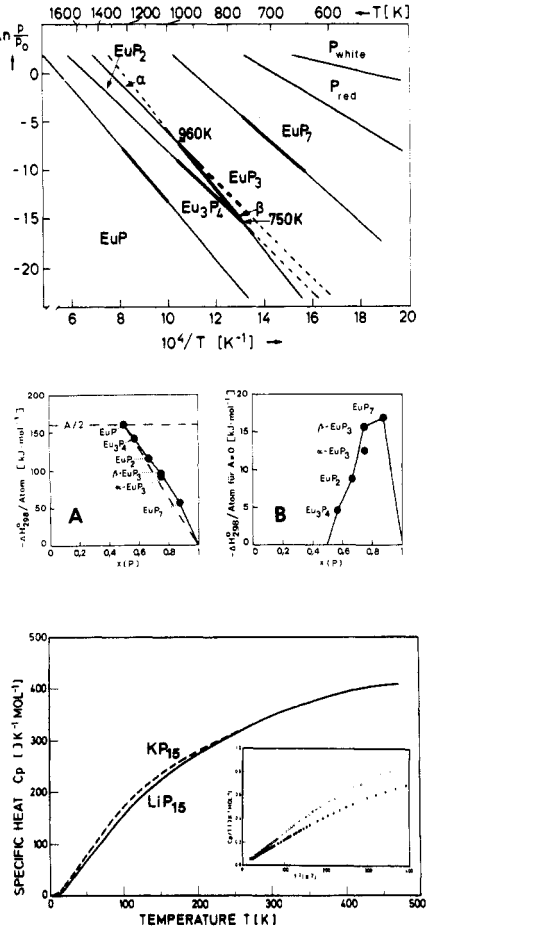

Figure 11. (Top) ln $(p/p°)$ vs T^{-1}, representing the stability regions of the europium phosphides (bold, measured region; thin, extrapolated; dashed, metastable; P_0 = 1013 mbar). (Center) (A) Heat of formation per atom $\Delta H°_{298}(EuP_x,s)$ relative to $A = \Delta H°_{298}(EuP,f) = -320$ kJ·mol^{-1}. Dashed lines indicate the value of EuP ($A/2$) and the curve for atomar heats of formation between EuP and P(red) in the case of ideal mixtures, respectively. The deviations of compounds from this line are a measure for the relative stability. (B) Relative heats of formation per atom for the hypothetical case $A = 0$. In this picture the relatively large gain of energy for the formation of polyphosphides from EuP and P is demonstrated. (Bottom) Specific heat of LiP_{15} (—) and KP_{15} (– – –) as a function of temperature. The insert gives the low-temperature molar heat capacity C_p/T vs T^2.

according to $MP_{15}(s) = {}^1/_3M_3P_7(s) + {}^{19}/_6P_4(g)$. This is surprising since there are many phases known between MP_{15} and M_3P_7 (Table I). However, experiments under an Ar atmosphere show increased decomposition temperatures and discontinuities in the TG curves, indicating the intermediate formation of the other phases. This is important in the synthesis of those compounds. In fact, the relative stability of the intermediate phases is strongly influenced by the unique behavior of the M_3P_7 phases (section X), whose stability changes rapidly with pressure and temperature. The thermodynamic data are given in Table VII. It is seen that the stability of MP_{15}(s) with respect to thermal decomposition is nearly identical for M = Na to Cs but is noticeably larger for LiP_{15}, which is related to the different behavior of Li_3P_7. With respect to red phosphorus, the evaporation of P_4 from MP_{15} is strongly activated. Under vacuum conditions, e.g., it is possible to decompose MP_{15}(s) without evaporating an excess of elemental red phosphorus. However, it is not possible to reach vapor pressure equilibrium over Hittorf's phos-

phorus even in the Knudsen cell with the smallest orifice.

Similar results are obtained with the higher polyphosphides of the rare-earth metals.[300] The heptaphosphides LnP_7 (La to Pr) decompose at about 600 K, forming the corresponding pentaphosphides. At about 750 K further decomposition starts, yielding the diphosphides. All other pentaphosphides LnP_5 (Nd to Lu) decompose directly to the monophosphides. Knudsen cell vapor pressure measurements show that the mean enthalpy for vaporizing one $P_4(g)$ is about 150 kJ mol^{-1} for LnP_7, but about 200 kJ mol^{-1} for LnP_5 and 170 kJ mol^{-1} for YbP_5 (α, β). Although the $P_4(g)$ equilibrium pressure at a given temperature increases with decreasing cation radius, in general, it shows some irregularities, which obviously are affected by the electron configuration of Ln^{3+} as well as by the different stabilities of the decomposition products.

3. The bright yellow compounds M_3P_7 (M = Na to Cs) were found to sublime congruently[301] according to the general reaction $M_3P_7(s) = 3M(g) + {}^7/_4P_4(g)$, whereas Li_3P_7 decomposes to lower phosphides under similar conditions. $\Delta H°_{298,f}$ of $Na_3P_7(s)$, $K_3P_7(s)$, $Rb_3P_7(s)$, and $Cs_3P_7(s)$ were found to be −119, −114, −118, and −66 kJ mol^{-1}, and $\Delta S°_{298}$ is 509, 612, 689, and 756 J K^{-1} mol^{-1}, respectively. The large entropy contribution to the stability of these compounds makes them unique among alkali-metal phosphides. Furthermore, it is shown that the $M_3P_7(s)$ compounds are stable with respect to both phosphorus-rich and metal-rich compounds in the corresponding systems. $\Delta H°_T$ and $\Delta S°_T$ for the crystalline so plastically crystalline phase transition were found to be 35.5 kJ mol^{-1} and 47 J K^{-1} mol^{-1} (Na_3P_7), 10.1 kJ mol^{-1} and 19 J K^{-1} mol^{-1} (K_3P_7), 5.8 kJ mol^{-1} and 12 J K^{-1} mol^{-1} (Rb_3P_7), and 19.6 kJ mol^{-1} and 35 J K^{-1} mol^{-1} (Cs_3P_7), respectively, by DSC measurements.

4. The heat capacities of LiP_{15} and KP_{15}[302] (Figure 11 (bottom)) were measured in the temperature range 2–470 K and the thermodynamic functions for these compounds were calculated. The absolute entropies of LiP_{15} and KP_{15} at 298 K were found to be 386.0 and 411.4 J K^{-1} mol^{-1}, respectively. The low-temperature limiting values of the Debye temperature are $\theta_0(LiP_{15})$ = 238.3 K and $\theta_0(KP_{15})$ = 220.0 K, and the ratio is $\theta_0(LiP_{15})/\theta_0(KP_{15})$ = 1.08. This ratio is much larger than would be expected from the square root of the mass ratio (1.02) and, therefore, not all atoms may participate in the soft vibrational modes at low temperatures. But, taking only the lattice vibrations of the six nearest neighbors of the metal cation into account, the ratio $\theta_0(LiP_{15})/\theta_0(KP_{15})$ takes on a value of 1.08, which is in excellent agreement with the experiment. This indicates that the covalent bonding within the P_{15}^- tubes and the ionic interaction between the cation and the polyanion produce two distinctly separate sets of vibrational excitations within the structure (section XII). At low temperatures, obviously interchain vibrations occur, which are partially transmitted through the cations. At higher temperatures ($T \geq \theta/10$), intrachain vibrations, propagated through the covalently bonded tubes are the dominant vibrational modes. The unusual temperature dependence of the Debye temperatures, $\theta(T)$, of LiP_{15} and KP_{15} is caused by these high-frequency vibrations. The Debye temperature of these compounds increases almost threefold from low temperature to room temperature [at 50 K, $\theta(LiP_{15})$ = 370 K, $\theta(KP_{15})$ = 345 K; at 200 K, $\theta(LiP_{15})$ = 580 K, $\theta(KP_{15})$ = 565 K] as a result of intrachain lattice vibrations.[302,312]

X. Phase Transitions and Plastically Crystalline Phases

Second-order phase transitions are very similar in character to S_N2 reactions, because both processes progress homogeneously and continuously and are controlled by an "order parameter", e.g., the deviation from the transition-state structure. In this context Dunitz and Bürgi[303] have shown that similar information on chemical reaction paths can be obtained by simple comparison of appropriate static crystal structures. Only few investigations exist about real transitions, but some possibilities should be mentioned here.[9]

(i) The pentaphosphides of the trivalent lanthanoid cations, LnP_5, form a $^1_\infty(P_5^{3-})$ polyanion, consisting of condensed P_{12} rings. The structure is a derivative of a hypothetical P modification with condensed six-membered rings in the boat form. The polyanion adapts itself optimally to the size of the cation in the series La to Lu by altering the P–P bond lengths and conformational changes. β-YbP_5 forms a more closely packed variant of this structure, resulting from the α-modification by a relative shift of the twelve-membered rings. The structures of the LnP_5 series can be interpreted as stages of a reaction path brought about by application of pressure.[9]

(ii) Th_2P_{11} is a particularly attractive example of a frozen-in ring-opening reaction with an S_N2 mechanism.[98] Inserted into the $^1_\infty(P_{16}^{10-})$ bands are isolated P_6 rings (chair) and P_3 fragments of such rings. The P_3 fragments are bonded to the polyanion bands. A periodic modulation is present in the crystal, caused by valency and generated by the turning of a single P–P bond. At room temperature both boundary states are frozen in, giving the environment of the "mobile" P atom the configuration of the boundary states of an S_N2 reaction. At higher temperatures this process may take place in the crystal (perhaps with varying modulation wavelengths).

(iii) Triclinic CaP_3 passes through a phase transition at 990 K into the monoclinic $SrAs_3$-type structure with a very long induction period. The bonding in the polyanion remains unchanged, but remarkable variations in dihedral angles occur.[58,349] By comparison with the isostructural mixed crystal series $Ca_xEu_{1-x}As_3$ it is suggested that T_c can be changed progressively with substitution. In this context it is remarkable that the supposed reaction path from $CaAs_3$ (triclinic) to $SrAs_3$ (monoclinic) represents a transition from a semiconductor to a semimetal.[304]

An interesting field of phase transitions between the crystalline and plastically crystalline state is provided by molecules and molecule-like anions, e.g., P_4S_3, M_3P_7, and M_3P_{11} (M = alkali metal).[10,33,346] Whereas the binary phosphides in the high-temperature form (β) match the structure of the intermetallic Li_3Bi (P_7 and P_{11} surround the Bi positions), β-P_4S_3 adopts the complex β-Mn type structure by substituting Mn atoms by the centers of P_4S_3 molecules. A similar plastically crystalline phase has been known for a long time for

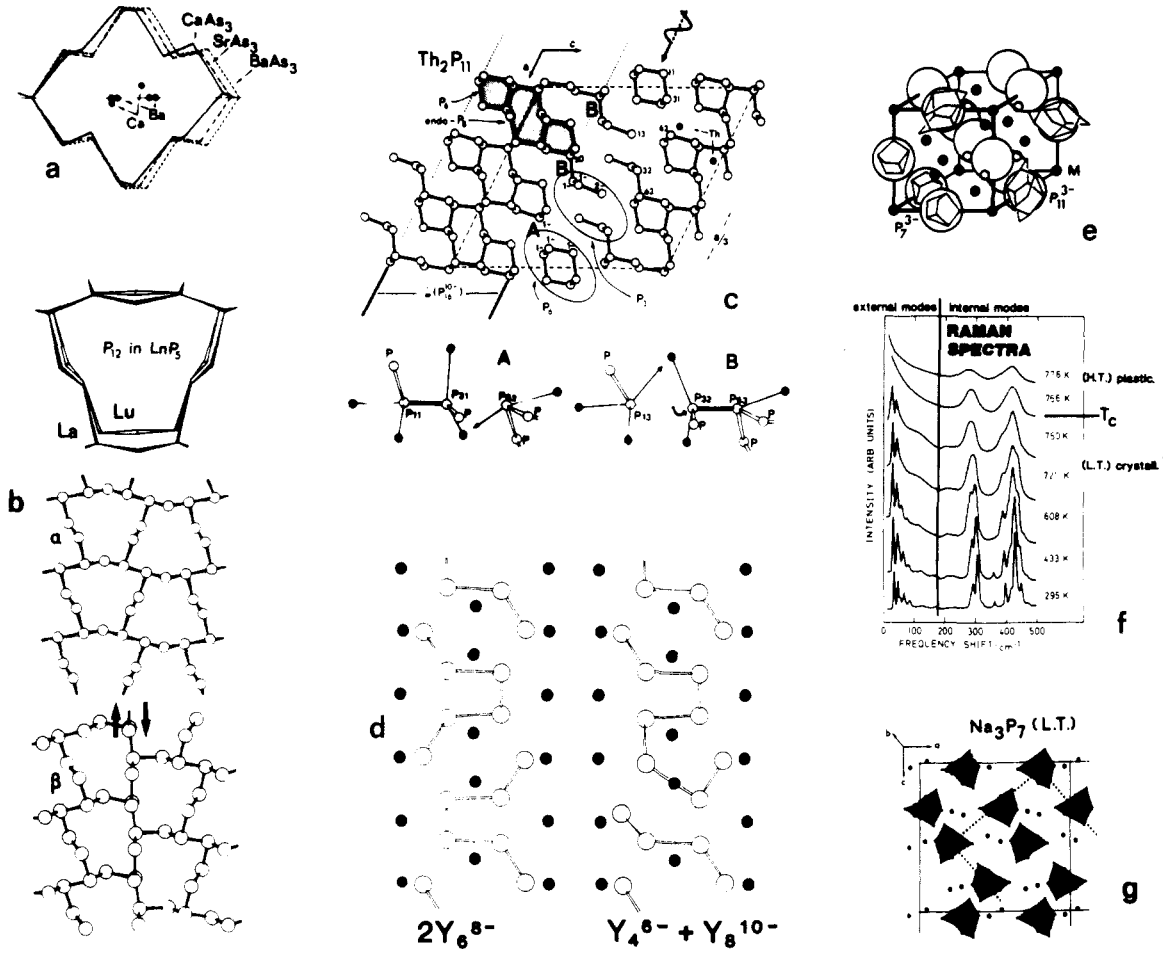

Figure 12. (Left) Stepwise adaptation of polyanionic nets to the size of cations, as visualized (a) in the case of triarsenides, isotypic with α-EuP_3, and (b) in the case of LnP_5. Relation between α- and β-YbP_5. The arrows indicate the relative shift, going from one type of *cyclo*-P_{12} catenation to the other. (Center) (c) $^1_\infty(P_{16}^{10-})$ substructure of Th_2P_{11} with inserted P_6^{6-} rings. The S_N2 reaction scheme for the opening and closure of P_6 is given. (d) Relationship between Y_6^{8-}, Y_4^{6-}, and Y_8^{10-} finite polyanions in a trigonal-prism structure. Note the relatively small atomic shifts, necessary for transformations. (Right) (e) Li_3Bi as the parent structure (Bi is indicated by large circles) of the plastically crystalline phases M_3P_7 and M_3P_{11}. (f) Raman spectra of Na_3P_7 as a function of temperature. Note the disappearing of the external modes just above T_c. (g) Na_3P_7 low-temperature crystal structure. The orientation of the plastically crystalline unit cell is indicated by dotted lines. Cf. (e) with (g).

P(white), where P_4 tetrahedra surround the 58 Mn positions in the α-Mn structure.[6,9] The electron density of the plastically crystalline phases in the region of the mobile clusters has been analyzed quantitatively in the case of Rb_3P_7, Cs_3P_{11}, and $Cs_3P_{8.33}$.[43] By careful assignment of the observed peak splitting (Figure 7) it was possible to evaluate a model with static disorder of P_7^{3-} and P_{11}^{3-} anions, such that their threefold principal axes point toward the cubic [111] direction. The alkali metals follow these orientational shifts.[38,347]

XI. Phosphorus/Arsenic Mixed Crystals

The variety of stable polyarsenides is not nearly as large as that of the polyphosphides. Therefore, investigation of mixed systems is very fruitful, because the chemical difference of both elements is offered in a simple way.

1. It is known that all molecule species $(P_{1-x}As_x)_4$ do exist.[305] However, the behavior is already different from that of orthorhombic black phosphorus and rhombohedral gray arsenic. There exist two *limited* series of mixed crystals.[306] This is remarkable, because both elements transform into the two modifications by pressure. The complicated and strained Hittorf phosphorus modification is not known for arsenic, and, indeed, only some percent of As can be introduced in that structure. On the other hand, the crystallization of Hittorf's phosphorus[307] is much easier in the presence of As, resulting in a mixed phase $P_{0.95}As_{0.05} \triangleq P_{20}As$. The reason is offered by the structure in which As is found to occupy exclusively the "roof" positions of the strained fivefold tubes (Figure 13). The accompanying reduction in strain may be simply demonstrated by a model kit as an analog computer.[348] The decreasing strain in the course of the substitution by arsenic is also reflected in the observed decrease of chemical reactivity; e.g., the formation of phosphoric acid with wet air is suppressed.

2. Similar to P_4 and black phosphorus, the molecule-like P_7^{3-} group as well as the defect variants of the strain-free black phosphorus structure (EuP_3 etc.) shows complete miscibility. The whole series of valence tautomeric systems $(P_{1-x}As_x)_7^{3-}$ was proved to exist in ethylenediamine solutions of $Rb_3(P_{1-x}As_x)_7$ mixed crystals[308] (Figure 13).

3. Mixed crystals in the whole range also exist with EuY_3, EuY_2, and EuY. Statistical distributions of P and As are found in the three completely different polyanionic substructures $^2_\infty(P_{1-x}As_x)_3^{2-}$, $^1_\infty(P_{1-y}As_y)_2^-$, and $(P_{1-z}As_z)_2^{2-}$. In $Eu(P_{1-x}As_x)_3$ a weak preference of As for the (2b)Y^- positions occurs, which form the most

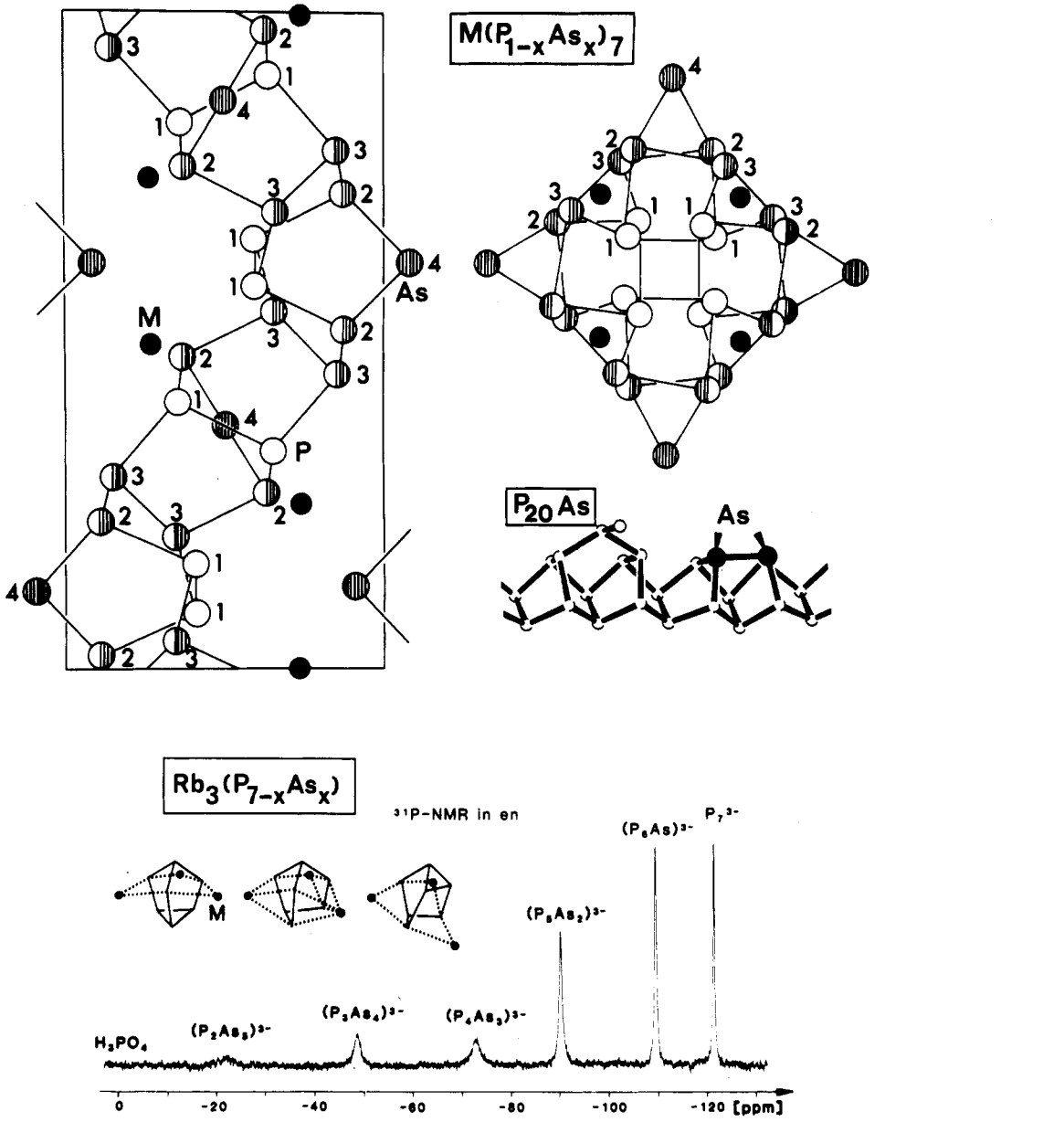

Figure 13. Mixed crystals $M(P_{1-x}As_x)_7$. Note the descending substitution on going from the periphery to the helix axis. (The numbers label the four different atomic sites.) Exclusive roof substitution by As (black dots) is observed in $P_{20}As$ with Hittorf's phosphorus structure. The As positions are occupied by $P_{0.5}As_{0.5}$. Mixed heptaheteronortricyclenes $(P_{7-x}As_x)^{3-}$ as visualized by ^{31}P NMR spectroscopy.

flexible part of the polymeric structure. During thermal decomposition the x:y:z ratio is changed systematically ($x < y < z$) and in accordance with an enrichment of As in the solid with a smaller Y:Eu ratio. Moreover, with $Eu(P_{1-z}As_z)_2$ a structural phase transition takes place from the EuP_2 to the $EuAs_2$ type, which mainly differs in the conformation of the polyanionic chains $^1_\infty(Y^-)$.[349]

Much more stimulating is the phase transition in the monopnictide series, because EuP belongs to the NaCl structure with Eu^{3+} and P^{3-}, but EuAs forms the Na_2O_2 structure with Eu^{2+} and As_2^{4-}. The polyanionic EuAs structure is stable within $0.05 \leq z \leq 1.00$. This large range corresponds with the observation that EuAs does not transform into the NaCl structure under pressure but decomposes.[350]

4. The relations are quite different in the strained helical polyanionic structures of LiP_7 and NaP_7. Here, the As atoms demonstrate pronounced preference for the peripheral atomic positions of the $^1_\infty(P_{1-x}As_x)_7^-$ helix[309] (Figure 13). The As substitution reaches $x = 0.50$, but the individual values at the four different atomic positions are $x_i = 0.0(1x), 0.60(2x), 0.65(2x)$, and $1.0(2x)$, going from the center to the periphery of the helix. With respect to the findings in Hittorf's phosphorus structure, this distribution seems to be affected by structural strain more than by differences in polarity. Again, this substitution can be seen as a chemical reaction, starting from the surface region with maximal strain ("corrosion").

The fourfold $^1_\infty(P_7^-)$ helix is a very rigid building unit, which is clearly demonstrated by the constant length of the helical axis in LiP_7 and NaP_7. This is clearly the reason for the nonexistence of that structure with the larger alkali metals. A free helix of this type should have a screw order >4 and a relative height $h^* = 7.1$ with respect to the mean P–P bond length. The lock-in to fourfold symmetry needs increasing curvature, which lowers h^* ($h^*_{obsd} = 6.7$) but stretches the peripheral bonds. Therefore, the concentration of the larger As

atoms in the peripheral region seems to be very reasonable.

XII. Vibrational, Electronic, and Magnetic Properties

From a chemist's point of view, the polyphosphides are valence compounds (section IV). How far the expected relationships between stoichiometry, structure, and properties hold can only be answered by complete measurements of the relevant physical properties. Such measurements are very rare as compared with the large number of compounds.

Vibrational spectra are suitable tools for demonstrating to what extent the separation of covalent-bonded polyanions and inserted cations holds, how strong the interactions between these partial structures are, and which modes are typical for the solid state (separation of lattice modes and cluster vibrations). Reliable assignments of definite partial structures then allow the identification of such units in amorphous materials.

Appearance and color—fundamental properties for chemists for emotional reasons—can only be quantified by transmission and reflectivity measurements. The band gaps, characteristic for the solid state, can be deduced from measurements of electrical conductivity, which, apart from that, allow conclusions on transport phenomena and doping concentrations as well as identification of charge carriers (extrinsic, intrinsic, etc.).

Magnetic properties are primarily important for the characterization of the electronic states of the transition-metal and rare-earth cations, which is necessary to prove the above-mentioned electron transfer to the phosphorus partial structures. Moreover, due to the consecutive separation of magnetic cations, the higher polyphosphides open up an unexpected richness for the study of electronic interactions and magnetic order phenomena.

The Raman and IR spectra of crystalline P_4S_3 (nortricyclene system) clearly show the separation of internal and external modes as expected. The external modes are strongly pressure and temperature dependent, whereas the internal cluster modes are nearly unaffected.[310] Approaching the crystalline to plastically crystalline phase transition, the external modes disappear completely. The same is true for the polyphosphides M_3P_7 and M_3P_{11}.[44,351] Again, the external vibrations vanish upon approaching T_c, and, moreover, the internal modes are still present (but broadened) in the melts, impressively demonstrating the molecule-like behavior as well as the high thermal stability of those polycyclic anions[355] (Figure 12). Derivatives of these cages, namely, P_7R_3 and $P_{11}R_3$, possess complicated spectra at first glance with strong frequency shifts caused by the substitution.[311,327] But once more the internal cage vibrations are nearly unaffected, even if the substituents are changed from R = Si(me)$_3$ to Pb(me)$_3$. Frequencies and their assignment of the cage vibrations with these quite different types of compounds are directly comparable to each other (Figure 14).

A striking example for the validity of the Zintl–Klemm treatment is provided by Rb_4P_6.[42] Despite the fact that the electronic stability of the planar P_6^{4-} ring is determined by the formation of hexagonal-bipyramidal $Rb_2P_6^{2-}$ subunits, the vibrational behavior of P_6^{4-} is like that of benzene!

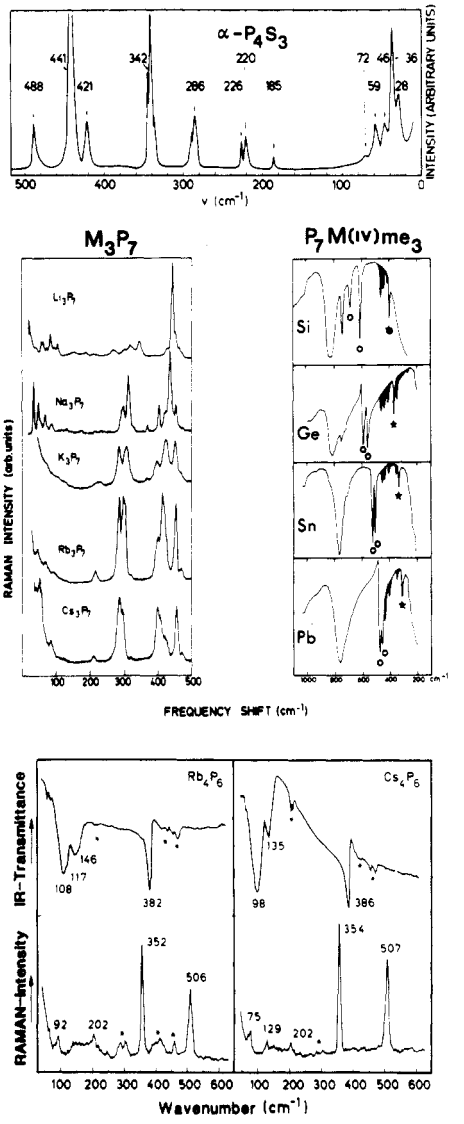

Figure 14. Raman spectra of α-P_4S_3 (top) and M_3P_7 (center left). IR spectra of $P_7M^{IV}(me)_3$ in the region 1000–200 cm^{-1}. The fundamental vibrations of the P_7 cage are marked black, the black stars indicate γ(P–M), and the circles indicate γ(M–C$_3$); the nonmarked strong bands are $\gamma C(H_3)$ (center right). Raman and IR spectra of Rb_4P_6 and Cs_4P_6 (bottom). Note the sequence of the fundamental vibrations of P_6^{4-}: $\tilde{\nu}(E_{2g}^{(1)}) < \tilde{\nu}(A_{1g}) < \tilde{\nu}(E_{1u}) < \tilde{\nu}(E_{2g}^{(2)}) = 202/202 < 352/354 < 382/386 < 506/507$ cm^{-1} (Rb_4P_6/Cs_4P_6), being equivalent to that of benzene. The dots indicate frequencies originating from M_3P_7 impurities.

The inter- and intratube variations of the 1D tubular polymers P_{15}^- in KP_{15}[312] as well as the similar units in the violet Hittorf's phosphorus[313] are separated in a very similar way. Moreover, one can assign the observed vibrations, typical for the respective subunits P_7, P_8, and P_9, by appropriate calculations. Comparison with vibrational spectra of amorphous red phosphorus (a-P) now really proves that a-P contains similar tubes with P_8 and P_9 as in violet P, that the number of P_8 cages is reduced, and that unambiguously P_7 cages of the nortricyclene type are present.

There is no indication for the presence of polymerized butterfly P_4 units as postulated earlier.[314] The upper frequency range (above 430 cm^{-1}) corresponds to extended breathing waves along the ladder-shaped spines of the tubes, which occur in all these tubular structures.

TABLE VIII. Band Gaps (E_g) (in eV) As Derived from Optical (o), Conductivity (c), and Photoconductivity (pc) Measurements[a]

P(white)	≥3.0	ZnP_2 (red)	2.05, o	EuP_3 (α, β)	~0.3, c	RuP_3	1.67, pc
P(black)	0.33, c	ZnP_2 (black)	1.33, o	EuP_7	0.9–1.1, c	RuP_4 (α)	0.19, c
P(Hittorf violet)	2.25, o	Cd_3P_2	0.5, o	CeP_5	0.4, c	RuP_4 (β)	0.32, c
P(amorph)	~2.0, o	Cd_6P_7	0.6, c	SmP_5	0.5, c	OsP_2	~1.2
M_4P_6 (K, Rb, Cs)	1.3–1.6, c	Cd_7P_{10}	1.6, o	Th_2P_{11}	0.3, c	OsP_4 (α)	0.20, c
LiP_5	~1.0, c	CdP_2 (α)	1.97, o	MnP_4 (6)	0.27, c	OsP_4 (β)	0.30, c
KP_{15}	~1.8, o	CdP_2 (β)	2.02, o	MnP_4 (8)	0.14, c	CoP_2	0.34, o
BaP_{10}	1.62, o	CdP_4	0.90, o	ReP_4	0.54, c		>0.02, c
B_6P	3.3, c		1.15, c	FeP_2	0.37, c	CoP_3	0.45, o
BP	2.0, o		1.02, o	FeP_4 (α)	0.32, c	RhP_2	~1, diff refl
AlP	2.42, o	SiP	2.0, o	FeP_4 (β)	0.1, c	IrP_2	1.1, o
GaP	2.24, o	GeP	0.95, o	FeP_4 (γ)	1.0, pc	NiP_2	0.73, o
InP	1.35, o	Eu_3P_2	0.3–0.5, c	RuP_2	~0.8, o	PtP_2	0.6–0.7, c
Zn_3P_2	1.2, o					Cu_2P_7	0.42, c

[a] In case of direct and indirect gaps, the direct E_g has been given. All E_g refer to 300 K or room temperature. For the references cf. Tables I–III, Landolt-Börnstein, New Series, Vol. 17, and ref 353.

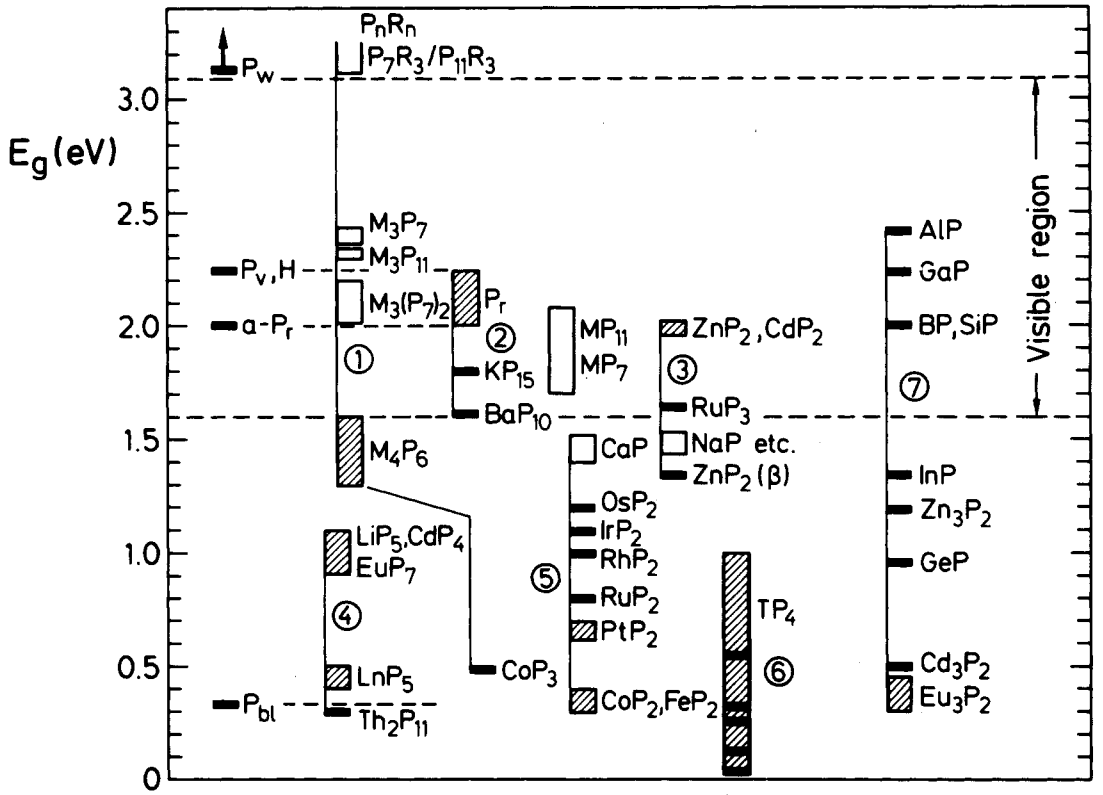

Figure 15. Ordering of E_g values according to structural relationships (Table VIII). Values estimated only from structure and color are represented by open rectangles. The structural correlations are (1) cycles and polycycles, (2) tubular and related structures, (3) infinite chain, (4) nets related to black phosphorus, (5) dumbbells, (6) nets with transition metals, and (7) isolated P^{3-}.

For the contribution of such vibrations to the specific heat, cf. section IX.4.

Going to 2D corrugated polyanionic nets, e.g., α-EuP_3, the separation of vibrations is still present. The high-frequency modes are mainly associated with vibrations within the layer, whereas the low-frequency modes are dominated by metal vibrations.[315]

The colors of the metal phosphides are collected in Table I from literature data. From the colors, the reflectivity, and the structures one can estimate that most of the polyphosphides are semiconductors. But for the metal-rich compounds (main group and RE are given only) semimetallic or metallic behavior may be expected. The available data are compiled in Table VIII and ordered in Figure 15 with respect to structural properties (P modifications are included). Some general trends can be seen as a very rough estimate, according to πd_{thumb} (πd_{thumb} is the scientific version of a workman's rule to make a rough estimate of something; it is synonymous to eyeballing something): (a) The band gap E_g is strongly affected by the polyanionic partial structure and increases with increasing P/M ratio, but only if the connectivities of the P substructures are comparable. (b) E_g decreases with increasing charge q(M) in compounds of comparable anionic structures. (c) E_g decreases with the heavier cation of the same group. (d) Crossing trends result if the character of the electronic states at the Fermi level is changed, e.g., $(P–P)^{nb}$←$(P–P)^*$ or $(P–P)^{nb}$←$(M–P)^*$, etc. Transition metals seem to lower E_g in general. (e) Compounds of family 4 (Figure 15) suggest that with decreasing mean charge q(P), one yields a "dilute" P(black) structure having more separated layers and, therefore, a larger E_g of about 1.3–1.5 eV. (f) Compounds of family 1 and family 5 show the influence of the increasing interconnection of isolated P_n systems via M atoms. (g) Tubular

and infinite chain structures are closely related to red phosphorus (families 2 and 3). (h) The large spread of E_g values with isolated P^{3-} ions demonstrates the influence of cation charge, P/M ratio, and electronegativity differences of M and P.

The magnetic properties of rare-earth monophosphides have been reviewed recently.[13] Magnetic susceptibility measurements show all europium polyphosphides to be Eu(II) compounds.[83] The rare-earth pentaphosphides are Ln(III) compounds, as expected.[76] In general, a Curie–Weiss behavior is obeyed, and the deviations are caused by mainly three phenomena: (i) transition to magnetically ordered phases at low temperatures (Sm, Gd, Dy, and Tb); (ii) crystal field splitting of the degenerate ground states (Ce, Nd, and Tm); and (iii) contributions of van Vleck's TIP (Sm and Pr). The phase transitions of SmP_5 and GdP_5 occur in two steps. The magnetic structure of TbP_5 and DyP_5 show ferromagnetic ordering within cation layers and antiferromagnetic ordering—coupled via P atoms—between adjacent layers. Angular overlap calculations show that the measured crystal field splittings as well as the susceptibilities can be simulated. An optimal fit, however, could only be reached by assuming two different interaction parameters, corresponding to $(2b)P^-$ and $(3b)P^0$, respectively.[76]

The phosphides and arsenides $M(P_{1-x}As_x)_3$ (M = Ca, Sr, Ba, Eu; $0 \leq x \leq 1$) are excellent examples to demonstrate how measurements on new materials yield interesting physical phenomena[317-323] caused by the interplay of several properties, e.g., semimetallic behavior ($SrAs_3$, $EuAs_3$) or small energy gaps, low crystal symmetry (monoclinic, triclinic), magnetic properties of Eu(II), complete miscibility, and insensitivity to air and moisture. The successful crystal growth of the relatively simple phases was a necessary prerequisite. In a series of publications the following have been shown: (i) The longitudinal Hall effect—expected for low symmetry—has been observed for the first time. (ii) The strip-line technique has been shown to be a suitable tool for the detection of magnetic phase transitions. (iii) The unexpected large anomalies in the magnetoresistance are caused by the coexistence of the galvanomagnetic properties of group 5 elements and the magnetic properties of rare-earth ions. (iv) Multiple magnetic phase transitions occur in the (T,B) phase diagrams, which are changed by pressure as well as concentration x(As) and exhibit a rich variety (paramagnetic; incommensurate ordered; antiferromagnetic; spin-flop phases).

XIII. Chemical Reactions

In general, the polyanions may be transferred into molecules and other derivatives by appropriate chemical reactions.[10] The highly reactive (not only versus oxygen and moisture) phosphides of the alkali and alkaline-earth metals are especially suitable synthons, and, in particular, those with finite polyanions. Of course, the scheme given in Figure 16 can be generalized for application to polymeric anions. Heterogeneous as well as homogeneous reactions have been investigated, and suitable solvents were shown to be ethylenediamine (en), liquid ammonia, THF, and glyme. It is not sure whether the heterogeneous reactions are really heterogeneous or not. Nevertheless, well-crystallized and pure

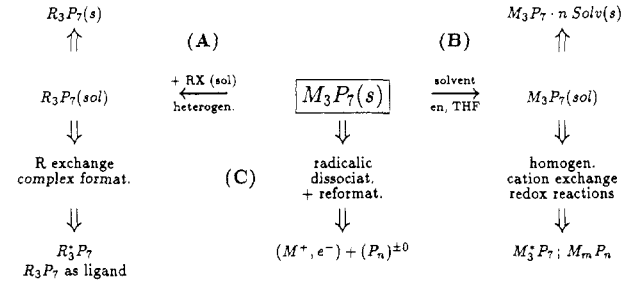

Figure 16. Scheme of chemical reactions exemplified by $M_3P_7(s)$.

solvent-free compounds, in general, dissolve only very poorly and slowly, whereas the respective solvates show good solubility.

Heterogeneous Reactions (Path A)

In a typical heterogeneous reaction, e.g., crystalline $M_3P_7(s)$ is transferred to solvated molecules $R_3P_7(sol)$ with suitable reactants RX (e.g., $ClSi(me)_3$). From the solutions the crystalline $R_3P_7(s)$ are obtained. Via R-to-R* exchange, new compounds are available, often in high yield.[311,327]

Homogeneous Reactions (Path B)

Solutions of binary metal phosphides are accessible with polar solvents cited above. Highest purity of the phosphide (surfaces) as well as of the solvent is necessary. It may be pointed out here that progress was mainly prevented for these reasons in this field for some decades. One believed for a long time that the deep red colored solutions are typical. However, it was recently shown that completely colorless solutions can be obtained[10,324] and that the onset of oxidation processes results in deep red solutions immediately. Indeed, recently the first oxidation products of phosphanes have been characterized by ^{31}P NMR spectroscopy.[325] For obtaining high reaction yields, the precipitation of amorphous (or microcrystalline) compounds by adding nonpolar solvents is useful. Suitable single crystals may be grown by countercurrent crystallization. The state of the metal phosphides in solution is considerably uncertain. However, remarkable progress has been obtained by 2D NMR spectroscopy.[1] There is some evidence for the presence of solvated ion complexes.

Radical Decomposition (Path C)

This further reaction path is rather unexplored but promises, e.g., the synthesis of new metastable modifications of the element or alloys. Important examples are the formation of *allo*-Ge[288] and *allo*-Si[286] from appropriate metal compounds and $(ph)_2CO$ in THF. Indeed, Na_3P_7 also reacts under formation of Na^+, the deep blue $(ph)_2CO^-$, and light red amorphous residues of new, but not yet characterized forms of elementary phosphorus[9,10] ($[P_7]_n$?; section XI). Thermal decomposition may also be discussed in terms of radical reactions. This is especially true if the alkali metal vaporizes.[37]

Some Results

Path A

Important examples are $P_7(M(me)_3)_3$,[311] $P_{11}(M(me)_3)_3$,[326] and $P_7(M(ph)_3)_3$[327] with M = Si, Ge, Sn, and

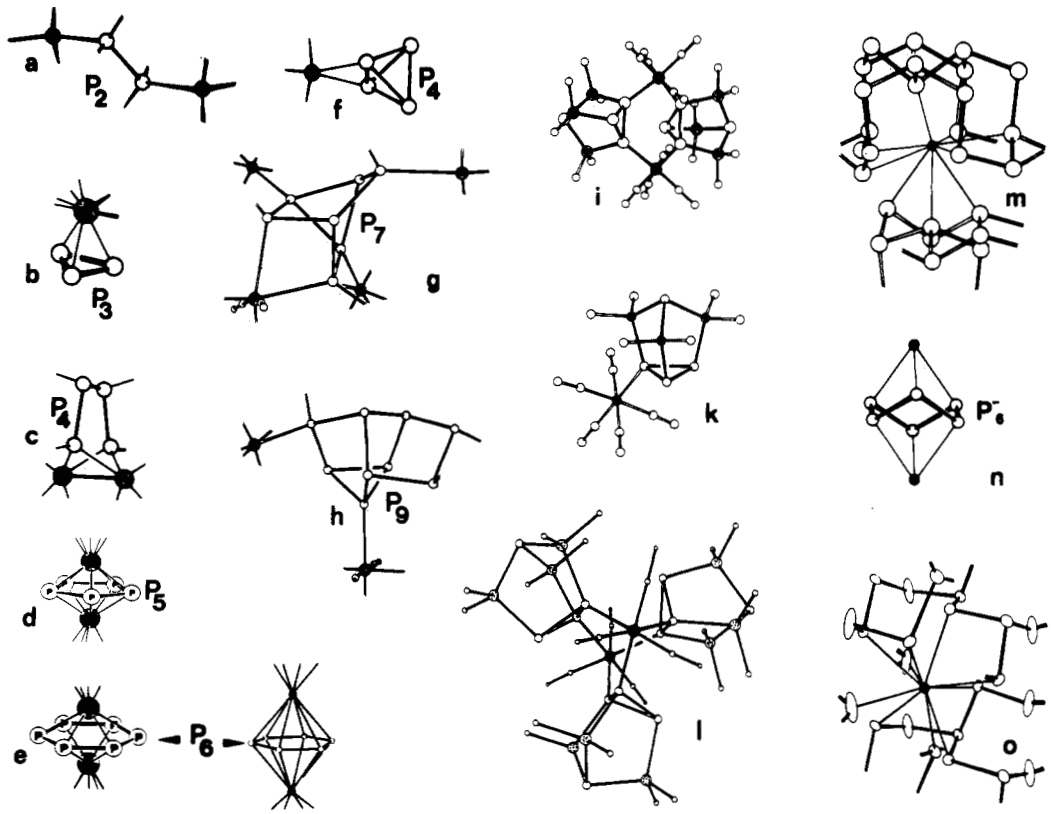

Figure 17. Donor properties of polyphosphides and phosphanes: (a) μ,η^1,η^1-P_2R_4; (b) η^3-P_3; (c) μ,η^2,η^2-P_4R_4; (d) μ,η^5,η^5-P_5; (e) μ,η^6,η^6-P_6; (f) η^2-P_4; (g) η^1,η^1,η^1,μ-P_7R_3; (h) η^1,η^1-P_9R_3; (i) μ,η^1,η^1-$P_4Si_3(me)_6$; (k) η^1-$P_4Si_3(me)_3$; (l) μ,η^1,η^1-$P_4Si_3(me)_3$; (m) Eu coordination in EuP_7; (n) μ,η^3,η^3-P_6^{6-} in Th_2P_{11}; (o) Th coordination in ThP_7.

Pb, making use of $Si(me)_3Cl$ as leaving group. A milestone is the preparation of P_7H_3 as the first polycyclic phosphane in pure colorless samples.[328]

Path B

The preparation of hydrogen phosphides[1,352] like $Li_2HP_7(solv)_x$ and $LiH_2P_7(solv)_x$ should be noted [$Li_3P_7(solv)_x + P_2H_4$; $Li_3P_7(solv)_x + P_7H_3$]. Na_3P_{21} is formed from P_4 and Na in solution, crystallizes as $Na_3P_{21}(thf)_{15}$, and can be transformed into $NaP_{21}R_2(solv)_x$[329] and then into $HP_{21}R_2$.[330] The latter reaction steps demonstrate directly the difference in nucleophilicity of the three P^- atoms. On the other hand, steric effects surely play an important role, especially in those parts of structures containing the nucleophilic $(2b)P^-$ in the central part of the roof line. Oxidation with P_4 in en leads from Na_3P_7 to $Na_4P_{14}(en)_6$[10] and from Cs_4P_6 to $Cs_3P_{11}(en)_3$.[235] The latter reaction corresponds to the solid-state reaction $Na_3P_7(s) + P_4(g) \rightarrow Na_3P_{11}(s)$.

Path C

The reaction of K_4P_6 with $(ph)_2CO$ in solution is remarkable, in particular, because of the easy abstraction of only one part of potassium ($K + (ph)_2CO \rightarrow K^+ + (ph)_2CO^-$) yielding K_3P_7. This partial homolytic cleavage is completely equivalent to the thermal reaction of K_4P_6 with SiO_2 (quartz wall) at $T \sim 470$ K, forming K_3P_7 and (K_2O + Si) from K(g) and SiO_2(s).[37]

XIV. Donor Properties

Polyphosphorus structures are involved in a manifold of donor–acceptor interactions with metal atoms. Such interactions are especially interesting because of the variable and polyfunctional donor properties of the phosphorus substructures as ligands. This is observed in numerous isolated complex compounds[246-274] as well as in the M–P coordinations of solid metal phosphides. The latter exhibit some types of arrangements having no analogy in classical complexes.

1. Complexes

Despite the compounds with diphosphanes(4),[246-253] acting as η^1 or as η^2 ligands, numerous mono-, di-, and trinuclear complexes have been characterized. *cyclo*-P_n phosphanes(n) with $n = 3$,[257,258,260] $n = 4$,[263] $n = 5$,[267] and $n = 6$[271] react as uni-, bi-, and tridentate ligands, respectively. Complexes with P_4 molecules are remarkable, showing that even the element can act with suitably stabilized metals, namely Sacconi's $(triphos)NiP_4$[265] and Ginsberg's $(P(ph)_3)_2RhClP_4$.[264] Some insight into the degradation of P_4 was gained by trapping *cyclo*-P_3[255,256] as η^3-P_3 and $\mu(\eta^3$-$P_3)$. Important complexes are Scherer's complexes with *cyclo*-P_5^-[268,269] and *cyclo*-P_6,[270] because of their analogy to the cyclopentadienyl anion and benzene. Another important aspect originates from the different donor abilities of the heptaheteronortricyclene cages. Whereas P_4S_3 complexes with the apical P atom,[266] the cages $P_4(Si(me)_2)_3$[261,262] are bonded only via the basal P atoms (Figure 17). Central parts of those complexes correspond directly to hexahetero-2,2,2-barrelane and -cyclohexane, namely, $[Cr_2P_6]$[262] and $[Cr_2P_4]$[261] as well as $[Mo_2P_6]$[248] and $[Ag_2P_4]$.[247] All attempts for complexation of P_7R_3 (R = $Si(me)_3$) failed. By simply changing R to C_2H_5 or i-C_3H_7, a series of complexes was found.[275] Thus it was possible to study

step by step the different donor abilities of the cage atoms versus one, two, three, and four metal atoms: complexation starts with the bridging P atoms and ends with the basal P atoms. The highest donor ability at the bridging P atoms has also been observed with P_9R_3.[274]

2. Coordination in Solids

As pointed out, definite assignments exist in crystalline solids between the coordination of the metal atoms and the donor functions of the polyanion. This can be illustrated by some selected examples (Figure 17): (i) An extreme is $Cu_2P_3I_2$, which is in fact an adduct of CuI and elemental phosphorus (charge-transfer complex). One-dimensional chains of polycyclic P_{12} units cross the CuI substructure and complete the Cu coordination by one-third of the available lone pairs. (ii) The hexagonal-bipyramidal units $M_2Y_6^{2-}$ with the planar ring Y_6^{4-} are the most striking features of the M_4Y_6 phases (M = K, Rb, Cs; Y = P, As). INDO calculations show that the formation of $M_2[\mu\text{-}(\eta^6\text{-}Y_6)]$ complexes substantially stabilizes the unusual 2π system by the dominant lowering of the σ states of the planar Y_6^{4-}. The π character has already been posulated from the short bond distances Y–Y. (iii) In Th_2P_{11} a *cyclo*-P_6^{6-} chair acts as a twofold η^3 ligand bridging two Th atoms and forming a hexagonal scalenohedron ($\bar{3}m$ symmetry). In the same structure condensed skew-boat P_6 and *endo*-$P_8(C_{2v})$ rings coordinate Th atoms. The Th coordination of the phosphorus-richest M^{4+} phosphide, namely, ThP_7, is built by a corrugated 3D net of condensed P_6 and P_{12} rings forming proper cavities. (iv) The trivalent rare-earth metals are sandwich-like, enveloped by two *cyclo*-P_{12} in the pentaphosphide structures, and attain a tetragonal-antiprismatic eightfold coordination. Various modifications of the M–P coordination are further known with M^{2+} and M^{3+} bonded to chains and rings of multiple configurations and conformations. (v) The donor qualities of polyphosphides can clearly be shown by comparison of crystal structures of solvent-free and solvated compounds (section VI). Obviously, complete separation of cation and polyanion is only possible with the help of crown ether and cryptate. Figure 10 gives some examples. The participation of (bonded) metal atoms in the important valence tautomerism of P_7^{3-} (and Pb_9^{4-} and Sn_9^{4-}) in solution must be expected. This is another striking proof of the donor qualities of such polyanions. (vi) A novel complex system represents $[NbAs_8]^{3-}$ (not known with P up to now), which shows quite unexpected abilities of polyanions as ligands. The monocyclic Zintl anion As_8^{8-}, isostructural and isoelectronic with the S_8 crown, is *centered* by Nb(V). This is unusual because the stronger donor functions of the As_8^{8-} crown are expected to point outward. INDO calculations explain the electronic structure of this complex, which has $\bar{8}2m$ symmetry.[331]

XV. Solid-State Volumes

The old idea of Biltz and Klemm[332] that the molecular volume of solids at 0 K may be composed of specific increments ($V_m = \sum V_i$) has been discussed recently for the metal phosphides.[333] Saltlike and semimetallic compounds behave differently, but there is no difference between compounds of A and B metals. The observed relations allow for some valuable analysis with respect to structure and properties and give very good estimations of the unit cell content. In the case of saltlike phosphides the volume increment of phosphorus, V_P, which is obtained after subtraction of the cation increment, increases with increasing negative charge q(P) and decreases with increasing cation charge q(M). A suitable empirical relation is given by $V_p(q(P),q(M)) = \exp(\alpha q(P)q(M) + \beta q(P) + \gamma q(M) + \delta)$ [cm^3 mol^{-1}], with $\alpha = 0.046$, $\beta = -0.368$, $\gamma = -0.066$, and $\delta = 2.630$. In the case of semimetallic phosphides, in general V_P(sm) is smaller and depends on the mole fraction X(P): $V_P(sm) = 7.0X(P) + 4.0$ [cm^3 mol^{-1}]. With electropositive metals the observed volume V_{obsd} is much smaller than the sum of the volumes of the elements, but the difference decreases with increasing X(P). The incremental values $\sum V_i$(saltlike) and $\sum V_i$(sm) span the region of V_{obsd}, and the better fit to one or the other corresponds with the physical properties. Larger deviations indicate peculiarities, e.g., cluster anion formation or metals.

The two SiP_2 modifications are suitable examples to show that in special cases the volume can be used to judge the bonding type. Black pyrite-type p-SiP_2 and red $GeAs_2$-type SiP_2 have the volumes $V_m = 27.3$ and $V_m' = 35.7$ cm^3 mol^{-1}, respectively, with the ratio $V_m/V_m' = 0.76$. The volumes of the elements (Si: 12.0, P(black): 11.4) yield 34.8 cm^3 mol^{-1}, which only fits the larger value. On the other hand, one calculates from the increments 31 (saltlike) and 24 (sm) cm^3 mol^{-1}, respectively, with the correct ratio of about 0.77, as well as with the correct prediction of properties. It should be pointed out that the knowledge of the structures is not necessary, e.g., whether $2P^{2-}$ or (P^{3-} + P^-) are present.

Another example is Cu_2P_7: again the observed volume (95 cm^3 mol^{-1}) corresponds to the elemental values (Cu, P(black)). From the increments, however, one expects 105–110 and 80 cm^3 mol^{-1}, respectively, from which one expects semiconductor properties, and this is true ($E_g = 0.42$ eV).

An important statement is the theorem of *optimal volumes*,[332,333] which are expected to be defined by $\sum V_i$ in a series of homologous compounds. It is shown that in those series the fit of the optimal volume line is maintained by changing the structure type if the volume of one structure type becomes insufficient.

XVI. Defect Structures

As mentioned above, a large part of the polyphosphide structures can be derived from the P modifications or from possible P modifications by defect formation. The defect is formed by electron transfer from the metal atom onto the nearly unchanged P network. Analogues are structures formed by trigonal prisms of M atoms, in which their centers are occupied by P atoms. A whole series of examples exists in which defects are formed in the network of the polyanion by electron transfer. An analysis of such defect structures has been given in ref 9 and 334.

Especially interesting are the variations of the $ThSi_2$ and AlB_2 structures. The defect formation results in finite chains, according to $MX_m\square_n$ (X = P;) ($m + n = 2$). These structures differ in the relative orientation

of the M_6 prisms, which, because of the three square faces of these polyhedra, can be varied in many different ways. In the hexagonal AlB_2 type, all M prisms are oriented in the same way. The occupation of all centers by X atoms generates the well-known two-dimensional honeycomb structure of graphite. M_4P_6 (M = K, Rb, Cs) are direct derivatives of this Al_4B_8 type, since, according to $M_4P_6\square_2$, a quarter of the possible P sites remain vacant in an ordered way and leave isolated plane X_6 rings. The defects and their order apparently depend on the valency. Rotating the prisms by 90° from one layer to the next, the $ThSi_2$ type structure results, which, on complete occupation of the prism centers, shows a characteristic three-dimensional network of three-bonded X atoms. By rotating every second layer, an unknown tetragonal MX_2 type would result, containing a three-dimensional network of X_6 rings rotated with respect to each other. The compounds Sr_3P_4, Ba_3P_4, and Eu_3P_4 are examples for a M_3X_6 defect type $M_3P_4\square_2$. Another example, not yet verified with phosphorus, but with the congeners arsenic and antimony, is provided by the compounds Ca_2As_3 and Sr_2Sb_3, because a simple reorder of defects in the M_6 prisms would follow the conproportionation $X_4^{6-} + X_8^{10-} \rightarrow 2X_6^{8-}$ (Figure 12).

The examples given above certainly show how nature uses basic structural principles as far as possible.

XVII. The Eulerian Polyhedra Theorem

It is astonishing to see how the efforts to describe chemical structures diverge, which are known to be 3D objects. On one side, there is the large progress in the 3D representation of molecules and crystal structures, which is a success of the rapid development of graphic systems. On the other side, one can find the successful efforts of several commissions of nomenclature to press each 3D structure, with the aid of the graph theory, into the 2D space and on top of all to represent it in a linear structural form. The Eulerian polyhedra theorem[335] is a beautiful didactical tool to demonstrate the common root of those divergent efforts. For convex polyhedra Euler's theorem relates the number of corners C (atoms), the number of faces F (rings), and the number of edges E (bond): $C + F = E + 2$. The connectivity of all corners is correlated with the total number of ring members included in the system: $\sum$(bond number) = $\sum$(ring member) because the number of bonds = E = $^1/_2$(bond number). As a very important fact, polyhedra with threefold-bonded corners (3b)C can be enlarged by "improper corners" (2b)C* or at least by loops (2b)L to "improper convex polyhedra", which completely fulfill Euler's formula without changing the number of rings R by introducing (2b)C* or (2b)L. If the number of corners is (3b)C = 0, 2, 4, 6, 8, ..., then R = 2, 3, 4, 5, 6, ... rings are present, corresponding to C* = C*, C = C, tetrahedron, trigonal prism, cube, etc. An example is the ufosane system of P_{11}^{3-} and $P_{11}H_3$, respectively: P_{11}^{3-} = (3b)P_8 + (2b)P_3^- = (3b)C_8(2b)C_3* and, therefore, C = 11; E = $^1/_2\sum$(bond number) = $^1/_2$((8 × 3) + (3 × 2)) = 15; 11 + R = 15 + 2 yields R = 6. P_{11}^{3-} and $P_{11}H_3$ are hexacyclic systems with a total of 2 × 15 = 30 ring members, and these relations are not changed within the group of all isomers [C = 11; 30 ring members; $(3b)_8(2b)_3$]. The known polyanion P_{11}^{3-} represents the solution (5_6), a system of six five-membered rings (Figure 3), and it is a cubane derivative.

With some training a lot can be learned about the relationships between polyhedra and graph theory, e.g., how one has to deal with connected polycyclic systems. First of all, it is very impressive to imagine the system projected out onto a sphere. This holds especially for simple cyclic systems, e.g., benzene. One can also choose a 2D representation (graph theory), in which the periphery of the system has to be counted as an additional ring for the Euler formalism. The correct counting of cycles with respect to the nomenclature can be achieved by excluding the periphery and changing the Euler formula to $C + F = E + 1$. The formalism holds for atoms with other linkages too.

XVIII. Epilogue

We have tried to demonstrate the manifold relationships between different fields and disciplines by the polyphosphides. The huge field of synthetic chemistry seems to be inexhaustible, and at least the test tube seems to be still the best analog computer. However, modern theoretical methods promise relevant progress, which will be equivalent to that analog computer in the future. Regarding the large number of polyphosphides, one can imagine a lot of potential for interesting materials which are rather unexplored, but challenging.

XIX. References

(1) "Chemistry and Structural Chemistry of Phosphides and Polyphosphides. 48. For part 47, see Chattopadhyay, T.; Brown, P. J.; Thalmeier, P.; Bauhofer, W.; von Schnering, H. G. *Phys. Rev. B*, submitted.
(2) Baudler, M. *Angew. Chem.* **1987**, *99*, 429; *Angew. Chem., Int. Ed. Engl.* **1987**, *26*, 419.
(3) Baudler, M. *Angew. Chem.* **1982**, *94*, 520; *Angew. Chem., Int. Ed. Engl.* **1982**, *21*, 492.
(4) Baudler, M. *Pure Appl. Chem.* **1980**, *52*, 755; *ACS Symp. Ser.* **1981**, *No. 171*, 261; *Z. Chem.* **1984**, *24*, 352.
(5) Aronsson, B.; Lundström, L.; Rundquist, S. *Borides, Silicides and Phosphides*; Methuen & Co. Ltd.: London, 1965.
(6) Corbridge, D. E. C. *The Structural Chemistry of Phosphorus*; Elsevier: Amsterdam, 1974.
(7) Corbridge, D. E. C. *Phosphorus*; Elsevier: Amsterdam, 1978.
(8) von Schnering, H. G. In *Homoatomic Rings, Chains and Macromolecules of Main Group Elements*; Rheingold, A. L., Ed.; Elsevier: Amsterdam, 1977; Chapter 14.
(9) von Schnering, H. G. *Angew. Chem.* **1981**, *93*, 44; *Angew. Chem., Int. Ed. Engl.* **1981**, *20*, 33.
(10) von Schnering, H. G. *Nova Acta Leopold. N.F. Nr. 264* **1985**, *59*, 165; *ACS Symp. Ser.* **1983**, *No. 232*, 69. von Schnering, H. G. Rheinisch-Westfälische Akademie der Wissenschaften, Vorträge N325, p 7, Westdeutscher Verlag, Opladen, 1984.
(11) Jeitschko, W. *Int. Rev. Sci., Inorg. Chem., Ser. Two* **1974**, *5*, 219.
(12) Jeitschko, W.; Flörke, U.; Möller, M. H.; Rühl, R. *Ann. Chim. Fr.* **1982**, *7*, 413.
(13) Hulliger, F. *Struct. Bonding (Berlin)* **1968**, *4*, 83. Gschneidner, K. A., Jr.; Eyring, L., Eds. *Handbook on the Physics and Chemistry of Rare Earths*; North-Holland: Amsterdam, 1979; Chapter 33. (a) Kosyakov, V. I.; Vasil'eva, I. G. *Russian Chem. Rev. (Engl. Transl.)* **1979**, *48*, 153.
(14) Krebs, H.; Müller, K.-H.; Pakulla, I.; Zürn, G. *Angew. Chem.* **1955**, *67*, 524.
(15) Krebs, H.; Pakulla, I.; Zürn, G. *Z. Anorg. Allg. Chem.* **1955**, *278*, 274.
(16) Krebs, H.; Weitz, H.; Worms, K. H. *Z. Anorg. Allg. Chem.* **1955**, *280*, 119.
(17) Krebs, H.; Müller, K.-H.; Zürn, G. *Z. Anorg. Allg. Chem.* **1956**, *285*, 15.
(18) Krebs, H.; Ludwig, Th. *Z. Anorg. Allg. Chem.* **1958**, *294*, 257.
(19) Klemm, W. *Proc. Chem. Soc. (London)* **1958**, 329.
(20) Klemm, W. *Trab. Reun. Int. React. Sólidos, 3rd* **1956**, *1*, 447.
(21) Dorn, F. W. Dissertation, Münster University, 1956. Korte, H. D. Dissertation, Münster University, 1960.
(22) Pearson, W. B. *Acta Crystallogr.* **1964**, *17*, 1.
(23) Zintl, E. *Angew. Chem.* **1939**, *52*, 1. See also ref 9.
(24) Brauer, G.; Zintl, E. *Z. Phys. Chem., Abt. B* **1937**, *37*, 323.
(25) Mansmann, M. *Z. Kristallogr.* **1965**, *122*, 399.

(26) Hönle, W.; von Schnering, H. G. *Z. Kristallogr.* **1981**, *155*, 307.
(27) Manriquez, V.; Hönle, W.; von Schnering, H. G. *Z. Anorg. Allg. Chem.* **1986**, *539*, 95.
(28) Hönle, W.; von Schnering, H. G. *Int. Conf. Phosph. Chem., Collect. Abstr.*, Halle/Saale (GDR), 1979, p 418.
(29) von Schnering, H. G.; Wichelhaus, W. *Naturwissenschaften* **1972**, *59*, 78.
(30) Wichelhaus, W. Dissertation, Münster University, 1973.
(31) von Schnering, H. G.; Hönle, W. *Z. Anorg. Allg. Chem.* **1979**, *456*, 194.
(32) Manriquez, V. Dissertation, Stuttgart University, 1983.
(33) von Schnering, H. G. *Int. Conf. Phosph. Chem., Collect. Abstr.*, Halle/Saale (GDR), 1979, p 199. von Schnering, H. G.; Hönle, W.; Manriquez, V.; Meyer, T.; Mensing, Ch.; Giering, W. *2nd Int. Conf. Solid State Chem., Collect. Abstr. FV 54*, Eindhoven, 1982.
(34) Wichelhaus, W.; von Schnering, H. G. *Naturwissenschaften* **1973**, *60*, 104.
(35) Gnutzmann, G.; Dorn, F. W.; Klemm, W. *Z. Anorg. Allg. Chem.* **1961**, *309*, 210.
(36) Schmettow, W.; Lipka, A.; von Schnering, H. G. *Angew. Chem.* **1974**, *86*, 10; *Angew. Chem., Int. Ed. Engl.* **1974**, *13*, 5.
(37) Abicht, H.-P.; Hönle, W.; von Schnering, H. G. *Z. Anorg. Allg. Chem.* **1984**, *519*, 7.
(38) Meyer, T. M. Dissertation, Stuttgart University, 1985.
(39) Peters, K. Dissertation, Münster University, 1971.
(40) Schmettow, W. Dissertation, Münster University, 1975.
(41) von Schnering, H. G.; Schmidt, H. *Angew. Chem.* **1967**, *79*, 323.
(42) von Schnering, H. G.; Meyer, T.; Hönle, W.; Schmettow, W.; Hinze, W.; Bauhofer, W.; Kliche, G. *Z. Anorg. Allg. Chem.* **1987**, *553*, 261.
(43) Meyer, T.; Hönle, W.; von Schnering, H. G. *Z. Anorg. Allg. Chem.* **1987**, *552*, 69.
(44) Somer, M. Dissertation, Clausthal University, 1979.
(45) von Schnering, H. G.; Schmidt, H.; Makus, D., unpublished.
(46) von Stackelberg, M.; Paulus, R. *Z. Phys. Chem., Abt. B* **1933**, *22*, 305.
(47) El Maslout, A.; Motte, J. P.; Courtois, A.; Protas, J.; Gleitzer, C. *J. Solid State Chem.* **1975**, *15*, 223.
(48) Brice, J.-F.; Gerardin, R.; Zanne, M.; Gleitzer, C.; Aubry, J. *Mater. Res. Bull.* **1975**, *10*, 1237.
(49) L'Haridon, P.; David, J.; Lang, J.; Parthé, E. *J. Solid State Chem.* **1976**, *19*, 287.
(50) Zintl, E.; Husemann, E. *Z. Phys. Chem., Abt. B* **1933**, *21*, 138.
(51) von Schnering, H. G.; Menge, G. *Z. Anorg. Allg. Chem.* **1976**, *422*, 219.
(52) El Maslout, A.; Zanne, M.; Jeannot, F.; Gleitzer, C. *J. Solid State Chem.* **1975**, *14*, 85.
(53) Gibinski, T.; Cisowska, E.; Zcanowicz, W.; Henkie, Z.; Wojakowski, A. *Kristall. Techn.* **1974**, *9*, 161.
(54) Weibke, F. Dissertation, Hannover University, 1930.
(55) Iandelli, A.; Franceschi, E. *J. Less-Common Met.* **1973**, *30*, 211.
(56) Schmettow, W.; von Schnering, H. G. *Int. Conf. Phosph. Chem., Collect. Abstr.*, Halle/Salle (GDR), 1979, p 234.
(57) von Schnering, H. G.; Wittmann, M.; Sommer, D. *Z. Anorg. Allg. Chem.* **1984**, *510*, 61.
(58) von Schnering, H. G.; Schmettow, W.; Wittmann, M., unpublished.
(59) Dahlmann, W.; von Schnering, H. G. *Naturwissenschaften* **1973**, *60*, 518.
(60) Maass, K. E. *Z. Anorg. Allg. Chem.* **1970**, *374*, 19.
(61) Dahlmann, W.; von Schnering, H. G. *Naturwissenschaften* **1973**, *60*, 429.
(62) Dahlmann, W.; von Schnering, H. G. *Naturwissenschaften* **1972**, *59*, 420.
(63) Maass, K. E. *Z. Anorg. Allg. Chem.* **1970**, *374*, 1118.
(64) von Schnering, H. G.; Dahlmann, W. *Naturwissenschaften* **1971**, *58*, 623.
(65) von Schnering, H. G.; Menge, G. *Z. Anorg. Allg. Chem.* **1982**, *491*, 286.
(66) Berger, R. *Acta Chem. Scand., Ser. A* **1981**, *A35*, 635.
(67) Berger, R. *Acta Chem. Scand., Ser. A* **1980**, *A34*, 231.
(68) Parthé, E.; Parthé, E. *Acta Crystallogr.* **1963**, *16*, 71.
(69) Vu, D.; von Schnering, H. G., in preparation. Cf. Annual Report of the Max-Planck-Institut für Festkörperforschung, Stuttgart, 1983.
(70) Ono, S.; Nomura, K.; Hayakawa, H. *J. Less-Common Met.* **1974**, *38*, 119.
(71) von Schnering, H. G.; Wichelhaus, W.; Schulze-Nahrup, M. *Z. Anorg. Allg. Chem.* **1975**, *412*, 193.
(72) Hayakawa, H.; Nomura, K.; Ono, S. *J. Less-Common Met.* **1976**, *44*, 327.
(73) Wichelhaus, W.; von Schnering, H. G. *Z. Anorg. Allg. Chem.* **1976**, *419*, 77.
(74) Wichelhaus, W.; von Schnering, H. G. *Naturwissenschaften* **1975**, *62*, 180.
(75) Hassler, E.; Johnsson, T.; Rundquist, S. *Acta Chem. Scand., Ser. A* **1974**, *A28*, 123.
(76) Hartweg, M. Dissertation, Stuttgart University, 1987.
(77) von Schnering, H. G.; Wichelhaus, M.; Weber, H. P. *Z. Anorg. Allg. Chem.*, in preparation. See also: Weber, H. P. Staatsarbeit, Münster University, 1975.
(78) Franceschi, E.; Olcese, G. L. *J. Phys. Chem. Solids* **1969**, *30*, 903.
(79) von Schnering, H. G.; Wichelhaus, W., in preparation. See also ref 83 and 76.
(80) Iandelli, A.; Botti, E. *Atti Accad. Naz. Lincei, Cl. Sci. Fis., Mat. Nat., Rend., Ser. 7* **1937**, *25*, 638.
(81) See ref 70 and: Mirnov, K. E. *Izv. Akad. Nauk SSSR, Neorg. Mater.* **1983**, *19*, 714.
(82) Iandelli, A. *Z. Anorg. Allg. Chem.* **1956**, *288*, 81.
(83) Wittmann, M. Dissertation, Münster University, 1978.
(84) von Schnering, H. G.; Wittmann, M. *Z. Anorg. Allg. Chem.*, in preparation.
(85) Hulliger, F.; Vogt, O. *Solid State Commun.* **1970**, *8*, 770.
(86) von Schnering, H. G.; Wittmann, M., in preparation.
(87) Howell, I. K.; Pytlewski, L. L. *Inorg. Nucl. Chem. Lett.* **1970**, *6*, 681.
(88) Wittmann, M.; von Schnering, H. G. *5th Eur. Cryst. Meet., Collect. Abstr.*, Kopenhagen, 1979, 80-P1-5a.
(89) Schmettow, W.; Mensing, Ch.; von Schnering, H. G. *Z. Anorg. Allg. Chem.* **1984**, *510*, 51.
(90) Bauhofer, W.; Gmelin, E.; Möllendorf, M.; Nesper, R.; von Schnering, H. G. *J. Phys. C.: Solid State Phys.* **1985**, *18*, 3017.
(91) von Schnering, H. G.; Wittmann, M. *Z. Naturforsch.* **1980**, *356*, 824.
(92) Yaguchi, K. *J. Phys. Soc. Jpn.* **1966**, *21*, 1226.
(93) Menge, G.; von Schnering, H. G. *Z. Anorg. Allg. Chem.* **1976**, *422*, 226.
(94) Iandelli, A. *Rare Earth Research, Arrowhead Research Conference Calif.* 1960, Macmillan: New York, 1961; p 135.
(95) Heimbrecht, M.; Zumbusch, M.; Biltz, W. *Z. Anorg. Allg. Chem.* **1941**, *245*, 391. Leciejewicz, J.; Troc, R. *J. Nucl. Mater.* **1981**, *99*, 129.
(96) Meisel, K. *Z. Anorg. Allg. Chem.* **1939**, *240*, 300.
(97) Hulliger, F. *Nature (London)* **1966**, *209*, 499.
(98) von Schnering, H. G.; Wittmann, M.; Nesper, R. *J. Less-Common Met.* **1980**, *76*, 213.
(99) von Schnering, H. G.; Vu, D. *J. Less-Common Met.* **1986**, *116*, 259.
(100) Wojakowski, A.; Damieu, D.; Hery, Y. *J. Less-Common Met.* **1982**, *83*, 169.
(101) Marples, J. A. C. *J. Phys. Chem. Solids* **1970**, *31*, 2431.
(102) Zumbusch, M. *Z. Anorg. Allg. Chem.* **1941**, *245*, 402.
(103) Troc, R.; Leciejewicz, J.; Ciszewski, R. *Phys. Status Solidi* **1966**, *15*, 515; **1967**, *24*, 763. Pietraszko, D.; Lukaszewicz, K. *Roczn. Chem. Ann. Soc. Chim. Pol.* **1971**, *45*, 1105.
(104) Damieu, D.; Haire, R. G.; Peterson, J. R. *J. Less-Common Met.* **1979**, *68*, 159.
(105) Damieu, D.; Haire, R. G.; Peterson, J. R. *J. Inorg. Nucl. Chem.* **1980**, *42*, 995.
(106) Santandrea, R. P.; Mensing, Ch.; von Schnering, H. G. *Thermochim. Acta* **1987**, *117*, 261.
(107) Steenberg, B. *Ark. Kemi. Mineral. Geol.* **1938**, *A12*, 1.
(108) Schlenger, H.; Jacobs, H.; Juza, R. *Z. Anorg. Allg. Chem.* **1971**, *385*, 177.
(109) Olofsson, O. *Acta Chem. Scand.* **1965**, *19*, 229.
(110) Möller, M. H.; Jeitschko, W. *Z. Anorg. Allg. Chem.* **1982**, *491*, 225.
(111) Möller, M. H.; Jeitschko, W. *Inorg. Chem.* **1981**, *20*, 828.
(112) Jeitschko, W.; Möller, M. H. *Acta Crystallogr., Sect. B* **1979**, *B35*, 573.
(113) von Stackelberg, M.; Paulus, R. *Z. Phys. Chem., Abt. B* **1935**, *28*, 427.
(114) Smolyarenko, E. M.; Yakimovich, V. N. *Dokl. Akad. Nauk BSSR* **1983**, *27*, 517.
(115) White, J. G. *Acta Crystallogr.* **1965**, *18*, 217.
(116) Fleet, M. E.; Mowles, Th. A. *Acta Crystallogr., Sect. C* **1984**, *C40*, 1778.
(117) Rubtsov, V. A.; Smolyarenko, E. M.; Trukhan, V. M.; Yakimovich, V. N. *Cryst. Res. Technol.* **1986**, *21*, K93.
(118) Berak, J.; Pruchnik, Z. *Roczn. Chem. Ann. Soc. Chim. Pol.* **1968**, *42*, 1403.
(119) Zavalishin, E. I.; Aleinikova, K. B.; Rabotkina, N. S.; Arsenov, A. V. *Zh. Strukt. Khim.* **1979**, *20*, 146.
(120) Goodyear, J.; Steigmann, G. A. *Acta Crystallogr., Sect. B* **1969**, *B25*, 2371. Olofsson, O.; Gullman, J. *Acta Crystallogr., Sect. B* **1970**, *B26*, 1883.
(121) Horn, J. *Bull. Acad. Polon. Sci.* **1969**, *17*, 69.
(122) Krebs, H.; Müller, K. H.; Zürn, G. *Z. Anorg. Allg. Chem.* **1956**, *285*, 15.
(123) Slack, G. A.; McNelly, T. F.; Taft, E. A. *J. Phys. Chem. Solids* **1983**, *44*, 1009.

(124) Wang, C. C.; Spinar, L. H. *J. Phys. Chem. Solids* **1963**, *24*, 953.
(125) Amberger, E.; Rauh, P. A. *Acta Crystallogr., Sect. B* **1974**, *B30*, 2549.
(126) Addamiano, A. *Acta Crystallogr.* **1960**, *13*, 505.
(127) Jamieson, J. C. *Science (Washington, D.C.)* **1963**, *139*, 845.
(128) Kinomura, N.; Terao, K.; Kikkawa, S.; Horiuchi, H.; Koizumi, M. *Mater. Res. Bull.* **1983**, *18*, 53.
(129) Olofsson, O.; Gullman, J. *Acta Chem. Scand.* **1971**, *25*, 1327.
(130) Wadsten, T. *Chem. Scr.* **1975**, *8*, 63.
(131) Osugi, J.; Namikawa, R.;f Tanaka, Y. *Rev. Phys. Chem. Jpn.* **1966**, *36*, 35.
(132) Wadsten, T. *Acta Chem. Scand.* **1967**, *21*, 593.
(133) Wadsten, T. *Acta Chem. Scand.* **1967**, *21*, 1374.
(134) Donohue, P. C.; Siemons, W. J.; Gillson, J. L. *J. Phys. Chem. Solids* **1968**, *29*, 817.
(135) Chattopadhyay, T. K.; von Schnering, H. G. *Z. Kristallogr.* **1984**, *167*, 1.
(136) Osugi, J.; Namikawa, R.; Tanaka, Y. *Rev. Phys. Chem. Jpn.* **1967**, *37*, 81.
(137) Donohue, P. C.; Young, H. S. *J. Solid State Chem.* **1970**, *1*, 143.
(138) Gullman, J.; Olofsson, O. *J. Solid State Chem.* **1972**, *5*, 441.
(139) Olofsson, O. *Acta Chem. Scand.* **1970**, *24*, 1153.
(140) Eckerlin, P.; Kischio, W. *Z. Anorg. Allg. Chem.* **1968**, *363*, 1.
(141) Donohue, P. C. *Inorg. Chem.* **1970**, *9*, 335.
(142) Katz, G.; Kohn, J. A.; Broder, J. D. *Acta Crystallogr.* **1957**, *10*, 607.
(143) Hönle, W. Dissertation, Münster University, 1975.
(144) von Schnering, H. G.; Menge, G. *Z. Anorg. Allg. Chem.* **1981**, *481*, 33.
(145) Möller, M. H.; Jeitschko, W. *J. Solid State Chem.* **1986**, *65*, 178.
(146) Donohue, P. C. *J. Solid State Chem.* **1972**, *5*, 71.
(147) Rebbah, A.; Yazbeck, J.; Landé, R.; Deschanvres, A. *Mater. Res. Bull.* **1981**, *16*, 525.
(148) Rebbah, A.; Yazbeck, J.; Deschanvres, A. *Acta Crystallogr., Sect. B* **1980**, *B36*, 1747.
(149) Rebbah, A.; Yazbeck, J.; Deschanvres, A. *Rev. Chim. Miner.* **1980**, *17*, 96.
(150) Braun, D. J.; Jeitschko, W. *Acta Crystallogr., Sect. B* **1978**, *B34*, 2069.
(151) Jeitschko, W.; Hofmann, W. K. *J. Less-Common Met.* **1983**, *95*, 317.
(152) Meisen, V.; Jeitschko, W. *Z. Kristallogr.* **1984**, *167*, 135.
(153) von Schnering, H. G.; Menge, G. *J. Solid State Chem.* **1979**, *28*, 13.
(154) Hönle, W.; von Schnering, H. G. *Z. Kristallogr.* **1980**, *153*, 339.
(155) Hayakawa, H.; Ono, S.; Kobayashi, A.; Sasaki, Y. *Nippon Kagaku Kaishi* **1978**, *9*, 1214.
(156) Guerin, R.; El Ghadraoui, E. H.; Sergent, M.; Monceau, P. *J. Solid State Chem.* **1983**, *50*, 304.
(157) Flörke, U.; Jeitschko, W. *Inorg. Chem.* **1983**, *22*, 1736.
(158) Scholz, U. D.; Jeitschko, W. *Z. Anorg. Allg. Chem.* **1986**, *540/541*, 234.
(159) Donohue, P. C. *Mater. Res. Bull.* **1972**, *7*, 943.
(160) Jeitschko, W.; Braun, D. *Acta Crystallogr., Sect. B* **1977**, *B32*, 3401.
(161) Grandjean, F.; Gérard, A.; Braun, D. J.; Jeitschko, W. *J. Phys. Chem. Solids* **1984**, *45*, 877.
(162) Zemni, S.; Tranqui, D.; Chaudouet, P.; Madar, R.; Senateur, J. P. *J. Solid State Chem.* **1986**, *65*, 1.
(163) Kruger, O. L.; Moser, J. B. *J. Phys. Chem. Solids* **1967**, *28*, 2321.
(164) Ott, W. Dissertation, Stuttgart University, 1977.
(165) Hulliger, F.; Schmelczer, R. Schwarzenbach, D. *J. Solid State Chem.* **1977**, *21*, 371.
(166) Jeitschko, W. *Acta Crystallogr., Sect. B* **1974**, *B30*, 2565.
(167) Donohue, P. C.; Bierstedt, P. E. *Inorg. Chem.* **1969**, *8*, 2690.
(168) Jeitschko, W.; Meisen, U.; Möller, M. H.; Reehuis, M. *Z. Anorg. Allg. Chem.* **1985**, *527*, 73.
(169) Hofmann, W. K.; Jeitschko, W. *J. Solid State Chem.* **1984**, *51*, 152.
(170) Jeitschko, W.; Jaberg, B. *J. Solid State Chem.* **1980**, *35*, 312.
(171) Jeitschko, W.; Hofmann, W. K. *J. Less-Common Met.* **1983**, *95*, 317.
(172) Mewis, A. *Z. Naturforsch., B* **1984**, *B39*, 713.
(173) Mewis, A. *Z. Naturforsch., B* **1980**, *B35*, 141.
(174) Wenski, G.; Mewis, A. *Z. Naturforsch., B* **1986**, *B41*, 38.
(175) Elfström, M. *Acta Chem. Scand.* **1965**, *19*, 1694.
(176) Larsson, E. *Ark. Kemi* **1965**, *23*, 335.
(177) Rundquist, S. *Acta Chem. Scand.* **1962**, *16*, 287.
(178) Guérin, R.; Sergent, M.; Prigent, J. *Mater. Res. Bull.* **1975**, *10*, 957.
(179) Rühl, R.; Flörke, U.; Jeitschko, W. *J. Solid State Chem.* **1984**, *53*, 55.
(180) Dietrich, L. H.; Jeitschko, W. *J. Solid State Chem.* **1986**, *63*, 377.
(181) Jeitschko, W.; Donohue, P. C.; Johnson, V. *Acta Crystallogr., Sect. B* **1976**, *B32*, 1499.
(182) Snell, P. O. *Acta Chem. Scand.* **1968**, *22*, 1942.
(183) Hulliger, F. *Nature (London)* **1964**, *204*, 775.
(184) Gölin, M.; Carlsson, B.; Rundquist, S. *Acta Chem. Scand., Ser. A* **1975**, *A29*, 706.
(185) Rundquist, S. *Nature (London)* **1966**, *211*, 847.
(186) Jeitschko, W.; Donohue, P. C. *Acta Crystallogr., Sect. B* **1973**, *B29*, 783.
(187) Rühl, R.; Jeitschko, W. *Mh. Chem.* **1983**, *144*, 817.
(188) Holseth, H.; Kjekshus, A. *Acta Chem. Scand.* **1968**, *22*, 3284.
(189) Jeitschko, W.; Flörke, U.; Scholz, U. D. *J. Solid State Chem.* **1984**, *52*, 320.
(190) Rundquist, S. *Ark. Kemi* **1962**, *20*, 67.
(191) Kjekshus, A. *Acta Chem. Scand.* **1971**, *25*, 411.
(192) Zacharisen, W. H. *Acta Crystallogr.* **1963**, *16*, 1253.
(193) Donohue, P. C.; Bither, T. A.; Young, H. S. *Inorg. Chem.* **1968**, *7*, 998.
(194) Rühl, R.; Jeitschko, W. *Z. Anorg. Allg. Chem.* **1980**, *466*, 171. Guerin, R.; Potel, M.; Sergent, M. *Mater. Res. Bull.* **1979**, *14*, 1335.
(195) Kanno, R.; Kinomura, N.; Koizumi, M. *Acta Crystallogr., Sect. B* **1980**, *B36*, 2206.
(196) Rühl, R.; Jeitschko, W. *Inorg. Chem.* **1982**, *21*, 1886.
(197) Rühl, R.; Jeitschko, W. *Acta Crystallogr., Sect. B* **1982**, *B38*, 2784.
(198) Rundquist, S.; Ersson, N. O. *Ark. Kemi* **1969**, *30*, 103.
(199) Hönle, W.; von Schnering, H. G. *Z. Kristallogr.* **1987**, *179 & 180*, 443.
(200) Jeitschko, W.; Donohue, P. C. *Acta Crystallogr., Sect. B* **1972**, *B28*, 1893.
(201) Rühl, R.; Jeitschko, W.; Schwochau, K. *J. Solid State Chem.* **1982**, *44*, 134.
(202) Jeitschko, W.; Rühl, R. *Acta Crystallogr., Sect. B* **1979**, *B35*, 1953.
(203) Braun, D. J.; Jeitschko, W. *Z. Anorg. Allg. Chem.* **1978**, *445*, 157.
(204) Flörke, U.; Jeitschko, W. *J. Less-Common Met.* **1982**, *86*, 247.
(205) Dahl, E. *Acta Chem. Scand.* **1969**, *23*, 2677.
(206) Noläng, B. I.; Tergenius, L. E. *Acta Chem. Scand., Ser. A* **1980**, *A34*, 311.
(207) Jeitschko, W.; Rühl, R.; Krieger, U.; Heiden, C. *Mater. Res. Bull.* **1980**, *15*, 1755.
(208) Rühl, R.; Jeitschko, W. *Acta Crystallogr., Sect. B* **1981**, *B37*, 39.
(209) Jeitschko, W.; Donohue, P. C. *Acta Crystallogr., Sect. B* **1975**, *B31*, 574.
(210) Jeitschko, W.; Braun, D. J. *Acta Crystallogr., Sect. B* **1978**, *B34*, 3196.
(211) Sugitani, M.; Kinomura, N.; Koizumi, M.; Kume, S. *J. Solid State Chem.* **1978**, *26*, 195.
(212) Evain, M.; Brec, R.; Fiechter, S.; Tributsch, H. *J. Solid State Chem.* **1987**, *71*, 40.
(213) Kinomura, N.; Terao, K.; Kikkawa, S.; Koizumi, M. *J. Solid State Chem.* **1983**, *48*, 306.
(214) Vincent, R.; Pretty, S. F. *Philos. Mag. A* **1986**, *53*, 843.
(215) von Schnering, H. G.; Hönle, W.; Schwarz, A., in preparation. See also ref 10.
(216) Leung, Y. C.; Waser, J. *Acta Crystallogr.* **1957**, *10*, 574.
(217) Chattopadhyay, T. K.; May, W.; von Schnering, H. G.; Pawley, G. S. *Z. Kristallogr.* **1983**, *165*, 47.
(218) May, W. Dissertation, Stuttgart University, 1977.
(219) Minshall, P. C.; Sheldrick, G. M. *Acta Crystallogr., Sect. B* **1978**, *B34*, 1326.
(220) Griffin, A. M.; Minshall, P. S.; Sheldrick, G. M. *J. Chem. Soc., Chem. Commun.* **1976**, 809.
(221) Vos, A.; Olthof, R.; van Bolhuis, F.; Botterweg, R. *Acta Crystallogr.* **1965**, *19*, 864.
(222) Griffin, A. M.; Sheldrick, G. M. *Acta Crystallogr., Sect. B* **1975**, *B31*, 2738.
(223) Dixon, D. T.; Einstein, F. W. B.; Penfold, B. R. *Acta Crystallogr.* **1965**, *18*, 221.
(224) Hilmer, W. *Acta Crystallogr., Sect. B* **1969**, *B25*, 1229.
(225) Keulen, E.; Vos, A. *Acta Crystallogr.* **1959**, *12*, 323.
(226) Blachnik, R.; Wickel, V. *Thermochim. Acta* **1984**, *81*, 185.
(227) Monteil, Y.; Vincent, H. *Z. Anorg. Allg. Chem.* **1975**, *416*, 181.
(228) Sheldrick, G. M. Penney, G. J. *J. Chem. Soc. A* **1971**, 245.
(229) Baudler, M.; Düster, D.; Ouzomis, D. *Z. Anorg. Allg. Chem.* **1987**, *544*, 87.
(230) Hönle, W.; von Schnering, H. G.; Schmidtpeter, A.; Burget, G. *Angew. Chem.* **1984**, *96*, 796; *Angew. Chem., Int. Ed. Engl.* **1984**, *23*, 817.
(231) Hönle, W.; von Schnering, H. G., to be published.
(232) Baudler, M.; Faber, W. *Chem. Ber.* **1980**, *113*, 3394.
(233) Härer, J. Dissertation, Karlsruhe University, 1981.
(234) Hönle, W.; Borrmann, H.; von Schnering, H. G., in preparation.
(235) Hönle, W.; von Schnering, H. G. *Phosphorus Sulfur* **1987**, *30*, 775.

(236) Hönle, W.; Manriquez, V.; Mujica, C.; Weber, D.; von Schnering, H. G. *29th IUPAC Congress, Köln 1983, Abstracts of Papers*, p 36.
(237) Baudler, M.; Heumüller, R.; Hahn, J. *Z. Anorg. Allg. Chem.* **1985**, *529*, 7.
(238) Baudler, M.; Exner, O. *Chem. Ber.* **1983**, *116*, 1268.
(239) Fritz, G., and co-workers, unpublished.
(240) Baudler, M.; Düster, D. *Z. Naturforsch. B: Anorg. Chem., Org. Chem.* **1987**, *42B*, 335.
(241) von Schnering, H. G.; Manriquez, V.; Hönle, W. *Angew. Chem.* **1981**, *93*, 606; *Angew. Chem., Int. Ed. Engl.* **1981**, *20*, 594.
(242) Baudler, M.; Düster, D.; Germeshausen, J. *Z. Anorg. Allg. Chem.* **1986**, *534*, 19.
(243) Baudler, M.; Düster, D.; Langerbeins, K.; Germeshausen, J. *Angew. Chem.* **1984**, *96*, 309; *Angew. Chem., Int. Ed. Engl.* **1984**, *23*, 317.
(244) Fritz, G.; Schneider, H.-W.; Hönle, W.; von Schnering, H. G., to be published.
(245) Baudler, M.; Heumüller, R.; Düster, D.; Germeshausen, J.; Hahn, J. *Z. Anorg. Allg. Chem.* **1984**, *518*, 7. Tebbe, K.-F.; Fehér, M.; Baudler, M. *Z. Kristallogr.* **1985**, *170*, 180.
(246) Hartung, H. *Z. Anorg. Allg. Chem.* **1970**, *372*, 150.
(247) Jones, P. G.; Roesky, H. W.; Grützmacher, H.-J.; Sheldrick, G. M. *Z. Naturforsch., B* **1985**, *40B*, 590.
(248) Roesky, H. W.; Amirzadeh-Asl, D.; Clegg, W.; Noltemeyer, M.; Sheldrick, G. M. *J. Chem. Soc., Dalton Trans.* **1983**, 855.
(249) Atwood, J. L.; Newell, J. K.; Hunter, W. E.; Bernal, I.; Calderazzo, F.; Mavani, I. P.; Vitali, D. *J. Chem. Soc., Chem. Commun.* **1976**, 441; *J. Chem. Soc., Dalton Trans.* **1978**, 1189.
(250) Huttner, G.; Friedrich, P.; Willenberg, H.; Müller, H. D. *Angew. Chem.* **1977**, *89*, 268; *Angew. Chem., Int. Ed. Engl.* **1977**, *16*, 260.
(251) Elmes, P. S.; Scudder, M.; West, B. O. *J. Organomet. Chem.* **1976**, *122*, 281.
(252) Hoge, R.; Lehnert, R.; Fischer, K. F. *Cryst. Struct. Commun.* **1977**, *6*, 359.
(253) Huttner, G.; Müllner, H. D.; Bejenke, V.; Orama, O. *Z. Naturforsch., B* **1976**, *31B*, 1160.
(254) Di Vaira, M.; Peruzzini, M.; Stoppioni, P. *J. Chem. Soc., Dalton Trans.* **1984**, 359. Bianchini, C.; Di Vaira, M.; Meli, A.; Sacconi, L. *J. Am. Chem. Soc.* **1981**, *103*, 1448; *Inorg. Chem.* **1981**, *20*, 1169; *Angew. Chem.* **1980**, *92*, 412; *Angew. Chem., Int. Ed. Engl.* **1980**, *19*, 405.
(255) Dapporto, D.; Sacconi, L.; Stoppioni, P.; Zanobini, F. *Inorg. Chem.* **1981**, *20*, 3834.
(256) Di Vaira, M.; Peruzzini, M.; Stoppioni, P. *Acta Crystallogr., Sect. C* **1983**, *C39*, 1210.
(257) Tebbe, K. F.; Fehér, M. *Z. Naturforsch., B* **1984**, *B39*, 37.
(258) Tebbe, K. F. *Acta Crystallogr., Sect. C* **1984**, *C40*, 1552.
(259) Scherer, D. J.; Sitzmann, H.; Wolmershäuser, G. *Acta Crystallogr., Sect. C* **1985**, *C41*, 1761.
(260) Huttner, G.; Müller, H. D.; Frank, A.; Lorentz, H. *Angew. Chem.* **1975**, *87*, 597; *Angew. Chem., Int. Ed. Engl.* **1975**, *14*, 572.
(261) Hönle, W.; von Schnering, H. G. *Z. Anorg. Allg. Chem.* **1980**, *465*, 72.
(262) Fritz, G.; Uhlmann, R.; Hoppe, K. D.; Hönle, W.; von Schnering, H. G. *Z. Anorg. Allg. Chem.* **1982**, *491*, 83.
(263) Rheingold, A. L.; Fountain, M. E. *Organometallics* **1984**, *3*, 1417.
(264) Ginsberg, A. P.; Lindsell, W. E.; McCullough, K. J.; Sprinkle, C. R.; Welch, A. J. *J. Am. Chem. Soc.* **1986**, *108*, 403.
(265) Dapporto, P.; Midollini, S.; Sacconi, L. *Angew. Chem.* **1979**, *91*, 510; *Angew. Chem., Int. Ed. Engl.* **1979**, *18*, 469.
(266) Cordes, A. W.; Joyner, R. D.; Shores, R. D.; Dill, E. D. *Inorg. Chem.* **1974**, *13*, 132.
(267) Bush, M. A.; Woodward, P. *J. Chem. Soc. A* **1968**, 1221.
(268) Scherer, O. J.; Schwalb, J.; Wolmershäuser, G.; Kaim, W.; Gross, R. *Angew. Chem.* **1986**, *98*, 349; *Angew. Chem., Int. Ed. Engl.* **1986**, *25*, 363.
(269) Scherer, O. J.; Brück, Th. *Angew. Chem.* **1987**, *99*, 59; *Angew. Chem., Int. Ed. Engl.* **1987**, *26*, 59.
(270) Scherer, O. J.; Sitzmann, H.; Wolmershäuser, G. *Angew. Chem.* **1985**, *97*, 358; *Angew. Chem., Int. Ed. Engl.* **1985**, *24*, 351.
(271) Elmes, P. S.; Gatehouse, B. M.; West, B. O. *J. Organomet. Chem.* **1974**, *82*, 235.
(272) Cecconi, F.; Ghilardi, C. A.; Midollini, S.; Orlandini, A. *Inorg. Chem.* **1986**, *25*, 1766.
(273) Jones, R. A.; Seeberger, M. H.; Whittlesey, B. R. *J. Am. Chem. Soc.* **1985**, *107*, 6424.
(274) Fritz, G.; Schneider, H.-W.; Hönle, W.; von Schnering, H. G., in preparation. Schneider, H.-W. Dissertation, Karlsruhe University, 1987.
(275) Schäfer, H.; Trenkel, M. *Z. Anorg. Allg. Chem.* **1972**, *391*, 11.
(276) Ugai, Y. A.; Gukov, O. Y.; Illarionov, A. A. *Izv. Akad. Nauk SSSR, Neorg. Mater.* **1978**, *14*, 1012.
(277) Glaum, R.; Gruehn, R. *Z. Kristallogr.* **1987**, *178*, 72.
(278) Flörke, U. *Z. Anorg. Allg. Chem.* **1983**, *502*, 218.
(279) Richardson, M. W.; Noläng, B. *J. Cryst. Growth* **1977**, *42*, 90.
(280) Wilke, K.-Th. *Kristallzüchtung*; VEB Deutscher Verlag der Wissenschaften: *Berlin*, 1973.
(281) Olego, D. J.; Baumann, J.; Schachter, R.; Michel, C.; Kuck, M.; Gersten, S.; Polgar, L. G. *Phys. Rev. B* **1985**, *31*, 2240.
(282) Bellavance, D.; Vlasse, M.; Morris, B.; Wold, A. *J. Solid State Chem.* **1969**, *1*, 82.
(283) Hartmann, H.; Orban, J. *Z. Anorg. Allg. Chem.* **1936**, *226*, 257.
(284) Mooser, E.; Pearson, W. B. *Phys. Rev.* **1956**, *101*, 1608. Cf. detailed discussion by: Kjekshus, A.; Rakke, T. *Struct. Bonding (Berlin)* **1974**, *9*, 45.
(285) Grimm, H. O.; Sommerfeld, A. *Z. Phys.* **1926**, *36*, 36.
(286) von Schnering, H. G.; Schwarz, M.; Nesper, R. *J. Less-Common Met.*, in press.
(287) Hurng, W.-M.; Corbett, J. D.; Wang, S. L.; Jacobson, R. A. *Inorg. Chem.* **1987**, *26*, 2392.
(288) Grüttner, A.; Nesper, R.; von Schnering, H. G. *Angew. Chem.* **1982**, *94*, 933; *Angew. Chem., Int. Ed. Engl.* **1982**, *21*, 912.
(289) Grüttner, A. Thesis, Stuttgart University, 1982.
(290) Simon, A.; Borrmann, H.; Craubner, H. *Phosphorus Sulfur* **1987**, *30*, 507.
(291) Thurn, H.; Krebs, H. *Acta Crystallogr., Sect. B* **1969**, *B25*, 125.
(292) Brown, A.; Rundquist, S. *Acta Crystallogr.* **1965**, *19*, 684.
(293) Pauling, L. *The Nature of the Chemical Bond*, 3rd ed.; Cornell University Press: Ithaca, NY, 1960.
(294) Chattopadhyay, T.; Werner, A.; von Schnering, H. G. *J. Phys. Chem. Solids* **1983**, *44*, 699.
(295) Chattopadhyay, T.; von Schnering, H. G., unpublished.
(296) Will, G.; Lauterjung, J.f Schmitz, H.; Hinze, E. *Mater. Res. Soc. Symp. Proc.* **1984**, *22*, 49.
(297) Wolf, J. Dissertation, Stuttgart University, 1986.
(298) Hönle, W.; von Schnering, H. G.; Somer, M. *Z. Kristallogr.* **1986**, *174*, 82.
(299) Martin, T. P. *Angew. Chem.* **1986**, *98*, 197; *Angew. Chem., Int. Ed. Engl.* **1986**, *25*, 197.
(300) von Schnering, H. G.; Mensing, Ch., unpublished results.
(301) Santandrea, R. P.; Mensing, Ch.; von Schnering, H. G. *Thermochim. Acta* **1986**, *98*, 301.
(302) Santandrea, R. P.; Gmelin, E.; Santandrea, C.; von Schnering, H. G. *Thermochim. Acta* **1983**, *67*, 263.
(303) Dunitz, J. D. *Perspect. Struct. Chem.* **1968**, *2*, 1. Bürgi, H.-B. *Angew. Chem.* **1975**, *87*, 461; *Angew. Chem., Int. Ed. Engl.* **1975**, *14*, 460.
(304) Bauhofer, W.; Wittmann, M.; von Schnering, H. G. *J. Phys. Chem. Solids* **1981**, *42*, 687.
(305) Ozin, G. A. *J. Chem. Soc. A, Inorg., Phys., Theor.* **1970**, 2307.
(306) Klemm, W.; Falkowski, I. V. *Z. Anorg. Allg. Chem.* **1948**, *256*, 343.
(307) Hönle, W.; von Schnering, H. G., unpublished.
(308) Hönle, W.; von Schnering, H. G. *Angew. Chem.* **1986**, *98*, 370; *Angew. Chem., Int. Ed. Engl.* **1986**, *25*, 352.
(309) Hönle, W.; von Schnering, H. G. *IVth Eur. Crystallogr. Meet. Oxford, Collect. Abstr. B*, **1977**, 552.
(310) Chattopadhyay, T.; Carlone, C.; Jayaraman, A.; von Schnering, H. G. *Phys. Rev. B* **1981**, *23*, 2471. Chattopadhyay, T.; von Schnering, H. G. *Phys. Status Solidi B* **1982**, *108*, 241.
(311) Fritz, G.; Hoppe, K. D.; Hönle, W.; Weber, D.; Mujica, C.; Manriquez, V.; von Schnering, H. G. *J. Organomet. Chem.* **1983**, *249*, 63.
(312) Olego, D. J. *Phys. Rev. B* **1985**, *31*, 2230.
(313) Fasol, G.; Cardona, M.; Hönle, W.; von Schnering, H. G. *Solid State Commun.* **1984**, *52*, 307.
(314) Pauling, L.; Simonetta, M. *J. Chem. Phys.* **1952**, *20*, 29.
(315) Olés, B.; Stolz, H. J.; von Schnering, H. G. *Phys. Status Solidi B* **1981**, *106*, 157. Olés, B.; von Schnering, H. G. *J. Phys. C* **1981**, *14*, 5559.
(316) von Schnering, H. G.; Wichelhaus, W.; Wittmann, M. *Abstracts, Vth International Conference on Solid Compounds of Transition Elements (ICSTE)*, Uppsala, 1976.
(317) Möllendorf, M. Thesis, Stuttgart University, 1982.
(318) Bauhofer, W.; Wittmann, M.; von Schnering, H. G. *Proceedings of the Conference on the Physics of Narrow Gap Semiconductors, Linz*; Henrich, H., Palmetshofer, L., Eds.; Springer: Berlin, 1981. *Lect. Notes Phys.* **1982**, *152*, 30.
(319) Bauhofer, W.; Gmelin, E.; Möllendorf, M.; Nesper, R.; von Schnering, H. G. *J. Phys. C* **1985**, *18*, 3017.
(320) Chattopadhyay, T.; Bartholin, H.; Voiron, J.; Bauhofer, W.; von Schnering, H. G. *J. Magn. Magn. Mater.* **1987**, *63/64*, 632.
(321) Möllendorf, M.; Bauhofer, W.; Staguhn, W.; Thielemann, J.; von Ortenberg, M. *Solid State Commun.* **1987**, *61*, 591.
(322) Chattopadhyay, T.; Brown, P. J.; Thalmeier, P.; Bauhofer, W.; von Schnering, H. G. *Phys. Rev. B*, in press.
(323) Bauhofer, W. Habilitationsschrift, Würzburg, 1987.
(324) See ref 236.

(325) Baudler, M.; Germeshausen, J. *Angew. Chem.* **1987**, *99*, 372; *Angew. Chem., Int. Ed. Engl.* **1987**, *26*, 348. Baudler, M.; Michels, M.; Pieroth, M.; Hahn, J. *Angew. Chem.* **1986**, *98*, 465; *Angew. Chem., Int. Ed. Engl.* **1986**, *25*, 471.
(326) von Schnering, H. G.; Fenske, D.; Hönle, W.; Binnewies, M.; Peters, K. *Angew. Chem.* **1979**, *91*, 755; *Angew. Chem., Int. Ed. Engl.* **1979**, *18*, 679.
(327) Mujica, C.; Weber, D.; von Schnering, H. G. *Z. Naturforsch., B* **1986**, *41B*, 991.
(328) Baudler, M.; Riekehof-Böhmer, R. *Z. Naturforsch., B* **1985**, *40B*, 1424.
(329) Baudler, M.; Becher, R.; Germeshausen, J. *Chem. Ber.* **1986**, *119*, 2510.
(330) Baudler, M.; Becher, R., unpublished. See ref 1.
(331) von Schnering, H. G.; Wolf, J.; Weber, D.; Ramirez, R.; Meyer, T. *Angew. Chem.* **1986**, *98*, 372; *Angew. Chem., Int. Ed. Engl.* **1986**, *25*, 353.
(332) Biltz, W.; Klemm, W. In *Raumchemie der festen Stoffe*; Biltz, W., Ed.; Leopold-Voss-Verlag: Leipzig, 1934. Cf. Klemm, W., book 2 in ref 332.
(333) Klemm, W.; von Schnering, H. G. *Z. Anorg. Allg. Chem.* **1982**, *491*, 9.
(334) Nesper, R.; von Schnering, H. G. *Tschermaks Mineral. Petrogr. Mitt.* **1983**, *32*, 195.
(335) Euler, L. "Elementa doctrinae solidorum", In *Novi Commentarii Academiae Scientiarum Imperialis Petrolitanae*, 1758, pp 109–140.
(336) Böhm, M. C.; Gleiter, R. *Z. Naturforsch., B* **1981**, *36B*, 498.
(337) Zheng, Ch.; Hoffmann, R. *J. Am. Chem. Soc.* **1986**, *108*, 3078.
(338) Hoffmann, R.; Zheng, Ch. *J. Phys. Chem.* **1985**, *89*, 4175.
(339) Jolibois, P. *C. R. Seances Acad. Sci.* **1910**, *150*, 106.
(340) Cf. ref 12 and references cited therein.
(341) E.g.: Kaner, R.; Castro, C. A.; Gruska, R. P.; Wold, A. *Mater. Res. Bull.* **1977**, *12*, 1143.
(342) Hugot, C. *C. R. Seances Acad. Sci.* **1895**, *121*, 207. Brauer, G.; Zintl, E. *Z. Phys. Chem.* **1937**, *37B*, 323. Evers, E. Ch. *J. Am. Chem. Soc.* **1951**, *73*, 2038. Royen, P.; Zschaage, H. *Z. Naturforsch., B* **1953**, *8B*, 777.
(343) Fritz, G.; Hölderich, W. *Naturwissenschaften* **1975**, *62*, 573.
(344) Kjekshus, A.; Nicholson, D. G. *Acta Chem. Scand.* **1971**, *25*, 886.
(345) Hönle, W.; von Schnering, H. G. *Z. Anorg. Allg. Chem.* **1978**, *440*, 171.
(346) Hönle, W.; Manriquez, V.; Meyer, T.; von Schnering, H. G. *Z. Kristallogr.* **1983**, *162*, 104.
(347) Hönle, W.; Meyer, T.; Mensing, Ch.; von Schnering, H. G. *Z. Kristallogr.* **1985**, *170*, 78.
(348) von Schnering, H. G., unpublished.
(349) Schmettow, W.; Sommer, D.; Mensing, Ch.; von Schnering, H. G. 2nd Vortragstagung der Fachgruppe Festkörperchemie der GDCh, Stuttgart, 1980.
(350) Werner, A.; Hochheimer, H. D.; Wittmann, M.; von Schnering, H. G.; Hinze, E. *J. Less-Common Met.* **1982**, *87*, 327.
(351) Henkel, W.; Strössner, K.; Hochheimer, H. D.; Hönle, W.; von Schnering, H. G. *Proceedings of the 8th International Conference on Raman Spectroscopy, Bordeaux, 1982*; Wiley: New York, 1982. Bolduan, F.; Hönle, W.; Hochheimer, H. D.; Henkel, W. *Phys. Status Solidi B* **1985**, *132*, 41.
(352) Fritz, G.; Härer, J.; Matern, E. *Z. Anorg. Allg. Chem.* **1983**, *504*, 38.
(353) Sharon, M.; Tamizhmani, G. *J. Mater. Sci.* **1986**, *21*, 2193.
(354) Belin, C. H. E. *J. Am. Chem. Soc.* **1980**, *102*, 6036.
(355) Cf. ref 44 and: Cyvin, B. M.; Cyvin, S. J.; Somer, M.; Brockner, W. *Z. Naturforsch., A* **1986**, *41A*, 549.
(356) Scholz, U. D.; Jeitschko, W. *J. Solid State Chem.* **1987**, *67*, 271.
(357) Jeitschko, W.; Glaum, R.; Boonk, L. *J. Solid State Chem.* **1987**, *69*, 93.